IDENTIFICATION OF NOVEL PICORNAVIRUS PROTEINASE SUBSTRATES USING TERMINAL AMINE ISOTOPIC LABELING OF SUSBTRATES

by

Julienne Jagdeo

B.Sc., Simon Fraser University, 2009

M.Sc., Simon Fraser University, 2012

A THESIS SUBMITTED IN PARTIAL FULFILLMENT OF

THE REQUIREMENTS FOR THE DEGREE OF

DOCTOR OF PHILOSOPHY

in

THE FACULTY OF GRADUATE AND POSTDOCTORAL STUDIES

(Biochemistry and Molecular Biology)

THE UNIVERSITY OF BRITISH COLUMBIA

(Vancouver)

April 2017

Abstract

Viruses have exploited strategies of proteolysis for the purposes of processing viral proteins and manipulating cellular processes to direct synthesis of new virions and subvert host antiviral responses. Many viruses encode proteases within their genome, of which many have been well studied among the family of positive-sense single-stranded RNA picornaviruses. A subset of host proteins have already been identified as targets of picornaviral proteinases; however, the full repertoire of targets is not known. In this thesis, a novel proteomics-based approach termed terminal amine isotopic labeling of substrates (TAILS) was used to conduct a global analysis of protease-generated N-terminal peptides by mass spectrometry and identify novel substrates of the 3C ($3C^{pro}$) and 2A ($2A^{pro}$) proteinases from poliovirus and coxsackievirus type B3 (CVB3). TAILS was performed on HeLa cell extracts subjected to purified poliovirus $3C^{pro}$ or CVB3 $2A^{pro}$, and on mouse HL-1 cardiomyocyte extracts subjected to purified CVB3 $3C^{pro}$. A list of high confidence candidate substrates for all three proteinases was generated, which included a peptide corresponding to the known poliovirus $3C^{pro}$ substrate polypyrimide tract binding protein at a known cleavage site, thus validating this approach. Furthermore, three identical peptides in both the poliovirus and CVB3 $3C^{pro}$ list of high confidence substrates were identified, suggesting that cleavage of these substrates may contribute to general strategy of picornaviral infection. A total of seven high confidence substrates were validated as novel targets of $3C^{pro}$ *in vitro* and during virus infection. Moreover, mutations in the TAILS-identified cleavage sites for these candidates blocked cleavage *in vitro* and during infection. Depletion of these proteins by siRNAs modulated virus infection, suggesting that cleavage of these substrates either promotes or inhibits virus infection. In summary, an *in vitro* TAILS assay can be utilized to identify novel substrates of viral proteinases that are cleave during infection. Moreover, TAILS

can identify common substrates of viral proteinases between different viral species, revealing general strategies of infection utilized by related viruses. Finally, the identification of novel host substrates provides new insights the viral-host interactions mediated by viral proteinases that are required for successful infection.

Preface

Chapter 3 and **Chapter 4** are based on a modified portions of the original research article Jagdeo J, Dufour A, Fung G, Luo H, Kleifeld O, Overall CM, Jan E. (2015) Heterogeneous nuclear ribonucleoprotein M facilitates enterovirus infection. *J Virol* 89: 7064-7078. I completed, or actively contributed to, all data analyses presented in this dissertation and in the original research article listed above. The reuse and reprint of all published work is with permission from all journals referenced. I also conducted additional projects and experiments with collaborating labs, resulting in contributions to three other co-author peer-reviewed research articles. All studies were approved by the University of British Columbia Research Ethics Board (Biosafety #B12-0119 and Animal #A13-0237).

Table of Contents

List of Tables

List of Figures

List of Abbreviations

$2A^{pro}$: 2A proteinase

$3C^{pro}$: 3C proteinase

$3D^{pol}$: 3D polymerase

ACLY: ATP-citrate synthase

ALIX: programmed cell death 6-interacting protein

ARE: AU-rich element

ASC: apoptosis-associated speck-like protein containing a CARD

AUF1: AUF-rich element RNA-binding protein

BSA: bovine serum albumin

C3: complement component 3

CAR: coxsackievirus and adenovirus receptor

CMV: cytomegalovirus

COFRADIC: combined fractional diagonal chromatography

CREB: cAMP-responsive element-binding protein

CVB3: coxsackievirus type B3

DAF: decay accelerating factor

DAP5: death associated protein 5

DCM: dilated cardiomyopathy

DMEM: Dulbecco's Modified Eagle's Medium

DNA-PK: DNA-dependent protein kinase

eIF: eukaryotic initiation factor

EMCV: encephalomyocarditis virus

ERK: extracellular signal-regulated kinase

ESCRT: endosomal sorting complexes required for transport

EV: enterovirus

FBS: fetal bovine serum

FDR: false discovery rate

FMDV: foot and mouth disease virus

GAB1: Grb2-associated binding protein 1

G3BP1: Ras-GAP SH3 domain binding protein 1

HA: hemagglutinin

HAART: highly-active antiretroviral therapy

HAV: hepatitis A virus

HCV: hepatitis C virus

HIV-1: human immunodeficiency virus 1

hnRNP: heterogeneous nuclear ribonucleoprotein

h.p.i.: hours post infection

HRV: human rhinovirus

ICAM-1: intracellular adhesion molecule-1

IFN: interferon

IκB: I kappa B

IκBα: inhibitor of kappa B

IL: interleukin

IFNAR: interferon alpha/beta receptor

IRES: internal ribosomal entry site

IRF: interferon regulatory factor

ISG: interferon-stimulated gene

ITAF: IRES trans-acting factor

JAK-STAT: Janus kinase – signal transducer and activator of transcription

KH: hnRNP K homology

L^{pro}: leader proteinase

La: La lupus antigen

LC-MS/MS: liquid chromatography tandem mass spectrometry

MAP4: microtubule associated protein 4

MAVS: mitochondrial anti-viral signalling

MDA5: melanoma differentiation-associated protein 5

NEMO: NFkB essential modulator

NFkB: nuclear factor kappa-light chain-enhancer of activated B cells

NLR: NOD-like receptor

NLS: nuclear localization signal

NPC: nuclear pore complex

NUPS: nucleoporins

PABP: poly(A) binding protein

PAMP: pathogen associated molecular pattern

PBS: phosphate buffered saline

PCBP: poly(rC) binding protein

PFAS: phosphoribosylformylglycinamidine synthase

PKR: protein kinase R

PFU: plaque-forming units

PRR: pathogen recognition receptor

P/S: penicillin/streptomycin

PTB: polypyrimidine tract binding protein

PV: poliovirus

Q-TOF: quadrupole time-of-flight

RIG-I: retinoic acid-inducible gene-1

RIPA: radio-immunoprecipitation assay

RIPK1: receptor-interacting serine/threonine-protein kinase 1

RLR: RIG-I-like receptor

RRM: RNA recognition motif

SDS-PAGE: sodium dodecyl sulfate-polyacrylamide gel electrophoresis

SG: stress granule

SL-1: selective factor 1

SMN: survival of motor neuron complex

snRNP: small nuclear ribonucleoprotein

TAB: TGF-beta-activated kinase 1 and MAP3K7-binding protein

TAF: TBP-associated factor

TAILS: terminal amine isotopic labeling of substrates

TAK1: transforming growth factor beta-activated kinase 1

TANK: TRAF family member-associated NFκB activator

TBP: TATA box-binding protein

TBS-T: Tris-buffered saline-tween

TDP-43: transactive response DNA binding protein 43

TIA1: T-cell restricted intracellular antigen 1

TIAR: TIA-related protein

TLR: toll-like receptor

TRIF: toll/interleukin 1 receptor domain-containing adaptor inducing interferon beta

TF: transcription factor

USO1: general vesicular transport factor p115

UTR: untranslated region

VP1: viral structural protein 1

VPg: virus-encoded protein genome-linked

zVAD-FMK: z-valine-alanine-aspartate-fluoromethylketone

Acknowledgements

First and foremost, I would like to thank my senior supervisor Dr. Eric Jan for providing me with this opportunity to work on such a fascinating and challenging project. I would not have succeeded without his guidance and encouragement. I am also grateful for his support when perusing other learning opportunities outside of my research project. I extend this thank you to my committee members Dr. Honglin Luo, Dr. Leonard Foster, and Dr. Chris Overall. They have all made themselves available to me when I was in need of guidance and have always provided me with thoughtful advice.

I would especially like to thank Dr. Antoine Dufour for all the work and support he has contributed to this project, especially with the TAILS experiments. His french humour and knowledge in wine have also been quite helpful. I would also like to thank Dr. Theo Klein and Dr Gabriel Fung for the assistance they have provided me. To my fellow 'Jan-labbers' – Dr. Anthony Khong, Dr. Hilda Au, Craig Kerr, Dr. Qing Wang and Dr. Jennifer Bonderoff – thank you all for your guidance, criticism, conversations and coffee runs. You guys are an exceptional group of people to 'battle it out in the trenches' with. And thank you to the many undergrads that have contributed to this project.

Lastly, thank you to my family - especially my mom – for their unconditional love, support and patience. And to Jeremy – there are no words… except to say I owe you a long vacation ☺

Chapter 1: Introduction

1.1 Overview

Proteases play fundamental roles in cells by ultimately changing the fate and function of their substrates through proteolytic cleavage. Beyond protein degradation, proteases have now been established as key signalling molecules for many critical cellular functions, including cell death, cell-cell communication, the immune response, cellular localization and the cell cycle (1). Consequently, unregulated protease activity can play prominent roles in disease such as inflammation, cancer, and cardiovascular disease. Thus, the study of proteases has not only facilitated our understanding of fundamental cellular processes and has shed light into the pathological progression of several diseases, but may also help identify novel therapeutic targets.

Viruses have exploited strategies of protein hydrolysis by encoding proteases within their genome that are necessary for proteolytic processing of viral proteins and are thus essential for virus infection. The roles and function of viral proteases have been well studied in the positive-sense single-stranded RNA picornavirus family, which include many clinically and agriculturally relevant viruses such as the human hepatitis A (HAV), poliovirus, coxsackieviruses, and rhinoviruses (HRV), as well as foot and mouth disease (FMDV) and avian encephalomyelitis viruses that infect hoofed-livestock and chickens, respectively. Picornaviral genomes contain a single main open reading frame that is subsequently translated as a single polyprotein. The polyprotein must then be processed into individual viral proteins in order for the viral life cycle to proceed, which is the primary function of their virally-encoded proteinases. In addition, it is now well-established that picornaviral proteinases strategically target host proteins to modulate or inhibit cellular processes to facilitate viral replication and block host antiviral innate immune responses (Table 1.1 and 1.2). As shown with picornavirus proteinases, cleavage of host proteins

can impact a variety of cellular functions and influence many aspects of the viral life cycle, including viral translation and replication, to either promote or block the synthesis of new virions. As such, picornaviral proteinases are viable targets for antiviral therapy; however, little success has been achieved beyond clinical trials (2). An alternative approach may be to target the host proteins and/or pathways impacted by viral proteinases that are essential for virus infection. Thus, there is an unmet need to find new antiviral therapies for picornaviruses.

To date, there are approximately 45 host proteins that have been identified as substrates of picornavirus proteinases but the complete repertoire of host proteins targets remains unknown. Conventional approaches used to identify substrates of viral proteinases have included candidate approaches, bioinformatics, and two-dimensional gel electrophoresis coupled with mass spectrometry; however, these techniques have had their limitations (3-5). Terminal amine isotopic labeling of substrates (TAILS) is a recently developed gel-free strategy specifically designed for analysis of protease-generated peptides and has successfully identified novel substrates for matrix metalloproteases and dipeptidyl peptidases (6-8). The focus of this thesis was to establish TAILS as a method to identify novel substrates of viral proteases, using picornavirus proteinases as a model, to ultimately shed light into the complete proteolytic networks established by picornaviral proteinases during infection. Furthermore, uncovering the complete proteolytic network of picornaviral proteinases will provide further insights into the fundamental viral-host interactions that promote virus infection and the pathogenesis of picornaviral diseases.

Table 1.1 Known substrates of $2A^{pro}$, $3C^{pro}$, and L^{pro} picornavirus proteinases

Function	Protein Name	Gene Symbol	Virus	Proteinase	Cleavage Site
Translation	eukaryotic translation initiation factor 4G I	eIF4G I	PV, HRV, CVB3, FMDV	2A L	^{478}LSTR|GPPR^{485} ^{671}ANLG|RTTL^{677}
	eukaryotic translation initiation factor 4G II	eIF4G II		2A L	^{689}PGGR|GVPL^{696} ^{682}ADFG|RQTP^{689}
	polyadenylate-binding protein	PABP	PV	2A 3C	^{484}TQTM|GPRP^{491} ^{682}VHVQ|GQEP^{689} ^{689}AIPQ|TQNR^{696} ^{682}WTAQ|GARP^{689}
	eukaryotic translation initiation factor 5B	eIF5B	PV, HRV, CVB3	3C	^{475}VMEQ|GVPE^{482}
	death-associated protein 5	DAP5	CVB3	2A	^{430}MKSQ|GLSQ^{438}
Nuclear-Cytoplasmic Transport	nuclear pore complex protein 98	Nup98	PV, HRV	2A	^{370}LTTF|GSST^{377} ^{548}LQTT|GARP^{555}
	nuclear pore complex protein 153	Nup153	PV, HRV	2A	?
	nuclear pore complex protein 62	Nup62	PV, HRV	2A	^{99}LSNT|AATP^{106} ^{214}ITST|GPSL^{221} ^{243}VTTA|GAPT^{250} ^{294}LKPL|APAG^{301}
RNA Metabolism	polypyrimidine tract-binding protein 1/2/4	PTB 1/2/4	PV, EMCV, HRV, CVB3, HAV, FMDV, Aichivirus	3C	^{145}ARAQ|AALQ|AVNS^{156} ^{311}AIPQ|AAGL^{318}
	poly(rC)-binding protein 2	PCBP2	PV, CVB3, HRV	3C	^{250}ARQQ|SHFP^{257}
	heterogeneous nuclear ribonucleoprotein M	hnRNP M	PV, CVB3	3C	^{386}IAKQ|GGGG^{393}
	AUF-rich element RNA-binding protein	AUF1	CVB3, PV, HRV	3C	^{32}AATQ|GAAA^{39}
	La lupus autoantigen	La	PV, CVB3, EMCV, HAV	3C	^{355}VQFQ|GKKT^{362}
	Gemin 3	Gemin3	PV	2A	^{459}VHTY|GLSQ^{466}
	Gemin 5	Gemin5	FMDV	L	^{843}RKAR|SLLP^{850}
Transcription	TATA-binding protein	TBP	PV	2A 3C	^{15}ASPQ|GAMT^{22} ^{101}AVQQ|STSQ^{108}
	cAMP-responsive element binding protein	CREB	PV	3C	^{169}AITQ|GGAI^{176}
	octamer-binding transcription factor	Oct1	PV	3C	?
	transcription factor IIIC	TFIIIC	PV	3C	^{729}PVPQ|GEAE^{736}
	TATA-binding protein-associated factor 110	TAF110	PV	3C	^{262}IQLQ|GPVR^{269} ^{802}ACAQ|GVPS^{809}
Cytoskelaton	microtubule-associated protein 4	MAP4	PV, HRV	3C	?
	dystrophin	Dys	CVB3, CVB4	2A	^{802}LTTI|GASP^{809}
	cytokeratin 8	Cyt8	CVB4, HRV2	2A	^{12}VSTS|GPRA^{19}
Apoptosis	Ras GTPase-activating protein 1	RasGAP	CVB3	3C	?
	Grb2-associated binder 1	GAB1	CVB3	3C	^{172}ETLG|IQED^{179} ^{433}LTVG|SVSS^{440}

Table 1.2 Host antiviral substrates of $2A^{pro}$, $3C^{pro}$ and L^{pro} picornavirus proteinase

Function	Protein Name	Gene Symbol	Virus	Proteinase	Cleavage Site
Pathogen Recognition Receptors	retinoic acid induced gene I	RIG-I	PV, CVB3, HRV, EMCV, ECHO, EV71	3C	?
	melanoma differentiation associated protein 5	MDA-5	CVB3, EV71, PV	2A	?
	NLR family pyrin domain containing 3	NLRP3	EV71	3C, 2A	?
Innate Immune Response Signaling	TIR domain-containing adaptor inducing beta interferon	TRIF	CVB3, EV71, EV68	3C	^{187}DWSQ|GCSP^{194} ^{650}AFPQ|SLPF^{657} ^{656}PFPQ|SPAF^{663} ^{668}APPQ|SPGL^{675} ^{699}RGSQ|APED^{706}
	mitochondrial antiviral signaling protein	MAVS	CVB3, PV, EV71, HRV	3C	^{145}QETQ|APES^{152}
	NFkB essential modulator	NEMO	HAV, FMDV	3C	^{380}LPSQ|RRSP^{387}
	DNA-dependent protein kinase	DNA-PK	PV, CVB3	3C	?
	transcription factor p65	p65/RelA	PV, HRV, Echo, FMDV	3C, L	?
	interferon regulatory factor 7	IRF7	EV68, EV71	3C	^{164}AGLQ|APGP^{171} ^{186}AVQQ|SCLA^{193}
	inhibitor of kBa	IkBa	CVB3	3C	^{245}VTYQ|GYSP^{252}
	TRAF family member-associated NF-kappa-B activator	TANK	EMCV, FMDV	3C	^{288}FEIQ|GIDP^{295}
	TAK1/TAB1/TAB2/TAB3 complex	TAK1/TAB1-3	EV71	3C	^{110}GQLQ|GGQS^{117} ^{357}AKQQ|SCES^{364} ^{411}MPSQ|GQMV^{418} ^{448}THTQ|SSSS^{455} ^{170}SAMQ|GPSP^{177} ^{340}YQKQ|GSHS^{347}
	interferon alpha and beta receptor subunit 1	IFNAR	EV71	?	?
	complement C3	C3	PV, HRV	3C	?
Stress Granules	ras-GAP Sh3 domain-binding protein	G3BP1	PV, CVB3	3C	^{322}AGEQ|GDIE^{329}

1.2 Picornaviruses

1.2.1 Classification and genomic organization

The family *Picornaviridae* belongs to the order *Picornavirales* and is comprised of small positive, single-stranded RNA viruses that infect vertebrates. There are currently 54 species grouped into 31 genera.

Picornaviruses possess a compact RNA genome of approximately ~7.5 kb in length that contains a single open reading frame with a highly structured 5' untranslated region (UTR) and a 3' poly(A) tail (9-12). In place of a 5' cap, picornaviruses harbour a virus-encoded protein genome-linked (VPg) protein that functions in viral RNA replication. Translation of the open reading frame is directed by an internal ribosome entry site (IRES) located in the 5' UTR to generate a polyprotein that is subsequently processed into four structural proteins and seven or eight (depending on the genus) non-structural proteins by the virally-encoded proteinases (Figure 1.1). The structural proteins termed VP4, VP2, VP3 and VP1 adopt an icosahedral structure to form the viral capsid that is approximately 30 nm in diameter. Non-structural proteins include VPg (3B), a putative helicase (2C), proteinases ($3C^{pro}$, and $2A^{pro}$ or L^{pro} for some genres), and an RNA-dependent RNA polymerase ($3D^{pol}$) (13-18).

1.2.2 Picornaviral life cycle

The majority of picornaviruses gain entry into the host cell via endocytosis, with many requiring specific cell surface receptors to facilitate binding (Figure 1.2). For example, all poliovirus serotypes require the CD155 glycoprotein receptor for entry, whereas many human rhinovirus serotypes utilize intracellular adhesion molecule-1 (ICAM-1) (19, 20). While all coxsackieviruses recognize the coxsackievirus and adenovirus receptor (CAR) for entry, some

serotypes require a second receptor, decay-accelerator factor (DAF), to gain entry within tight junctions of polarized epithelial cells (21-23). Receptor-binding initiates capsid rearrangement to convert the infectious particle into the altered (A or 135S) form for release of the viral RNA into the cytoplasm (24-26). Upon release, the positive-sense RNA genome serves as a template for translation through the recruitment of ribosomes, minimal translation initiation factors, and IRES trans-acting factors (ITAFs) to the IRES (27, 28). The nascent polypeptide undergoes simultaneous processing by the virally-encoded proteinases (described in more detail below) to ultimately generate intermediate and mature forms of the viral proteins.

As infection progresses, cellular membranes undergo a dramatic rearrangement to alter or disrupt nuclear transport, releasing additional host proteins that support translation, and Golgi-body and endoplasmic reticulum membranes, for assembly of replication complexes that serve as anchoring point for viral RNA replication (29, 30). Viral proteins 2B and 2C have been shown to facilitate the formation of replication complexes through the disruption of Golgi-associated protein complexes (18, 31). RNA replication begins with negative-sense strand synthesis, whereby the positive-sense RNA genome becomes bound to the replication complexes via the viral proteins 3AB and serves as a template for replication. VPg undergoes 3CD and 3D-mediated uridylylation at a cis-acting CRE element, an RNA stem loop structure located internally within the genome, creating a VPg-linked polyU tail that is then transferred to the 3' end of the genome and serves as a primer for the RNA-dependent RNA polymerase (32, 33). Newly synthesized negative-sense strand RNA then serves as a template for more synthesis of positive-sense strand RNA, which is then packaged into pre-assembled capsid particles. Virus release occurs primarily by cell lysis; however, more recent studies have uncovered mechanism

of non-lytic spreading via exosomes or through hijacking of autophagy pathways that release a portion of new virions (34, 35).

Given the limited number of proteins expressed from their genomes, picornaviruses must rely on modulating a series of cellular processes to facilitate successful virus infection. Disruption of cellular pathways, modulation of cellular processes, hijacking or inhibition of host protein functions, and cell death are examples of cellular phenotypes observed as a consequence of successful picornavirus infection, which are ultimately orchestrated by a limited number of viral proteins, including the picornaviral proteinases. Examples of how picornavirus proteinase function supports virus infection are described in more detail below.

Many picornavirus infections are associated with disease in both humans and animals, and can contribute to their pathogenesis. Poliovirus through the fecal-oral route and primarily targets epithelial cells within the small intestines; however, infection can progress to the central nervous system (36). Upon gaining access to the central nervous system, poliovirus targets and subsequently destroys motor neuron, causing temporary or permanent paralysis, or poliomyelitis. While the development of a vaccine in the 1950s has significantly reduced the prevalence of infection, poliovirus still persists within certain areas of the world due to poor vaccination coverage. Similarly, FMDV infection remains prevalent among cloven-hoofed livestock in spite of the development of vaccines that protect against few serotypes, bearing significant economic loss to livestock (37). Coxsackievirus, classified within the enterovirus genus with poliovirus, is the most common cause of acute myocarditis in humans, causing inflammation and necrosis of cardiomyocytes (38). This can lead to the development of dilated cardiomyopathy, which accounts for ~20% of heart failure and sudden death in children and youth. There are currently no vaccines available for preventing coxsackievirus infections, or therapeutics for treatment of

dilated cardiomyopathy. Thus, there is still an unmet need for therapeutics for the treatment of picornavirus infections.

1.3 Picornavirus proteinases

Synthesis of a single polyprotein from picornaviral genomic RNA and the post-translational modifications utilized to derive the individual mature viral proteins were first described in the late 1960s (39, 40). The absolute requirement for extracts from infected lysates resulting in *in vitro* cleavage of the viral polyprotein led to the identification of the viral protein gamma, later defined as the 3C proteinase ($3C^{pro}$) (13). $3C^{pro}$ is a conserved proteinase amongst all known picornaviruses, and the primary proteinase responsible for most of the viral polyprotein processing events. A second proteinase, $2A^{pro}$, was later revealed among the enterovirus and rhinovirus genera of picornaviruses following the identification of a cleavage site within the polyprotein that was not targeted by $3C^{pro}$ (41). A third proteinase, L^{pro}, unique among the aphthovirus and erbovirus genera of picornaviruses has also been identified that bears no resemblance to either $2A^{pro}$ or $3C^{pro}$ (14). Within these viruses, the 2A protein does not possess proteolytic activity but instead uses a ‘stop-go’ translation mechanism that results in distinct proteins.

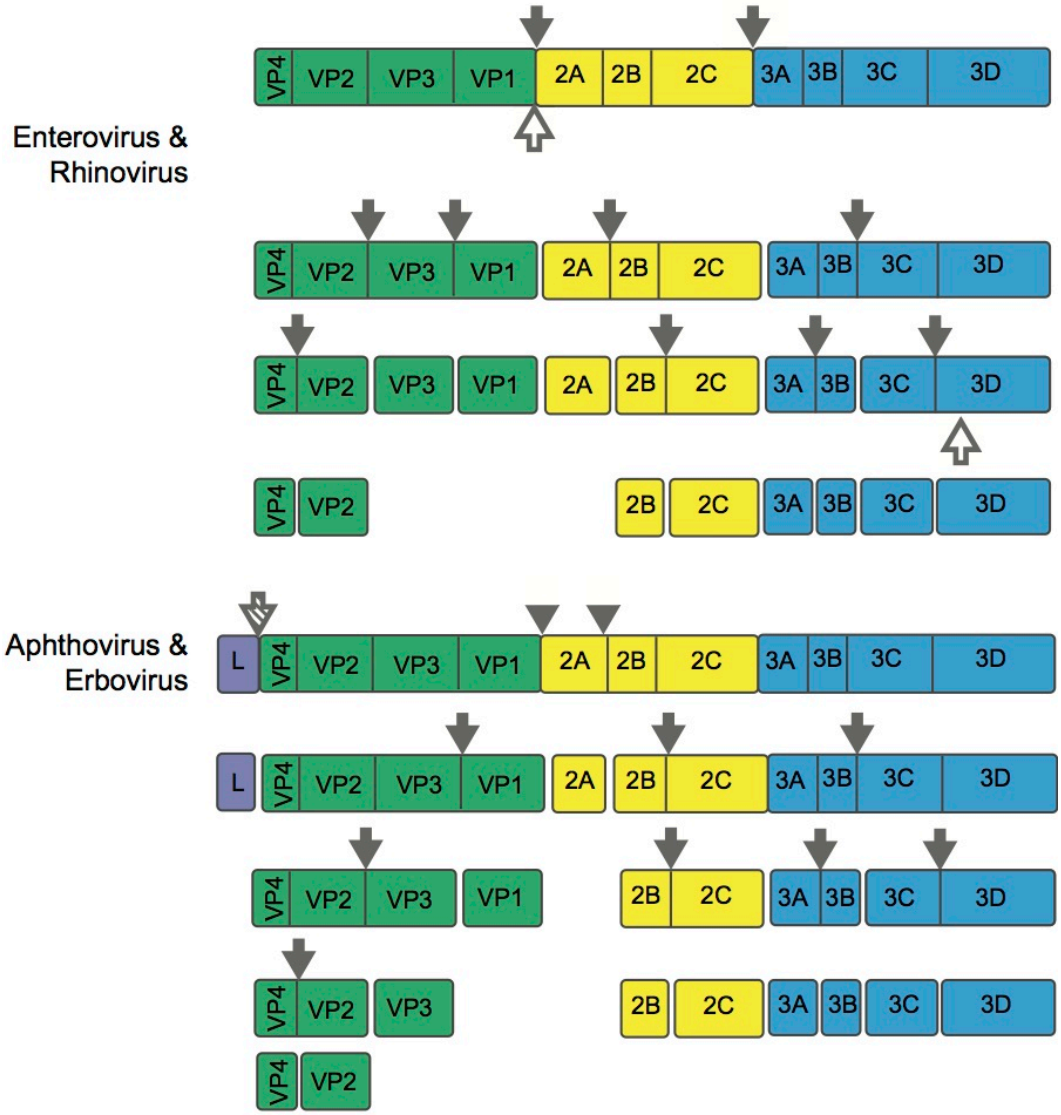

Figure 1.1 Proteolytic processing of picornavirus polyproteins. All picornaviruses translate their RNA genomes as a single polyprotein, which is subsequently processed into mature viral proteins by virally-encoded proteinases. $3C^{pro}$ mediates the majority of cleavages across all picornaviruses. Enteroviruses and rhinoviruses encode $2A^{pro}$ that targets a single cleavage site in *cis* directly upstream at its N-terminus. An alternative cleavage site carried out by $2A^{pro}$ between $3C^{pro}$ and $3D^{pol}$ has been identified in vitro; however, the biological significance of this cleavage site is unknown. Aphthoviruses and erboviruses also posses a second proteinase, L^{pro}, encoded by an additional gene located at the 5' end of its open reading frame. L^{pro} cleaves at a single site directly downstream of its C-terminus, releasing itself from the polyprotein. Within these viruses, the 2A protein does not contain proteolytic activity but instead uses a 'stop-go' translation mechanism that results in distinct proteins

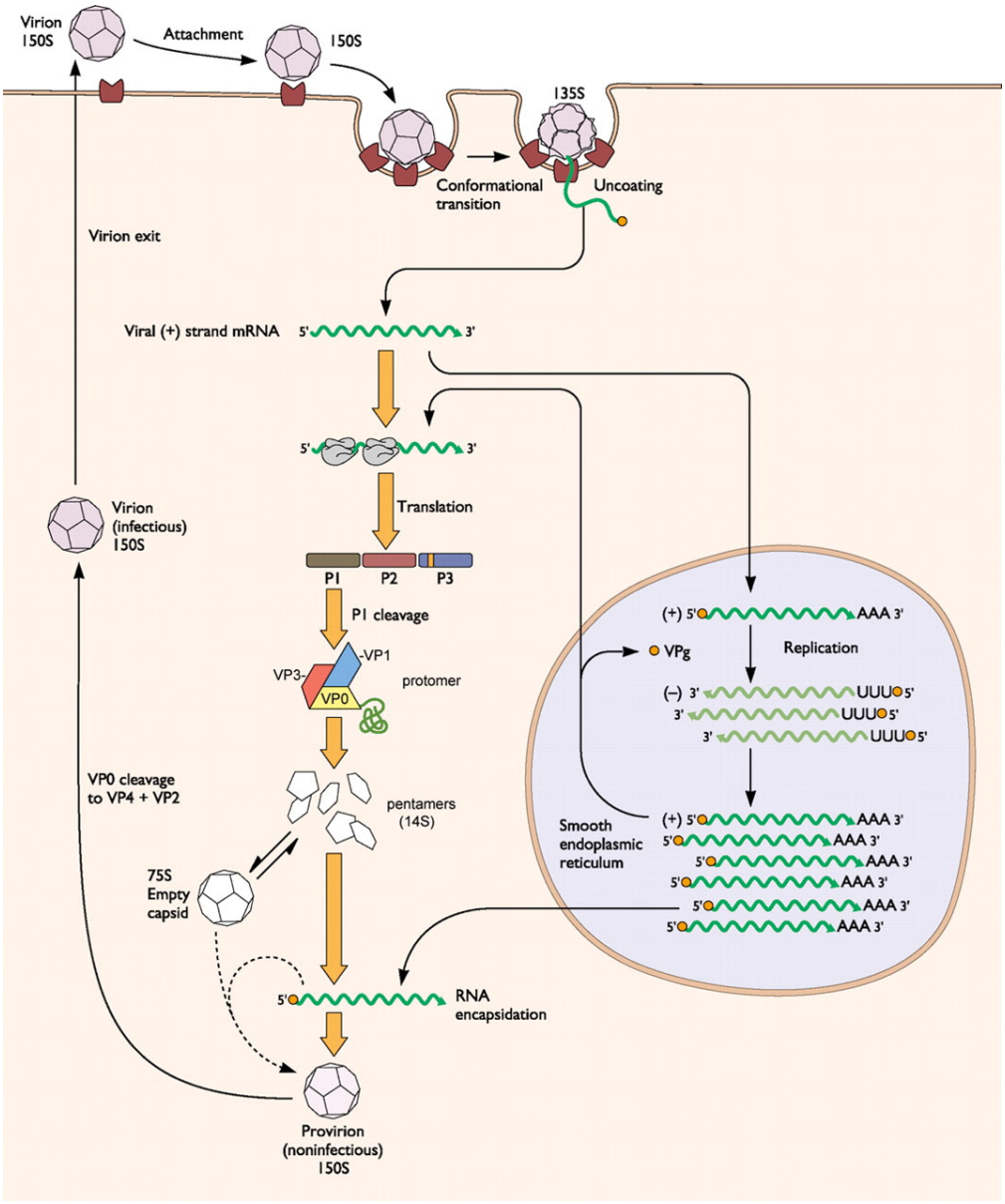

Figure 1.2 Overview of the picornavirus life cycle. The life cycle of poliovirus is illustrated above as a model for picornavirus infection. Infection begins by receptor-mediated endocytosis and viral RNA uncoating. Viral translation occurs in the cytoplasm, producing a polyprotein that is processed into mature viral proteins. Replication of the negative-sense strand proceeds at sites of replication complexes, which is then utilized as templates for positive-sense strand synthesis. New genomic RNA is packaged into preassembled procapsids, which are then released primarily by cell lysis. Adapted from Hogle (2002) (42).

1.3.1 Structure and biochemical properties

Sequence comparison and structural analysis of all three picornaviral proteinases have provided insights into their mechanism of action. Both $3C^{pro}$ and $2A^{pro}$ are most structurally similar to chymotrypsin proteases, comprising of two anti-parallel β-barrels linked together via a flexible loop (Figure 1.3) (43-48). Mutational analysis identified its catalytic core as a triad comprised of His-Cys-Glu/Asp located within the two β-barrels, with a cysteine nucleophile rather than a typical serine nucleophile utilized in chymotrypsin (49-57). Amino acids outside of the catalytic core of each proteinase have been reported to facilitate proteolytic activity in *cis* or *trans* (51, 55-57). During infection, $3C^{pro}$ is capable of performing its proteolytic function as itself or in its precursor form as $3CD^{pro}$, a fusion protein comprised of the $3C^{pro}$ and the 3D RNA-dependent RNA polymerase ($3D^{pol}$), which possesses proteinase activity but its polymerase is inactive (58). While mutational analyses and kinetic experiments have indicated that $3C^{pro}$ in its precursor form as $3CD^{pro}$ is the more efficient proteinase, the $3CD^{pro}$ crystal structure has provided little insight into the underlying mechanism as the proteinase retains a similar conformation (59-61). Although $3CD^{pro}$ is the predominant proteinase for viral polyprotein processing, it is likely that both $3C^{pro}$ and $3CD^{pro}$ contribute to the viral life cycle (59). In contrast to $3C^{pro}$ and $2A^{pro}$, the structure of L^{pro} is most comparable to that of the cysteine protease papain, and carries a cysteine nucleophile (62-65). The FMDV L^{pro} contains an α-helical domain juxtaposed to a β-sheet, with a Cys-His catalytic diad arranged in between the two domains (66, 67).

1.3.2 Substrate specificity

Activity and substrate specificity of the picornaviral proteinases were initially studied by elucidating the proteolytic processing events of the viral polyprotein to generate the individual mature viral proteins. All three proteinases participate in at least one cleavage event that occurs in *cis* immediately following translation of the polyprotein (14, 41, 68, 69). Primary cleavage events for all picornavirus include $3C^{pro}$ cleavage between the 2C and 3A junction, while $2A^{pro}$ targets its only cleavage site within the enterovirus and rhinovirus polyproteins at its N-terminus to generate the P1, P2 and P2 precursors. An alternative cleavage site carried out by $2A^{pro}$ between $3C^{pro}$ and $3D^{pol}$ has been identified *in vitro*, generating the alternative cleavage products designated 3C' and 3D', however the biological significance of this alternate cleavage site is still unknown (41). L^{pro} of aphthoviruses also possesses a single cleavage site within their polyprotein located directly downstream of its C-terminus, releasing itself from the P1 precursor. The remaining secondary and tertiary cleavage events to generate the 11 or 12 individual mature viral proteins occur in *trans* by $3CD^{pro}$. Since $3CD^{pro}$ is more efficient in processing the polyprotein than $3C^{pro}$, this may ensure rapid cleavage of its own proteins early in infection (59). Adoption of secondary and tertiary structures within the polyprotein is also required for efficient cleavage, providing additional means of regulating polyprotein cleavage (70).

Proteases identified among picornaviruses are termed endo-proteolytic peptidases, or proteinases, as they recognize and cleave at defined sites located internally within their substrates. Cleavage site analysis within the picornavirus polyprotein revealed a high level of substrate specificity as $3C^{pro}$ cleaves exclusively between Q and G at the P1 and P1' positions, respectively, at each of its 11 cleavage sites. The nomenclature of the residues surrounding the cleavage site is represented as P4-P3-P2-P1|P1'-P2'-P3'-P4', where the "|" denotes the scissile

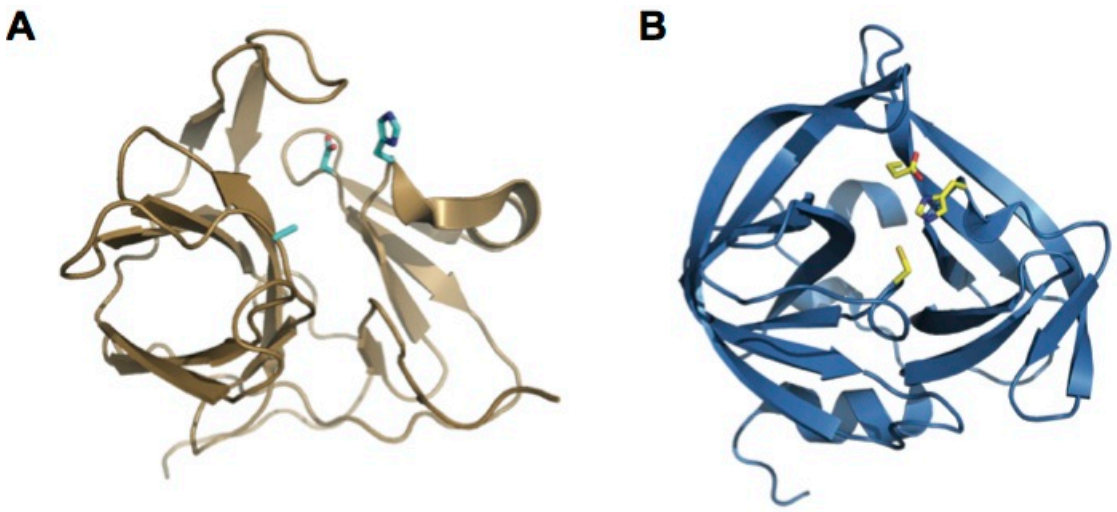

Figure 1.3 Structure of Picornavirus $3C^{pro}$ and $2A^{pro}$ Proteinases. Structures showing the two β-barrel domains and overall fold of the poliovirus $3C^{pro}$ (A) and CVB4 $2A^{pro}$ (B) proteinases. The catalytic residues of poliovirus (His 40, Glu 71, and Cys 147) and CVB4 $2A^{pro}$ (His 21, Asp 38, and Cys 110) are located in between the two β-barrel domains are indicated as balls and sticks. Structures are adapted from Mosimann, SC et al. (1997) and Baxter, NJ et al. (2006).

cleavage site. Extensive analysis of peptide substrates that have permutated amino acids within the cleavage sites has demonstrated that $3C^{pro}$ can accommodate other small amino acids, such as alanine or serine, at the P1' position (71, 72). This is attributed to its shallow binding pocket within the catalytic core, which can accommodate a more limited number of amino acids (47, 73). Additional amino acids outside the P1-P1' positions also contribute to substrate specificity, including alanine at the P4 position and proline at the P2' position, generated a preferred cleavage consensus motif of A-X-X-Q|G/A/S-P-X-X (5). In contrast, the active site of $2A^{pro}$ can accommodate a broader range of amino acids in the P1 position and thus has a more flexible cleavage consensus motif of I/L-X-T/S-Z|G-P-X-X, where z is a hydrophobic residue (5). Within the polyprotein, the P1 position is occupied by a tyrosine, however mutational analysis of peptide substrates has demonstrated equal proteolysis efficiency when substituted with alanine, threonine or valine.

Cleavage activity of L^{pro} has been the least well-characterized among the three proteinases. L^{pro} is responsible for a single cleavage event within the polyprotein and only a limited number of host substrates have thus far been identified. Initial investigations into its proteolytic activity suggest that the L^{pro} displays an unusually high degree of substrate specificity that extends through positions P7 to P5' (74, 75). Moreover, mutational analysis of the polyprotein cleavage site shows a preference for a basic residue at either the P1 or P1' position provided that the other amino acid next to the scissile bond is a G or S, as well as a requirement for L, A, or V at the P2 position (76).

In summary, much information on the specificity of picornaviral proteinase substrates has been gleaned from *in vitro* analysis of peptide sequences derived from known cleavage sites within the polyprotein. Whether the *in vitro*-derived consensus cleavage site is conserved *in vivo*,

and whether it is retained among host proteins targeted for cleavage, remains to be fully elucidated. Analysis of identified cleavage sites of known host proteins targeted by $2A^{pro}$ or $3C^{pro}$ suggests that a similar consensus cleavage site is preferred (Figure 1.4). Similar to the polyprotein consensus sequence, $3C^{pro}$ demonstrates strong preference for glutamine at the P1 position, as well as a high frequency of alanine and glycine at the P4 and P1', respectively. Likewise, glycine residues are highly preferred at the P1' position among $2A^{pro}$ host substrates, as well as a high frequency of threonine residues position at the P3, P2, and P1 positions. Identification of additional host targets and characterization of their cleavage sites would provide further insights into the true breadth of their substrate specificities, which my thesis aims to address.

1.4 Host substrates of picornaviral proteinases

Productive infection of picornaviruses depends on the permissive state of its host cell. Throughout its entire life cycle, the virus must rely on a series of cellular rearrangements to facilitate its translation and replication. The picornaviral proteinases play integral roles in infection by targeting host proteins to either directly or indirectly facilitate different steps of the viral life cycle. Much has been learned from identifying the host substrates that are cleaved by viral proteinases, including the cellular pathways and processes that are affected, and the adoption of secondary roles of cleavage products. Described below are examples of known host substrates and how their cleavage activity contributes to their role in virus infection.

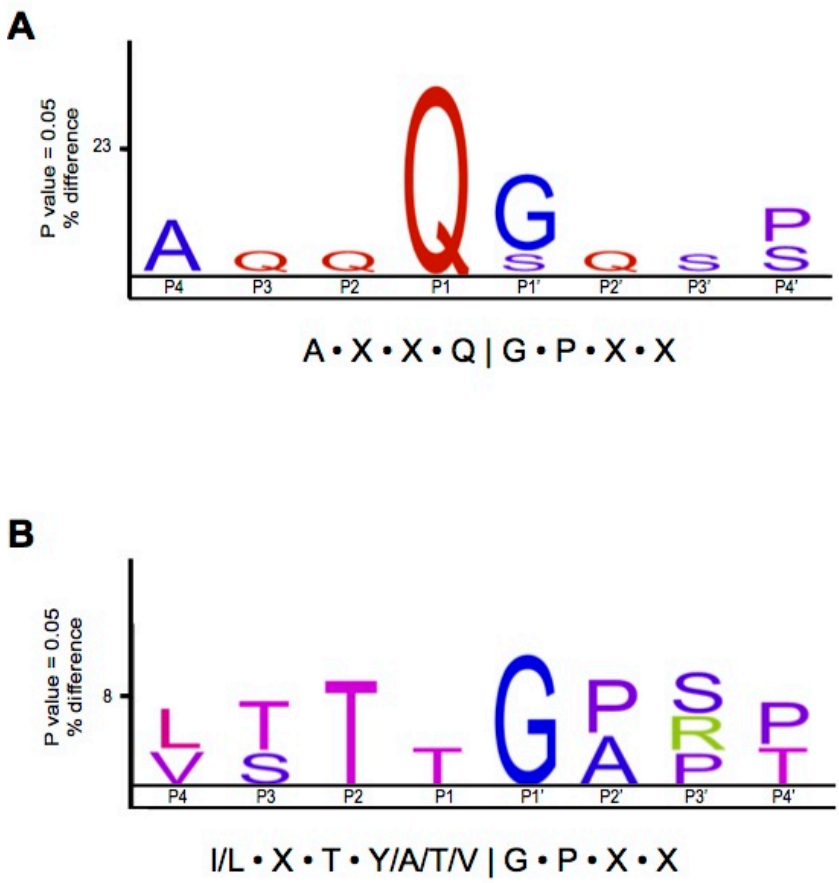

Figure 1.4 Comparison of consensus cleavage sequences derived from viral polyprotein processing sites and cleavage sites of known host substrates of 3C^{pro} and 2A^{pro}. IceLogos were derived from the P4-P4' amino acids sequences all known cleavage sites of host targets of 3C^{pro} (A) and 2A^{pro} (B), and the consensus sequence derived from known polyprotein cleavage sites is depicted below, where X denotes any amino acid. Amino acids are scored as percent differences that compares the frequency of an amino acid at a certain location between experimental and reference sets.

1.4.1 Host translation shutoff

A prominent characteristic of picornaviral infection is the rapid and near complete shutoff of host protein synthesis, concomitant with preferential viral translation and replication (77-80). Shutoff of host translation promotes viral translation by effectively inhibiting host antiviral responses and freeing the cellular pool of ribosomes for viral translation (81, 82). The viral proteinases contribute significantly to these effects; over-expression of either $2A^{pro}$ or $3C^{pro}$ in cells is sufficient to inhibit global cap-dependent translation (83-86). One of the best-characterized host substrates that participate in these events is the eukaryotic initiation factor 4G (eIF4G), which is a direct substrate of $2A^{pro}$ and is cleaved during poliovirus, CVB3, and HRV2 infection. eIF4G is a key factor in cap-dependent translation by acting as a scaffold for recruiting the core eIFs, including the cap-binding protein eIF4E, eIF3, eIF4A and the poly(A) binding protein (PABP), to the 5' cap of the mRNA (87-90). Cleavage by $2A^{pro}$ bisects eIF4G resulting in separation of the cap-binding protein and the ribosome recruitment domains, thus inhibiting ribosome recruitment and *de novo* protein synthesis. Mutant eIF4G that is cleavage-resistant is more resilient to $2A^{pro}$-mediated inhibition of cap-dependent translation, strongly suggesting that cleavage of eIF4G by $2A^{pro}$ plays a significant role in host protein translation shutoff in virus-infected cells (91). Although cleavages of both isoforms of eIF4G, I and II, are detected in infected cells, eIF4GII cleavage by $2A^{pro}$ coincides more closely with host translation shutoff (92, 93). In support of eIF4GII as the key substrate, treatment of virus-infected cells with inhibitors of virus replication decreases cleavage of eIF4GII but not eIF4GI. A recent report demonstrated that death-associated protein 5 (DAP5), a structural homolog of eIF4GI, is also cleaved by $2A^{pro}$ and contributes to both viral IRES translation and replication (94). Finally,

eIF4GI is also a direct substrate of L^{pro} during FMDV infection, indicating that targeting this step of cap-dependent translation by viral proteinases is a general strategy of picornaviruses (95, 96).

$3C^{pro}$, which does not target eIF4GI or II, also contributes to host translation shutoff during picornavirus infection. Key translation factors, PABP and eIF5B, are direct substrates of $3C^{pro}$, and are cleaved during poliovirus and CVB3 infection (85, 97-99). $3C^{pro}$ preferentially targets PABP associated with actively translating mRNAs, thus disrupting PABP-eIF4G interactions and the PABP oligomerization on poly(A) tails that promotes the circularization of mRNA for translation (97). Thus, cleavage of PABP allows the virus to target translating mRNAs in addition to inhibiting *de novo* translation through cleavage of eIF4G. Although eIF5B, which plays a role in 80S assembly, is cleaved by several enterovirus $3C^{pro}$, the significance of this cleavage in infected cells remains to be investigated. The targeting of translation factors also contributes to other aspects of the picornavirus life cycle. In EMCV-infected cells, PABP cleavage by $3C^{pro}$ does not affect viral protein synthesis, but instead contributes to viral replication (100). In summary, picornaviral proteinases mediate multiple cleavage events of translation factors to ensure sufficient host translation shutoff during infection.

1.4.2 Nuclear-cytoplasmic transport

Another common feature among many picornaviral infections is the remodeling of the nuclear pore complex (NPC), and consequent nuclear-cytoplasmic redistribution of proteins during infection (29, 101, 102). Inhibition of nuclear-cytoplasmic transport during virus infection not only prevents nuclear proteins from carrying out their endogenous functions within the nucleus, effectively impacting a number of cellular processes such as transcription and mRNA

metabolism, but also inactivates key antiviral response pathways such as NFκB signalling and Toll-like receptor signalling (103-106). Furthermore, although occurring exclusively within the cytoplasm, picornavirus replication and translation are promoted by a subset of nuclear factors that are redistributed to the cytoplasm during infection, allowing the virus to gain access to these key nuclear proteins (29, 107-113). These effects are primarily a consequence of alterations to the nuclear pore complex, a macromolecular structure embedded within the nuclear membrane and comprised of multiple copies of 30 distinct proteins called nucleoporins (Nups). Normally, proteins containing nuclear localization signals (NLS) are imported from the cytoplasm to the nucleus by interacting with importins that carry the proteins through the NPC using a Ran GDP-GTP cycle. Smaller molecules are also capable of transporting passively through minor channels of the NPC. Several NPC proteins are targeted by enterovirus proteinases. Nup98, Nup153 and Nup62 are cleaved by $2A^{pro}$ during poliovirus and rhinovirus infections, resulting in the block of nuclear import and subsequent accumulation of several nuclear proteins in the cytoplasm (114-117). Moreover, cleavage of Nups coincides with a block in export of mRNAs, rRNAs and U snRNAs from the nucleus to the cytoplasm (118). Interestingly, cleavage of these Nups occurs sequentially as cleavage of Nup98 take place early in poliovirus infection (1 hour post infection (h.p.i.)) whereas Nup153 and Nup62 are cleaved late (3-4 h.p.i.) (117). Late cleavage of Nup153 and Nup62 corresponds with the sequestration of nuclear-bound proteins, such as factors for transcription and mRNA splicing, and is dependent on viral replication. Conversely, cleavage of Nup98 is unaffected in the presence of viral replication inhibitors (117). Treatment of HeLa cells with interferon γ (IFNγ) rescues expression of Nup98 in cells expressing $2A^{pro}$, and more recently Nup98 has been shown to be involved in promoting transcription of antiviral genes (119). Thus, cleavage of Nup98 may occur earlier in poliovirus infection to contribute to

blocking host antiviral responses while cleavage of Nup153 and Nup62 primarily serves to relocalize host proteins that facilitate viral replication and/or translation, in addition to contributing to host transcription and translation inhibition. Taken together, modulating nuclear import via cleavage of nuclear pore proteins by proteinases impacts several cellular processes that facilitate viral synthesis and blocking host antiviral responses. Interestingly, the L protein of cardioviruses modifies the phosphorylation status of Nups and blocks function of RNA, thus cleavage of Nups is not common among all Picornaviruses (120-122).

1.4.3 RNA metabolism

A general theme from inhibiting nuclear-cytoplasmic import during infection is that several nuclear-resident RNA binding proteins are relocalized to the cytoplasm and are thus unable to carry out their normal functions in mRNA processing. It is now clear that these RNA-binding proteins have alternate functions that indirectly or directly impact viral translation and replication. Several members of the heterogeneous nuclear ribonucleoprotein (hnRNP) family of RNA binding proteins that normally shuttle between the nucleus and the cytoplasm, and whose primary functions involve many aspects of RNA metabolism, redistribute from the nucleus to the cytoplasm during picornavirus infections. The poly(rC) binding protein 2 (PCBP2, also known as hnRNP E2) was among the first identified, mislocalized hnRNP protein through its association with the poliovirus 5'UTR, and later established as a substrate for poliovirus, CVB3 and HRV16 $3C^{pro}$ (110, 123-125). Early in infection, full-length PCBP2 relocalizes from the nucleus to the cytoplasm, where it binds to distinct regions within stem loop IV of the 5'UTR of the viral RNA via its N-terminal RNA-binding domain to assist translation. As infection progresses, $3C^{pro}$ targets PCBP2 on translating viral RNAs to remove its N-terminal binding domain from stem

loop IV and inhibit its translation stimulatory effects, serving as a means to facilitate the switch from translation of viral RNA to its replication for viral packaging. Interestingly, upon removal of the N-terminus, the N-terminal cleavage product gains a secondary function whereby it binds to stem loop I of the 5'UTR to promote negative-sense strand synthesis (125, 126). Thus, the virus has adapted proteolytic strategies to usurp PCBP2 function for roles in both translation and replication on the same viral RNA by facilitating a switch from viral translation to replication.

Another hnRNP targeted by $3C^{pro}$ is the polypyrimidine tract binding protein (PTB, also called hnRNP I), which has been implicated in IRES translation for several picornaviruses (15, 127, 128). Like PCBP2, full-length PTB becomes relocalized during infection and binds to the 5'UTR to promote IRES translation, and is reported to promote ribosome pre-initiation complex formation and enhance viral RNA stability (129-131). Cleavage of PTB by $3C^{pro}$ results in PTB fragments that are no longer able to stimulate IRES translation (107). Thus, like the dual role of PCBP2, loss of PTB function upon cleavage contributes to the switch from viral translation to replication.

Not all hnRNPs characterized during picornavirus infection have facilitative roles. AUF-rich element RNA-binding protein (AUF1 or hnRNP D) binds to AU-rich elements (ARE) located in the 3'UTR of mRNAs targeted for decay but is also capable of interacting directly with the poliovirus IRES to inhibit viral translation (108, 132, 133). ARE-containing mRNAs include oncogenes and cytokines that play a critical role in the stability of mRNA during the inflammatory response (134, 135). During poliovirus, CVB3, and HRV infections, AUF1 redistributes from the nucleus to the cytoplasm and binds directly to stem loop IV of the 5'UTR to inhibit viral translation. Viruses have adapted to circumvent these antiviral effects by targeting AUF1 for cleavage by $3C^{pro}$, reducing its affinity for the 5'UTR. Interestingly, AUF1 has no

effect on EMCV infection, thus AUF1 does not serve a broad-spectrum defense mechanism against all picornaviruses (109).

Other RNA binding proteins that do not belong to the hnRNP family also have roles during infection. The La Lupus autoantigen (La) is a nuclear localized protein that protects RNA pol III transcripts from degradation by binding to it's 3' end. Like other nuclear RNA-binding proteins, La relocalizes from the nucleus to the cytoplasm early in infection and is cleaved (136). However, unlike other RNA-binding proteins that are cleaved in the cytoplasm upon relocalization, La is cleaved by $3CD^{pro}$ in the nucleus, resulting in separation of its nuclear-localization signal domain, thereby allowing La relocalization into the cytoplasm. $3CD^{pro}$ has been observed in the nucleus early during poliovirus and EMCV infection, which likely contributes to cleavage of nuclear proteins prior to complete Nup cleavage (137). La facilitate poliovirus and coxsackievirus infection as depletion of La decreases viral infectivity and IRES translation (138). La acts as a dimer in complex with other nuclear RNA binding proteins such as PTB to bind to viral 5'UTRs, possibly to promote formation of 40S and 80S ribosome complexes (139, 140). Over-expression of the La C-terminal cleavage fragment inhibits poliovirus IRES translation, suggesting a possible dominant negative function upon cleavage to further support the switch from translation to replication.

As noted earlier, cytoplasmic relocalization of RNA-binding proteins prevents many from carrying out their normal functions in mRNA processing within the nucleus. Over-expression of $2A^{pro}$ promotes aberrant exon splicing events; however, it remains unclear which targeted host substrates directly impact this process (141). Gemin3, a core component of the survival or motor neuron (SMN) complex that functions in assembly of U small nuclear ribonucleoprotein (snRNP) spliceosome complexes, is targeted by $2A^{pro}$ during poliovirus infection (142).

Cleavage of Gemin3 may contribute to the observed decrease in snRNP complex biogenesis during poliovirus infection, and in turn may deregulate splicing by blocking spliceosome complex assembly. Defects in assembly of U snRNP spliceosome complexes are characteristic of neurodegenerative disorders and may also provide a clue into the degeneration of motor neurons observed during poliomelytis. Gemin5, another core component of the SMN complex, is cleaved during FMDV infection by L^{pro} (63, 143). Cleavage of Gemin5 may not only contribute to inhibition of mRNA processing during infection as it has been reported that Gemin5 binds to and modulates FMDV IRES translation. PTB, which normally has a role in alternative splicing events, is relocalized to the cytoplasm during picornavirus infections and upon expression of $2A^{pro}$, which effectively may further facilitate deregulation of splicing.

1.4.4 Host transcription shutoff

Several picornaviruses inhibit cellular transcription that indirectly contributes to host translation shutoff and inhibition of innate immune responses (144). Transcription mediated through all three RNA polymerase (RNA Pol I/II/III) complexes is inhibited during infection; however, the RNA polymerases isolated from infected extracts are still functional, indicating that transcription factors specifically are targeted during infection. Several key proteins within core transcription complexes are cleaved by $3CD^{pro}$, which has been shown to enter the nucleus via a nuclear localization signal in $3D^{pol}$ (137, 145, 146). TATA-binding protein (TBP), which is a part of the transcription factor II D (TFIID) complex, is cleaved by $3CD^{pro}$, leading to inhibition of basal transcription (147-150). Expression of a cleavage-resistant TBP in infected cells results in a small-plaque phenotype, indicative of a less efficient viral life cycle (151).

Not all transcription factor complexes require TBP, or an intact TATA box sequence, for RNA Pol II transcription, including transcription factor complexes that target interferon-stimulated genes (ISG) (152). Not surprisingly, additional factors involved in RNA Pol II transcription are targeted by picornavirus proteinases, including the cAMP-responsive element-binding protein (CREB), which is stimulated by cyclic AMP, and Oct-1, a member of the POU domain transcription factor family (153, 154). $3C^{pro}$ cleaves both transcription factors to inactivate transcription of downstream genes. For example, CREB is a transcriptional regulator of several immune-related genes, thus cleavage of CREB to inactivate its transcriptional activity may directly contribute to blocking antiviral responses (155). Cleavage of Oct-1 blocks the transcription of several small nuclear RNA, histone and immunoglobulin genes as well as stress response pathways that may impact virus infection (156, 157). Thus, cleavage of transcription factors by viruses may be a strategy for inhibiting specific cellular pathways.

Picornaviral proteinases also target RNA Pol I and III transcription complexes directly. TFIIIC is a multi-subunit transcription factor that initiates transcription of tRNA genes by recruiting additional transcription factors and RNA Pol III. During infection, poliovirus $3C^{pro}$ cleaves the α and β subunits of TFIIIC, resulting in disassembly of the RNA Pol III transcription complex (158). Similarly, inhibition of RNA Pol I-mediate transcription is partially attributed to cleavage of TBP-associated factor 110 (TAF110), a component of the selective factor 1 (SL-1) complex required for RNA Pol I-mediated transcription.

In summary, picornaviruses have adapted several mechanisms utilizing proteolytic cleavage to mediate global and specific inhibition of transcription, thereby ensuring that cellular signalling and antiviral pathways are disarmed and to indirectly affect RNA metabolism that contributes to host translation shutoff.

1.4.5 Cytoskeletal proteins

Cytoskeletal proteins play an integral role in picornavirus infection by interacting with viral replication complexes to facilitate viral release. Many picornavirus infections exhibit cytopathic effects, including cell rounding and increased permeability of the plasma membrane, all of which are attributed to alterations of cytoskeletal proteins. $3C^{pro}$ contributes to the modulation of cytoskeletal proteins by cleaving microtubule associated protein 4 (MAP4), a microtubule binding protein that promotes microtubule assembly (159, 160). MAP4 is cleaved late in poliovirus and HRV14 infected cells, contributing to the collapse of the tubulin network and an increase in cell lysis to enhance viral release. Collapse of microtubules is also observed in FMDV-infected cells, along with Golgi fragmentation, and is dependent on its $3C^{pro}$ activity; however, the mechanism underlying this remains to be investigated (161, 162).

Transgenic mice with inducible, cardiac-specific expression of CVB3 $2A^{pro}$ develop severe dilated cardiomyopathy (DCM), a disease phenotype of CVB3-infected cardiomyocytes. Although the pathological mechanisms leading to disease are poorly understood, one contributing factor is $2A^{pro}$-mediated proteolytic cleavage of dystrophin (163-165). Dystrophin connects the cytoskeletal actin to the β-dystroglycan extracellular matrix; thus, its cleavage leads to the disruption of the cytoskeletal architecture and myocyte membrane integrity (163). Cleavage of dystrophin facilitates viral replication due to more efficient viral release. Generation of a knock-in cleavage resistant dystrophin showed decreased symptoms of cardiomyopathy and reduced viral titre, suggesting that cleavage of dystrophin is significant for clinical progression of the disease (166). However, a direct causal relationship has not been established and *dystrophin*$^{-/-}$ mice have a mild DCM phenotype attributed to the compensatory upregulation of the dystrophin

homologue, utrophin (167, 168). Since utrophin is not cleaved during CVB3 infection, dystrophin-cleavage alone is insufficient to explain the severe DCM phenotype observed in $2A^{pro}$-expressing transgenic mice. Cytokeratin 8, an intermediate filament protein, has also been identified as a substrate for CVB4 and HRV2 $2A^{pro}$ (4). Cleavage occurs near its N-terminus that is required for the polymerization of cytokeratin filaments; thus, like dystrophin, cleavage of cytokeratin 8 may contribute to disruptions in the cytoskeletal architecture. More recently, dysferlin, a plasma membrane protein involved in skeletal and cardiac muscle repair, has been identified as a $2A^{pro}$- and $3C^{pro}$-mediated substrate cleaved targeted during CVB3 infection (169). *Dysferlin-/-* mice displayed enhanced cardiac membrane lesions and increased viral production, demonstrating that dysferlin cleavage promotes the pathogenesis of CVB3-induced cardiomyopathy. The precise contribution of $2A^{pro}$-mediated cleavage of host substrates, including dysferlin, towards CVB3 infection-associated disease pathogenesis has yet to be fully characterized.

1.4.6 Apoptosis

Activation of apoptosis is a characteristic of certain picornavirus infections (170-172). Viruses may modulate apoptosis in infected cells to enhance cell lysis and viral spread. Furthermore, apoptosis is responsible for many of the pathological consequences of picornaviral infection such as dilated cardiomyopathy caused by cell death of cardiomyocytes and the poliovirus-induced cell death of neuronal cells that leads to poliomyelitis (173, 174). Over-expression of picornavirus $3C^{pro}$ and $2A^{pro}$ can lead to hallmarks of apoptosis, including activation of caspases and the mitochondrial release of cytochrome C, whereas expression of a catalytically inactive proteinase does not, demonstrating that viral proteolytic activity is required

for apoptosis activation (175). Viral proteinases may mediate this regulation by targeting effectors of extracellular signal-regulated kinases 1/2 (ERK1/2) signalling (176). Under normal physiological conditions, Grb2-associated-binding protein 1 (GAB1) mediates activation of ERK1/2, which occurs in response to many stimuli, including growth factors, cytokines and hormones, and leads to its phosphorylation and recruitment of adaptor proteins SOS and Grb2. This in turn mediates further interactions with a wide range of downstream effector proteins, such as RasGAP, to regulate a variety of cellular functions, including apoptosis (177, 178). CVB3 hijacks ERK1/2 function through cleavage of RasGAP and GAB1 to promote phosphorylation of ERK1/2 and activate apoptosis (179-181). Inhibition of apoptosis and loss of GAB1 both result in a decrease viral titres and protein production, demonstrating that apoptosis promotes viral infection and this effect may be mediated through disruption of ERK1/2 signalling.

1.4.7 Pathogen recognition receptors

Cells initiate a variety of antiviral mechanisms that can suppress steps in the viral life cycle, target viral proteins for degradation, or promote cell survival responses. Many viruses; however, are able to persist by evolving strategies to inhibit or circumvent cellular antiviral defense mechanisms. Such strategies utilized by many viruses, including picornaviruses, involve virus-mediated proteolytic cleavage of host proteins, some of which have been described above that contribute indirectly to inhibit host antiviral responses, including shutoff of host protein transcription and translation, and the blocking of nuclear-cytoplasmic transport. In addition, picornaviral proteinases can interfere directly with host antiviral response pathways through proteolytic cleavage, which are summarized below (Table 1.2).

Induction of the innate immune response is the first line of defense against invading foreign pathogens. Pathogen recognition receptors (PRRs), a family of ligand-binding receptors, recognize and bind to elements unique to foreign pathogens termed pathogen-associated molecular patterns (PAMPs) (182). Detection of RNA viruses primarily occurs through members of three PRR families: Toll-like receptors (TLR), RIG-I-like receptors (RLR) and nucleotide-binding oligomerization domain-like receptors (NLR). Both TLR and RLR signalling pathways converge to induce transcription of type I IFN via activation of interferon regulatory factor 3/7 (IRF3/7) and NFκB transcription factors (182). Despite having elements that would activate these pathways, such as an RNA genome, many picornaviruses have evolved mechanisms to counter type I IFN production.

Melanoma Differentiation-Associated protein 5 (MDA5) and retinoic acid-inducible gene I (RIG-I) are DexD/H box helicases, which belong to the RIG-I-like family of receptors that sense viral RNA in the cytosol (182). MDA5 binds to long dsRNA regions that occur during the replication phase of picornaviruses, whereas RIG-I recognizes 5'-triphosphates of ssRNA or short fragments of dsRNA or stem loops (183, 184). Upon RIG-I or MDA5 binding, both receptors interact with the mitochondrial antiviral-signalling protein (MAVS) to initiate NFκB signalling that leads to type I IFN induction (183, 185-187). While activation of either receptor induces the same antiviral response, only MDA5 appears to be essential for picornavirus recognition. Virus infection of MDA5 knockout mice that are unable to activate type I IFN result in increased viral loads of EMCV and HRV1A; however, viral loads remain unchanged upon infection in RIG-I knockout mice (184, 188-190). To antagonize this antiviral response, many picornavirus infections, including those in poliovirus, EV71 and CVB3, lead to alterations in MDA5 protein levels. EV71 infection leads to complete degradation of MDA5, whereas

poliovirus and CVB3 infections result in a moderate decrease in full-length protein with the accumulation of a smaller cleavage product as infection progresses (104, 191). Whether MDA5 is a direct target of picornavirus proteinases remains unclear. MDA5 cleavage in EV71 or poliovirus-infected cells is caspase- and proteasome-dependent; however, MDA5 is still cleaved during CVB3 infection in the presence of caspase and proteasome inhibitors (104, 191, 192). MDA5 is cleaved in cells expressing CVB3 $2A^{pro}$ and occurs late in CVB3-infected cells. Mengoviruses inhibit type I IFN responses but does not cleave MDA5, suggesting that other components of the pathway may be targeted, and that each picornavirus may have distinct pathways to disrupt type I IFN signalling (104, 191). Interestingly, while RIG-I is not essential for innate immunity to counter picornavirus infection, cleavage of RIG-I is still observed during poliovirus, HRV16, EV71 and CVB3 infection, and mediated by $3C^{pro}$ (191, 193). It is possible that cleavage of RIG-I ensures blockage of this arm of antiviral signalling and/or the effects observed for EMCV infection in *RIG-I-/-* mice, which are not indicative amongst all picornaviral infections.

Many picornavirus infections lead to an elevation of pro-inflammatory cytokines that are dependent on NLR activity. NLRs are a large family of intracellular PRRs, whereby a subset induce the assembly of the inflammasome, a multi-protein complex that activates expression of inflammatory cytokines interleukin-1β (IL-1β) and IL-18 upon detection of a foreign pathogen (194). Upon detection of viral dsRNA, the NLRP3-containing inflammasome is activated via complex formation of NLRP3 with the adaptor protein apoptosis-associated speck-like protein containing a CARD (ASC) and caspase-1, leading to the processing of pro-inflammatory cytokines IL-1β and IL-18 for secretion (195). To counter this pathway, EV71 cleaves NLRP3

via $2A^{pro}$ and $3C^{pro}$, effectively inhibiting inflammasome activation and reducing levels of IL-1β (196).

1.4.8 Type I interferon signalling proteins

PRR activation through MDA-5 and RIG-I is mediated through MAVS, a common signalling mediator for both receptors. MAVS in turn activates I-kappa-B (IκB) and TRAF family member-associated NFκB activator (TANK)-binding kinase complexes to promote NFκB and IRF3-mediated transcription of ISGs, respectively. Not surprisingly, cleavage of MAVS serves as a mechanism to inhibit antiviral responses mediated during picornavirus infections. During CVB3 infection, MAVS cleavage by $3C^{pro}$ occurs at the mitochondrial membrane, removing its N-terminus to disrupt both IRF- and NFκB-mediated IFN stimulation (104, 191, 197). Similar to MAVS, TIR-domain-containing adapter-inducing interferon-β (TRIF), which is an adaptor molecule of TLR3 signalling, is cleaved by CVB3, EV71, HAV and EV86 $3C^{pro}$, blocking its ability to stimulate NFκB-mediated transcription (104, 198, 199). Additional downstream activators, including NFκB essential modulator (NEMO), a downstream activator of MAVS, is also a target by HAV and FMDV $3C^{pro}$, disrupting transcriptional activation of NFκB and IRF3 (200, 201). DNA-dependent protein kinase (DNA-PK), which is a molecular sensor for DNA damage and is involved in DNA repair, may also have roles in the immune response as DNA-PK is required for IRF-3-dependent activation of IFN genes in response to DNA, but not RNA, viral infections (202, 203). Cleavage of DNA-PK is mediated by $2A^{pro}$ and occurs early during poliovirus infection, resulting in loss of its kinase activity. However, the significance of this during poliovirus infection remains to be investigated (204).

Components of transcription factor complexes targeting ISGs are also subject to proteolysis. p65/RelA, a factor of the NFκB signalling complex, is targeted for cleavage by $3C^{pro}$, contributing to inhibition of the host IFN response (105). Degradation of p65 also occurs during FMDV infection in a L^{pro}-dependent manner (103). IRF7 is also subjected to proteolytic cleavage by EV71 and EV68 $3C^{pro}$, inhibiting its transcription activation ability (205, 206). Cleavage of IRF3 has not been observed; however, expression of the IRF7 N-terminal cleavage product suppresses IRF3-mediated transcription activity and retains the ability to bind with full-length IRF3, possibly acting in a dominant-negative manner.

Factors that regulate IRF and NFκB transcription are also altered during picornavirus infection. Inhibitor of κBα (IκBα) is an inhibitor of NFκB transcription factor function, by preventing its translocation into the nucleus. During CVB3 infection, NFκB undergoes translocation to the nucleus but no NFκB signalling occurs (106, 207). IκBα is cleaved by $3C^{pro}$ and its cleavage fragment relocalizes to the nucleus whereby it acts as a negative regulator of NFκB. Thus, like IRF7, the IκBα cleavage fragments may retain functions to exacerbate inhibition of antiviral responses. Similar to IκBα, TANK is also a negative regulator of NFκB signalling that is cleaved during EMCV infection; however, its role in inhibiting NFκB signalling is not yet clear (158). The transforming growth factor beta-activated kinase 1 (TAK1) complex, comprised of TAK1, TGF-beta-activated kinase 1 and MAP3K7-binding protein 1 (TAB1), TAB2 and TAB3 proteins, is required for activation of TLR-mediated NFκB signalling pathways. EV71 $3C^{pro}$ interacts with TAB2 of the TAK1 complex, targeting all four proteins for cleavage and effectively inhibiting their transcriptional activity (208). In summary, several components of the PRR signalling pathways and IFN-mediated responses are targeted through

the action of picornavirus-encoded proteinases, thereby ensuring fail-safe inhibition of the antiviral responses.

1.4.9 Activators of other signalling pathways

Picornavirus proteinases not only target the induction of signalling pathways of IFN, but also the secondary signalling cascade via the Janus kinase – signal transducer and activator of transcription (JAK-STAT) pathway downstream of IFN signalling, which regulates the expression of several antiviral ISGs (209). Type I IFN binds to the interferon-α/β receptor (IFNAR), comprised of two subunits called IFNAR1 and IFNAR2, to initiate the JAK-STAT pathway involving activation of JAK kinases and phosphorylation of STAT transcription activators. Phosphorylated STAT1 and STAT2 complex with IRF9 to form the transcription factor ISGF3, which targets many ISGs that inhibit viral growth, including protein kinase R (PKR) and 2'-5' oligoadenylate synthase. EV71 $2A^{pro}$ and $3C^{pro}$ target IFNAR1 and IRF9, respectively, resulting in their inactivation that contributes directly to the inhibition of ISG induction (210, 211).

Humoral immunity contributes to host antiviral response by inhibiting the systemic spread and clearance of the virus though sensing of foreign pathogens by antibodies in the blood (212-215). The complement system mediates this response by facilitating the binding of the complement component C3 protein to surfaces of foreign pathogens and inducing lysis of the foreign pathogen or infected cell (216). Mechanisms for evading complement activation have been described for some viruses (217, 218). During enterovirus infection, C3 is capable of gaining entry into the cell by covalently binding to the viral capsid, and inducing a MAVS-dependent innate immune response. Poliovirus and HRV circumvent this by targeting C3 for

cleavage by $3C^{pro}$ (219). Thus, the examples described above collectively demonstrate how viral proteolytic cleavage is used to block host antiviral response at multiple levels and thus is a key player for its successful infection.

1.4.10 Stress granules

Cellular stresses that inhibit protein synthesis lead to the formation of dynamic cytoplasmic granular RNA structures, called stress granules (SGs), which serve as temporary storage compartments of mRNAs, ribosomes, translation initiation factors, and RNA-binding proteins (220). The function of stress granules is still poorly understood but it is thought to regulate mRNA metabolism during cellular stress and concentrate signalling factors important for apoptosis and/or antiviral innate immunity. Several proteins have been implicated in SG formation and/or identified as SG markers. SG components Ras GTPase-activating protein-binding protein 1 (G3BP1), T-cell-restricted intracellular antigen 1 (TIA1), and TIA1-related protein (TIAR), are considered hallmark RNA binding proteins that contain aggregation domains for SG assembly (221-223). SG formation has been of interest to virologists, as SGs are inhibited in many virus-infected cells, suggesting a role of SG in viral infection (224-226). In poliovirus and coxsackievirus-infected cells, SG formation is inhibited late in infection via cleavage of G3BP by $3C^{pro}$, allowing replication to proceed, while over-expression of a cleavage-resistant G3BP allows SGs to persist longer, decreasing viral yield, thus suggesting that SGs are antiviral (225, 226). Indeed, recent studies have demonstrated a role for stress granules in innate immunity, whereby PRRs localize within SGs to facilitate their activation and elicit innate immune responses (227-230).

1.5 Approaches to identifying candidate substrates

It is clear from the examples described above that proteolytic activity of viral proteinases plays an essential role in the hijacking and inhibition of cellular pathways and factors to promote the viral life cycle. It is also apparent that viral proteinases do not degrade indiscriminately but rather selectively, thereby allowing precise control of biological processes. Proteases catalyze hydrolytic reactions irreversibly, thereby controlling the fate and activity of the target proteins. Some targeted proteins undergo degradation; however, as described in examples above, it is clear that some truncated fragments can have functions distinct from the full-length protein (106, 125, 206, 225). The challenge now is to identify the cleaved fragments within a population of proteins. In spite of the advances in identifying novel substrates of viral proteinases, the full repertoire of host proteins targeted for cleavage during infection has not been fully defined.

Previous attempts to identify novel targets of viral proteinases have included candidate approaches, two-dimensional gel electrophoresis coupled with mass spectrometry, and bioinformatics; however, these techniques have their limitations. Candidate approaches such as detection by immunoblotting are hypothesis-driven based on a candidate's previously established function that either participates in a cellular pathway affected during virus infection or is similar to the function of a known substrate. However, this is time-consuming and depends on the availability of antibodies. Bioinformatics approaches identify candidate substrates based on the presence of a preferred proteinase (i.e. $2A^{pro}$ or $3C^{pro}$) consensus cleavage site established from phylogenetic and mutagenesis studies of known polypeptide cleavage sites as well as systematic cleavage of permutated peptides (5). Although useful, this does not take into account protein expression or accessibility of cleavage sites within the cell. Furthermore, cleavage sites of host proteins may deviate from the preferred consensus site and thus may limit the range of potential

substrate that can be identified. For example, non-canonical cleavage sites are often identified in target proteins from studies of the degradome of metalloproteinases (231). Thus, cleavage site specificities do not reliably identify native substrates *in vivo*. Exosites, which are non-active site recognition surfaces that affect substrate specificity and cleavage activity, also cannot be modeled with certainty yet (1). Thus, it is important to keep an unbiased approach in identifying protease targets. Two-dimensional gel electrophoresis in combination with mass spectrometry has been used to successfully identify a few novel substrates; however, it is also limited by the poor quality of peptide resolution achieved by gel electrophoresis and does not allow for identification of proteolytic cleavage sites occurring near the protein termini or for proteins products found in low abundance (4).

More recent mass spectrometry-based techniques have developed gel-free strategies that have been specifically designed for analysis of protease-generated peptides (232). Traditional shot-gun proteomics involves analysis of the entire proteome between two different samples, such as comparing wild-type versus mutant protease-treated samples. Coupled with the ability to isotopically label proteins, this can serve as a more sensitive approach to identify candidate substrates by measuring the relative abundance of proteins between two samples. This approach; however, still comes with its limitations as cleavage products can be masked by more abundant proteins, especially in highly complex samples such as in tissues. To resolve these issues, positive and negative selection strategies have been employed to enrich for N-terminal peptides, each of which have advantages and disadvantages. N-terminal biotinylation of peptides through enzymatic or chemical methods followed by streptavidin pull-down can positively enrich for N-terminal peptides (233). However, its labeling efficiency is relatively low and not always

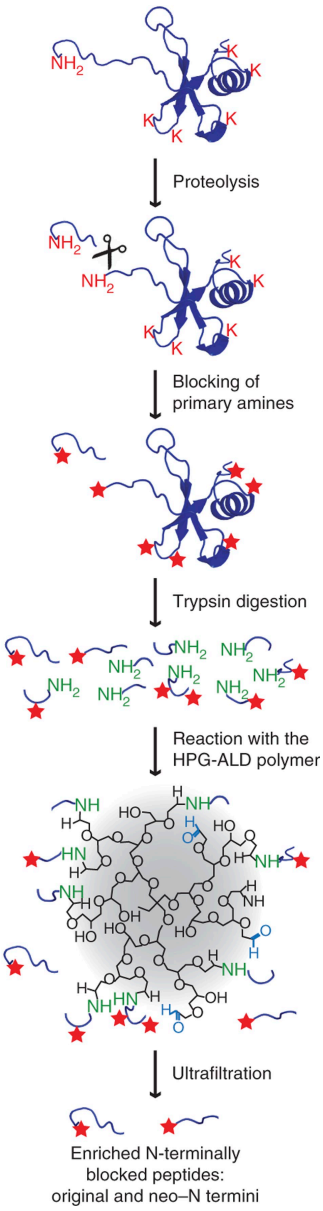

Figure 1.5 Schematic of TAILS workflow. The protease (represented by scissors) is incubated with proteome samples, resulting in protease-generated cleavage products with neo-N-termini. Primary amine groups of natural and protease-generated neo-N-termini (NH_2), as well as within lysine resides (K), are isotopically-labeled and subsequently blocked. Proteome samples are further digested with trypsin, generating internal tryptic peptides with an unlabeled free N-terminal amine group. Internal tryptic peptides are removed through reaction with a aldehyde-derivative polymer, which is then removed through ultafiltration. The remaining sample enriched with natural and neo-N-terminal peptides are then analyzed and quantified by LC-MS/MS. Adapted from Kleifeld et al (2011) (234)

compatible with isotopic labeling for quantification. Moreover, many protein N-termini are subjected to several post-translational modifications that can interfere with methods of positive selection, which posses a challenge for positive selection methods and results in a significant proportion of protease-generated N-terminal peptides unaccounted for. Other approaches such combined fractional diagonal chromatography (COFRADIC) and terminal amine isotopic labeling of substrates (TAILS) employ a negative selection strategy to enrich for N-terminal peptides (231, 234-237). Both approaches use whole protein amine isotopic labeling that effectively blocks the reactivity of protein N-termini (as well as internal lysines), followed by trypsin digestion and removal of unlabeled internal trypsin-generated peptides. In the COFRADIC method, the trypsin generated peptides are treated with an oxygen-18 isotopic label, generating highly hydrophobic peptides that can then be removed through multiple chromatography steps. COFRADIC has been successful in the negative selection of N-termini peptides; however, larger amounts of starting sample is required and the extensive fractionation requires considerable mass spectrometry time (238). Alternatively, TAILS utilizes a dendritic polyglyceraldehyde polymer that covalently binds to the free amines of trypsin-generated peptides, which are then removed by filtration (Figure 1.5). Use of this polyglyceraldehyde polymer allows for lower starting material, fewer samples for mass spectrometry analysis, and more options for peptide labeling. TAILS has been successful at identifying novel substrates for a variety of proteases, including matrix metalloproteases and dipeptidyl proteases (6-8, 239). N-terminal enrichment methods like COFRADIC and TAILS are still limited by the occurrence of N-terminal post-translational modifications that interfere with N-terminal labeling methods, and thus complete proteome enrichment cannot be achieved. Methods for C-terminal enrichment of

peptides have been described; however, complete C-terminal labeling has been difficult to achieve (240, 241).

1.6 Thesis rationale, hypothesis and specific aims

Research thus far into the substrates of picornaviral proteinases and the proteolytic events that ensue during virus infection has provided key insights into viral-host interactions required for successful picornaviral infection. Many of such proteolytic events involve a plethora of host proteins to effectively and efficiently inhibit major cellular signalling pathways that induce antiviral responses. To date, there are approximately 45 known host proteins that serve as substrates of picornavirus proteinases; however, we **hypothesize** that these viral proteinases target other host proteins to support virus infection that have yet to be identified through conventional methods. Thus, the **objective** of my thesis was to establish TAILS as a method for identifying novel substrates of picornavirus proteinases. To accomplish this, I addressed the following **specific aims**:

1. Develop an in vitro approach to perform TAILS using picornavirus proteinases.

We applied TAILS using cellular extracts from HeLa cells subjected to model picornavirus proteinases from the enterovirus genre, poliovirus $3C^{pro}$ and CVB3 $2A^{pro}$. For comparison, we applied TAILS using HL-1 cardiomyocytes subjected to CVB3 $3C^{pro}$ to more closely recapitulate a physiological setting of virus infection, and to identify conserved and unique substrates among $3C^{pro}$ of two different enteroviruses (Chapter 3).

2. Validate candidate substrates identified by TAILS as novel targets of picornavirus proteinases.

I applied a series of *in vitro* and *in vivo* experiments to validate select candidate substrates identified by TAILS as bona fide novel substrates of picornavirus proteinases, as well as to confirm the cleavage site identified by TAILS (Chapters 3, 4, and 5).

3. Characterize the functions of novel substrates during picornavirus infection and explore the biological significance of cleavage.

The functional importance of select validated candidate substrates during virus infection was explored utilizing a series of experiments, including siRNA knockdown and over-expression of wild-type and cleavage resistant forms to monitor changes in viral titres (Chapters 4 and 5).

Chapter 2: Materials and Methods

2.1 Cell culture and virus stocks

HeLa cells were cultured in Dulbecco's modified Eagle medium (DMEM) supplemented with 10% fetal bovine serum (FBS) and 1% penicillin/streptomycin (P/S) at 37°C. HL-1 murine cardiac muscle cells were cultured in Claycomb media (Sigma) supplemented with 10% FBS, 1% P/S, 2 mM L-glutamine, and 0.1 mM norepinephrine in ascorbic acid. Poliovirus (Mahoney type 1 strain) was generated from transfection of *in vitro* transcribed RNA from a poliovirus infectious clone, pT7pGemPolio (generously provided by Kurt Gustin, University of Arizona) into HeLa cells. Poliovirus and CVB3 (Kandolf strain) were both propagated and titred in HeLa cells.

2.2 Plasmids and transfections

The full-length open reading frames of the following proteins were PCR-amplified and cloned into a p3xFlag-CMV-7.1 vector (Sigma) with a 3xHA-tag cloned downstream using *XbaI* and *BamHI* sites: hnRNP M (NM_005968), hnRNP K (NM_ 002149), ALIX (NM_013374), RIPK1 (NM_003804), ACYL (NM_001096), PFAS (NM_012393) and USO1 (NM_001290049). Full-length CVB3 $3C^{pro}$ (M88483) and a CVB3 $3C^{pro}$ C147A mutant were PCR-amplified and cloned into the *NotI* and *NdeI* restriction sites of pET28b. Constructs were verified by sequencing. Full-length wild-type and mutant QG832EP USO1 was cloned into a mEGFP-C1 vector using *XhoI* and *BamHI* sites.

For DNA transfections, HeLa cells were transfected with 1-2 μg of plasmid using Lipofectamine 2000 (Invitrogen) according to the manufacture's protocol. Cells were transfected in antibiotic-free media for 5 hours, then replaced with complete media for 24-48 hours. For

siRNA transfections, HeLa cells were transfected (30-40% confluency) with the following siRNAs using Lipofectamine RNAimax (Invitrogen): hnRNP M (Ambion; s9259, s9261, s9260), hnRNP K (Ambion; s6739, s6738, s6737), PFAS (Ambion; s10331, s10332, s10330), RIPK1 (Ambion; s16651), ACLY (Ambion; s915), ALIX (Ambion; s19467, s19465, s19466) and USO1 (Ambion; s16392, s16391, s16390). Knockdown efficiency was validated by immunoblot analysis.

The pIRES-poliovirus and pIRES-dEMCV bicistronic reporter constructs (generously provided by Gabriele Fuchs and Peter Sarnow, Stanford University) were transfected into HeLa cells for 1 hour and then infected with poliovirus. Cells were harvested and luciferase activity was monitored using a dual Luciferase reporter assay kit (Promega). Luminescence was measured using a Centro LB 960 luminometer (Berthod Technologies).

2.3 Virus infections

Virus was absorbed with HeLa or HL-1 cells at the indicated multiplicity of infection (MOI) for 1 hour in serum-free DMEM at 37°C, then washed with phosphate buffered saline (PBS) and replaced with complete media. For virus infections in the presence of Z-Val-Ala-DL-Asp-fluoromethylketone (zVAD-FMK, Calbiochem), zVAD-FMK was added to serum-free DMEM containing virus at a final concentration of 50 μM.

For pulse chase experiments, media was replaced with methionine- and cysteine-free media containing 30 μCi of [^{35}S]-EasyTag™ Express Protein Labeling Mix (Perkin Elmer) for 30 minutes prior to harvesting. Cells were lysed in RIPA buffer (10 mM Tris pH 8, 1 mM EDTA, 0.5 mM EGTA, 140 mM NaCl, 1% Triton-X100, 0.02% Na-deoxycholate, 0.1% SDS) supplemented with protease inhibitors (Roche), and protein concentrations were determined by

Bradford assay. Proteins were resolved by sodium dodecyl sulfate-polyacrylamide gel electrophoresis (SDS-PAGE) and analyzed by phosphorimager analysis.

For plaque assays, virus-infected cells were washed twice with PBS, harvested in serum-free DMEM and lysed by 3 cycles of freeze thawing. Serial dilutions of cell supernatants were incubated with HeLa cells for 1 hour at 37°C. Cells were washed twice with PBS and overlaid with DMEM containing 2% FBS, 1% P/S and 1% methylcellulose. After 72 hours, cells were fixed with 50% methanol and stained with 1% crystal violet. Plaques were counted and viral titre was calculated as plaque forming units (PFU) per milliliter.

2.4 Immunoblot analysis

Equal amounts of protein were resolved by SDS-PAGE and transferred to a PVDF membrane. Antibodies used in this study were as follows: 1:1000 hnRNP M, 1:500 α-tubulin, 1:1000 actin (Santa Cruz Biotechnologies), 1:3000 G3BP1 (BD Transduction Science), 1:3000 VP1 (Dako), 1:1000 PABP (generously provided by Dr. Richard Lloyd, Baylor College of Medicine), 1:1000 PARP (Pharmingen), 1:1000 GAPDH (Abcam), 1:2000 AIP1/ALIX (Millipore), 1:4000 RIPK1, 1:7500 hnRNP K (Santa Cruz), 1:1000 PFAS (Abcam), 1:2000 ACLY (Millipore), 1:1000 VDP p115/USO1 (Novus Biologicals), 1:1000 HA (Covance), and 1:2000 FLAG (Sigma-Aldrich).

2.5 Northern blot analysis

Total RNA was isolated from cells using Trizol reagent (Invitrogen). RNA was resolved on a denaturing agarose gel and transferred to Zeta-probe blotting membrane (Biorad). Radiolabeled DNA hybridization probes were generated using the Deca labeling kit (Fermentas).

The amount of radiolabeled probe hybridized to the blot was analyzed and quantified using a phosphorimager (Typhoon, Amersham Biosciences).

2.6 Immunofluoresence

HeLa cells on coverslips were fixed with cold 100% methanol for 10 minutes, washed three times with PBS and then blocked with 5% bovine serum albumin (BSA) in PBS for 1 hour, followed by 1 hour incubation with primary antibody with 1% BSA in PBS at room temperature. The primary antibodies were used as follows: 1:25 hnRNP M and 1:50 HA (Santa Cruz Biotechnologies), 1:75 USO1 (Novus Biologicals), 1:400 double stranded RNA (dsRNA, English & Scientific Consulting Bt), 1:100 FLAG (Sigma), and 1:300 VP1 (Dako). Coverslips were washed three times with PBS then incubated with 1:500 secondary antibody (goat anti-rabbit or goat anti-mouse Texas red, and goat anti-mouse Alexa Fluor 488 (Life Technologies) with 1% BSA in PBS and Hoescht to stain for nuclei. Following three washes, coverslips were mounted onto slides using Prolong Gold Antifade Reagent (Life Technologies). Cells were imaged and analyzed using a Nikon Eclipse Ti confocal microscope and pictures were taken using the NIS-elements software.

2.7 Protein purification

Wild-type and catalytically inactive (C57A) CVB3 $2A^{pro}$ and His-tagged wild type and catalytically inactive mutant (C147A) poliovirus $3C^{pro}$ were purified using expression plasmids, pET-Cx2A, pET-Cx2A C109A, pET3Chc and pET3Chc C147A (generously provided by Richard Lloyd, Baylor College of Medicine). Wild-type CVB3 $3C^{pro}$ and a C147A catalytically inactive mutant proteinase were cloned into a pET28b expression vector containing an N-

terminal His-tag. $2A^{pro}$ proteinases were expressed in and purified from BL21 bacterial cells by ion exchange chromatography and size exclusion chromatography as previously described (87, 98). $3C^{pro}$ was expressed in and purified from BL21 bacterial cells by Nickle-nitrilotriacetic acid (Ni-NTA) chelating resin affinity chromatography. Fractions containing purified $3C^{pro}$ were then pooled and dialyzed in 20 mM Hepes pH 7.4, 100 mM NaCl, 7 mM β-mercaptoethanol, and 20% glycerol. Expression plasmid containing 3CD was generously provided by Bert Semler (UC-Irvine). Recombinant $3CD^{pro}$ was purified as described (133). The integrity and purity of the purified protein were verified by Coomassie R-250 staining using SDS-PAGE analysis.

2.8 *In vitro* cleavage assay

HeLa and HL-1 cell lysates were prepared by harvesting and pelleting cells in cold PBS and then resuspending in 2-3X pellet volumes of cleavage assay buffer (20 mM Hepes pH 7.4, 150 mM KOAc and 1 mM DTT) supplemented with protease inhibitors (Roche). Cells were incubated on ice for 10 minutes, and then lysed with 25 strokes in a dounce homogenizer. Lysates were then clarified by centrifugation at 13,000 rpm for 15 minutes at 4°C.

Purified hnRNP M (20 pg, Origene) or cell lysates were incubated with purified wild-type or catalytically inactive CVB3 $2A^{pro}$ (5 ng/µl), poliovirus $3C^{pro}$ (100 ng/µl) or CVB3 $3C^{pro}$ (100 ng/µl) in cleavage assay buffer at 37°C for different periods of times as indicated. Reactions were resolved by SDS-PAGE and proteins were assessed by immunoblot analysis.

2.9 Fluorescence-activated cell sorting analysis

HeLa cells were transfected with either wild-type or mutant QG832EP mEGFP-C1 USO1 for 24 hours and prepared for fluorescence-activated cell sorting (FACS) analysis by harvesting

cells by pelleting cells following trypsinization and washing cells in FACS sorting buffer (2 mM EDTA, 2% FBS, 1xPBS). Cells were resuspended at 10-20 million cells/ml in FACS sorting buffer, then sorted by FACS using a FACSAria or BD Influx (BD Biosciences) cell sorter. GFP-expressing cells were collected and allowed to recover for 24 hours in DMEM supplemented with 20% FBS and 1% P/S.

2.10 Mouse infection by CVB3

A/J mice (Jackson Laboratory #000646) at approximately 5 weeks of age were infected with 10^5 PFU by intraperitoneal injection. Mock infections were performed using equal volumes of PBS. At 9 days post-infection, mouse hearts were harvested, lysed and immunoblotted as indicated. These studies were performed in accordance with the recommendations in the Guide for the Care and Use of Laboratory Animals of the Canadian Council on Animal Care and were approved by the Animal Care Committee at the University of British Columbia (Animal #A13-0237).

2.11 N-terminal TAILS proteomics

TAILS was performed on HeLa cell extracts subjected to an *in vitro* cleavage assay as described above. Briefly, equal amounts of HeLa cell lysates were incubated with either purified wild-type or catalytically inactive mutant purified poliovirus $3C^{pro}$ or CVB3 $2A^{pro}$, while equal amounts of HL-1 cell lysates were incubated with either purified wild-type or catalytically inactive mutant purified CVB3 $3C^{pro}$, and incubated overnight at 37 degrees. TAILS was then performed as previously described (231, 242). In brief, after the protein was denatured and reduced, cysteines were alkylated and samples were isotopically labeled at the protein level by

reductive dimethylation of primary amines. Thus, any protein α amines on the natural N-terminus or the proteinase generated neo-N-terminus were labeled and so could be identified after trypsin digestion. Heavy (wild-type proteinase-treated) and light (catalytically-inactive proteinase-treated) isotopically labeled samples were combined, salts removed and the samples concentrated by methanol precipitation. The sample was then subject to trypsin digestion, followed by enrichment of labeled peptides by a negative selection step using a dendritic polyglycerol aldehyde polymer purchased from Flintbox (http://flintbox.com/public/project/1948). Unbound labeled N-termini peptides were separated from the polymer-bound peptides by centrifugation through a 10-kDa Microcon filter (Millipore). The flow through was collected and fractionated by strong-cation exchange high-performance liquid chromatography.

Samples analyzed on the LTQ-Orbitrap XL were loaded into a nano HPLC system (Thermo Scientific) coupled to an LTQ-Oribitrap hybrid mass spectrometer (LTQ-Orbitrap XL, Thermo Scientific) through a nanospray ionization source consisting of a fused-silica trap column (length, 2 cm; inner diameter, 100 μm; packed with 5 μm-diameter Aqua C-18 beads; Phenomenex), fused-silica fritted analytical column (length, 20 cm; inner diameter, 50 μm; packed with 3 μm-diameter Reprosil-Pur C-18-AQ beads; Dr. Maisch GmbH) and a silica gold-coated spray tip (20 μm inner diameter, 6 μm diameter opening, pulled on a P-2000 laser puller; Sutter Instruments; coated on EM SCD005 Super Cool Sputtering Device, Leica Microsystems). Buffer A consisted of 0.5% acetic acid, and buffer B consisted of 0.5% acetic acid and 80% acetonitrile (ACN). Gradients were run from 0% B to 15% B over 15 min, then from 15% B to 40% B in the next 65 min, then increased to 100% B over 10 min period, held at 100% B for 30 min. The LTQ-Orbitrap was set to acquire a full-range scan at 60,000 resolution (*m/z* 350–1,800)

in the Orbitrap and to simultaneously fragment the top five peptide ions in each cycle in the LTQ (minimum intensity 200 counts). Parent ions were then excluded from tandem mass spectrometry (MS/MS) for the next 180 s. The Orbitrap was continuously recalibrated against protonated (Si(CH3)2O)6; at *m/z* = 445.120025 using the lock-mass function.

For samples analyzed on the Aligent G6550A quadrupole time-of-flight (Q-TOF) mass spectrometer, samples were loaded without dilution into a 1200 Series nanoflow HPLC system (Agilent Technologies) connected to a 6550 Q-TOF (Agilent Technologies) through a Chipcube ion source. Peptide separation was performed by reversed phase chromatography using a micro-fluidic CHIP comprised of an analytical column; 75 μm ID, 150 mm length with a 300-Å C18 stationary phase and a 160 nL trap column of the same phase. Peptides were loaded in 0.1% (v/v) formic acid at 2 μL/min, and then resolved at 0.3 μL/min for 60 min, during which a linear gradient of acetonitrile was created from 5% to 40% in 0.1% (v/v) formic acid. Operating in auto MS/MS acquisition mode, the Q-TOF was set up to acquire full scan data over a mass range of 350 to 1700 m/z and MS/MS for the five most intense, multiply-charged ions.

For TAILS using CVB3 $3C^{pro}$, peptides were eluted from Stage tips in 80% ACN, 0.1% formic acid, SpeedVac concentrated to near-dryness and dissolved in approximately 20 μl mobile phase A (0.1% formic acid). Peptides were analyzed with an EASY nLC-1000 HPLC system (Thermo Scientific) online coupled to an Impact II high resolution, high mass accuracy QTOF system using a CaptiveSpray ion source (Bruker Daltonics) that was modified for minimal post-column dead volume as described in (Beck et al 2015 MCP). Peptides were loaded onto an in-house packed column (40 cm, 75 μm I.D.) packed with C18 material (Reprosil-Pur C-18-AQ beads 1.9 μm size; Dr. Maisch GmbH) and a silica gold-coated spray tip (20-μm inner diameter, 6-μm diameter opening, pulled on a P-2000 laser puller; Sutter Instruments; coated on EM

SCD005 Super Cool Sputtering Device, Leica Microsystems). Separation was performed using a linear gradient of 2-35% mobile phase B (100% ACN, 0.1% formic acid) over 90 min at a flowrate of 250 nL/min and heated to 50°C.

2.12 Mass spectrometry data analysis

For samples analyzed on the Q-TOF, MS peaks were searched by MASCOT (version 2.2, Matrix Science, London, UK) against a human database at a 1% false discovery rate (FDR). Queries originating from the same precursor (within 10 ppm and 1 min elution time) were searched as a group. Peptide and fragment mass error tolerances were set to 10 ppm and 0.4 Da, respectively. MASCOT searches of MS data were performed separately for heavy- and light-labeled peptides. Searches were performed using the following modifications: fixed carbamidomethylation of cysteines (+57.021 Da (Cys)), fixed heavy lysine (+34.0631 Da (Lys)), or light lysine (+28.0311 Da (Lys)); variable methionine oxidation (+15.995 Da (Met)), and fixed and variable modifications of the N-termini with heavy formaldehyde (+34.0641 Da (N termini)), light formaldehyde (+28.0311 Da (N-termini)), and acetylation (+42.011 Da (N termini)). The additional search criteria used were as follows: semi-ArgC cleavage specificity with up to three missed cleavages; a monoisotopic mass error window for the parent ion of 0.4 to 0.6 Da; and peptide mass tolerance of 0.4 Da for MS/MS fragment ions. Allowed peptide charge states were 1+, 2+, and 3+. Quantification of the heavy to light isotopically labeled peptides was achieved by using ProteoIQ. Statistically significant quantified peptides were determined by box plot analysis. All peptides identified within the upper fourth quartile were deemed statistically significant.

For samples analyzed on the Orbitrap XL and QExactive, spectra were matched to peptide sequences in the human UniProt protein database (October 2013) with appended standard laboratory and common contamination protein entries and reverse decoy sequences (in total 177,324 entries) using the Andromeda algorithm as implemented in the MaxQuant software package v1.4.12 at a peptide FDR of 0.01 (243, 244). Search parameters included a mass tolerance of 5 p.p.m. for the parent ion, 0.5 Da for the fragment ions in LTQ-Orbitrap XL data and 20 p.p.m. for fragment ions in QExactive data, carbamidomethylation of cysteine residues (+57.021464 Da), variable N-terminal modification by acetylation (+42.010565 Da) and variable methionine oxidation (+15.994915 Da).

Sequence logos were generated with IceLogo with a p-value of 5% (245).

2.13 Statistical analysis

All statistical analyses were performed using GraphPad Prism. All graphs represent the mean ± standard deviation (s.d.). P values were determined using an unpaired t-test and statistical significance was determined at the p-values indicated.

Chapter 3: Identification of Novel Host Substrates of $2A^{pro}$ and $3C^{pro}$ using *In Vitro* TAILS

3.1 Background

Picornaviral proteinases play a prominent role during infection by processing viral proteins and hijacking host protein function through proteolytic cleavage to facilitate infection (246). Much information has already been obtained on various mechanisms that direct the picornaviral life cycle and how host antiviral responses are circumvented through the identification of host protein substrates targeted for cleavage (85, 87, 89, 107, 116, 117, 125). Moreover, the identification of host protein substrates have provided insight into how viruses infection can contribute to the progression of disease (163). Currently, there are ~45 known host targets of picornaviruses; however, the full repertoire of targets is not known. Most targets have been identified through candidate approaches, two-dimensional gel electrophoresis coupled with mass spectrometry, and bioinformatics (4, 211, 247). However, these techniques have several limitations and biases (232). To overcome these limitations, recent mass spectrometry-based techniques have developed gel-free strategies that identify protease-generated peptides (231, 234, 235). TAILS has recently been developed as a gel-free proteomics-based approach to identify protease substrates at their cleavage site. TAILS has identified novel substrates for matrix metalloproteases and dipeptidyl peptidases, but has yet to be applied using a viral proteinase (6-8).

In this chapter, I summarize the results obtained for Aim 1 of this thesis. We have established an *in vitro* assay to perform TAILS as a novel approach to identify novel substrates of picornavirus proteinases. We utilized an *in vitro* assay for TAILS to offset the occurrence of

secondary cleavage events initiated as a result of virus infection, increasing the likelihood of identifying direct substrates of these viral proteinases. We utilized model picornavirueses proteinases from two enterovirues, the poliovirus and CVB3 $3C^{pro}$ and $2A^{pro}$, respectively, as both these proteinases have been extensively studied at both the biochemical and structural level. Moreover, as a subset of host proteins have already been identified as substrates of $3C^{pro}$ and $2A^{pro}$ within HeLa cell extracts, this provides a positive control for these studies. Furthermore, poliovirus and CVB3 infection in HeLa cells has already been established, thus providing a setting for validation of TAILS-identified candidate substrates *in vivo*. In addition to HeLa cell extracts, we applied TAILS to HL-1 cardiomyocyte extracts subjected to CVB3 $3C^{pro}$ to reflect a more physiological setting of virus infection as cardiomyocytes are the primary targeted cells upon CVB3-infection in humans (231, 232). Furthermore, we could identify both common and unique substrates of $3C^{pro}$ from two different enteroviruses. Upon completion of our TAILS experiments, a list of high confidence substrates was generated and a series of *in vitro* and *in vivo* experiments were performed to validate select high confidence substrates as bona fide targets of picornaviral proteinases.

3.2 Results

3.2.1 Purification and functional analysis of enteroviral proteinases

To establish an *in vitro* assay for applying TAILS using enteroviral proteinases, I first expressed and purified wild-type and catalytically inactive versions of the following His-tagged recombinant enteroviral proteinases from pET expression vectors: wild-type and C147A $3C^{pro}$ from poliovirus and CVB3, and wild-type and C57A $2A^{pro}$ from CVB3. Recombinant poliovirus

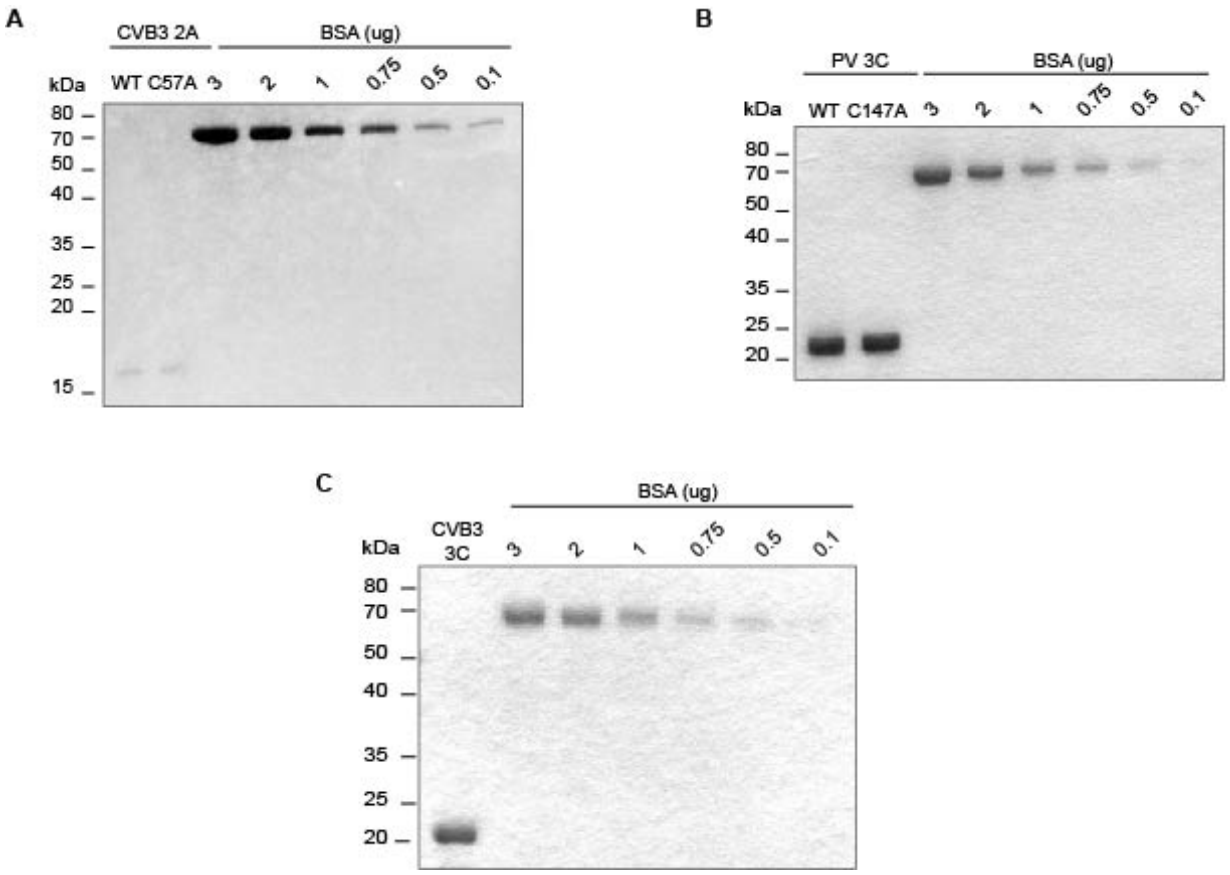

Figure 3.1 Purified Recombinant Enteroviral Proteinases. Coomassie-stained gel of expressed His-tagged wild-type (WT) and mutant recombinant CVB3 $2A^{pro}$ (A), poliovirus (PV) $3C^{pro}$ (B), and CVB3 $3C^{pro}$ (C) enteroviral proteinases. Protein concentration of a 10 µl sample of purified sample was estimated by comparing to known amounts of bovine serum albumin (BSA) as indicated above.

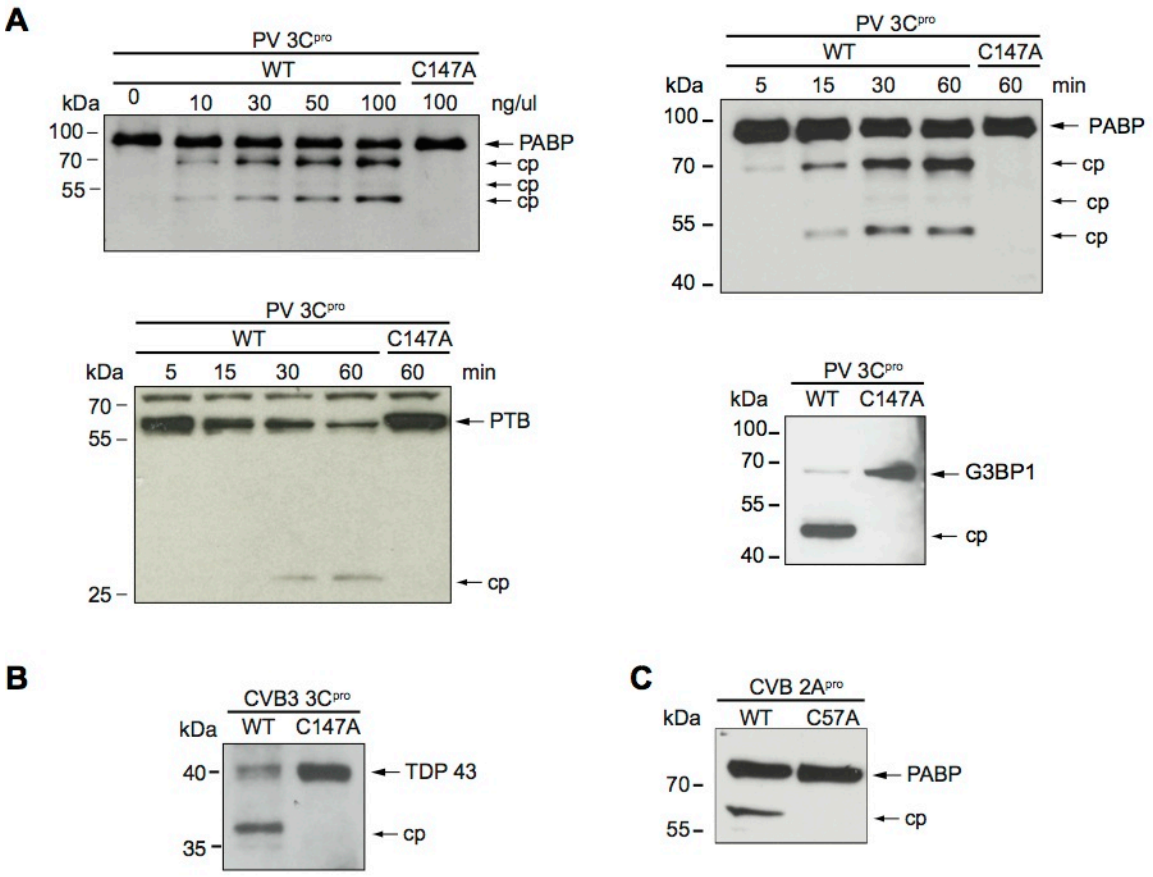

Figure 3.2 *In vitro* cleavage assay of known enterovirus 3C^{pro} and 2A^{pro} substrates. (A) Immunoblot showing cleavage of PABP in a dose-dependent (*top left)*, and time-dependent *(top right)* manner in HeLa cell extracts incubated with wild-type or mutant poliovirus (PV) 3C^{pro}. A proteinase concentration of 100 ng/µl was used for the time-dependent *in vitro* cleavage assays. Immnoblots showing cleavage of additional poliovirus 3C^{pro} substrates PTB *(bottom left)* over time, and G3BP *(bottom right)* at one hour. (B) Immunoblot following cleavage of TDP-43 in HL-1 cell lysates incubated with wild-type or mutant CVB3 3C^{pro} at one hour. (C) Immunoblot showing cleavage of PABP in HeLa cell extracts by CVB3 2A^{pro} at 10 ng/µl for 1 hour. cp, cleavage product.

$2A^{pro}$ is notoriously difficult to purify, and thus was not included in this study. His-tagged recombinant proteinases were expressed and purified from bacterial cells as described in the Materials and Methods. Protein concentrations were measured from a 10 µl aliquot of purified protein against a BSA standard (Figure 3.1).

Proteolytic activity of the wild-type recombinant proteinases was assessed by immunoblot using an *in vitro* cleavage assay in HeLa or HL-1 cellular extracts. *In vitro* cleavage assays with varying proteinase concentrations and incubation times were performed to determine optimal proteinase activity for TAILS. Incubation of wild-type but not mutant $3C^{pro}$ or $2A^{pro}$ in lysates resulted in cleavage of known target substrates PABP, PTB, G3BP1, and TAR DNA-binding protein 43 (TDP-43) (Figure 3.2) (85, 98, 225, 226, 248). The cleavage products observed were of known sizes previously published in the literature.

3.2.2 Identification of candidate substrates of $3C^{pro}$ from poliovirus and CVB3, and $2A^{pro}$ from CVB3 using *in vitro* TAILS

We applied TAILS using proteinases from two model enteroviruses, poliovirus and CVB3. Proteome samples prepared from HeLa cell extracts were incubated with purified wild-type or a catalytically inactive mutant poliovirus $3C^{pro}$ or CVB3 $2A^{pro}$ proteinase (C147A and C57A for $3C^{pro}$ and $2A^{pro}$, respectively) (Figure 3.3A). For comparison, proteome samples from HL-1 cardiomyocyte lysates were incubated with CVB3 wild-type or mutant (C147A) recombinant $3C^{pro}$ in order to more closely recapitulate a physiological setting of virus infection (249, 250). Furthermore, TAILS analysis of proteinases from two different enteroviruses that infect distinct cell lines should identify common and cell-specific host targets that may be

important for general enterovirus infection, including those that may contribute to specific pathogenesis of disease.

TAILS was performed on cellular extracts following an *in vitro* cleavage assay using a concentration 10 ng/µl and 100 ng/µl of $2A^{pro}$ and $3C^{pro}$, respectively, which were chosen based on optimal cleavage activity observed in Figure 3.2 (231, 234, 251). Following proteinase digestion, samples were isotopically labeled by reductive dimethylation of primary amines, applying a heavy (+32 Da) formaldehyde to the wild type sample and a light (+28 kDa) formaldehyde to the catalytically inactive mutant sample. The samples were mixed and trypsinized, followed by a negative selection step that removes unlabeled trypsin-generated N-terminal peptides using a dendritic aldehyde polymer, thus enriching for neo-N-termini and natural N-termini peptides (peptides that have a heavy/light (H/L) ratio) that are then identified by LC-MS/MS.

For poliovirus $3C^{pro}$ and CVB3 $2A^{pro}$, TAILS-enriched peptides from HeLa cell lysates were analyzed from a total of seven biological replicates using three different mass spectrometers and two search engines for peptide identification (Figure 3.3B). From the seven biological replicates for poliovirus $3C^{pro}$, we identified 3482 total peptides, of which 3210 were unique peptides from 1965 unique proteins. For CVB3 $2A^{pro}$, we identified 2688 unique proteins and 4156 unique peptides from 5221 total peptides (Figure 3.3C). For CVB3 $3C^{pro}$, we identified 347 unique peptides from 240 unique proteins, from a total of 364 identified peptides from three biological replicates (Figure 3.3D).

Peptides with a high H/L ratio were identified and ranked to represent candidate substrates that were cleaved in lysates containing wild-type proteinase compared to that containing mutant proteinase. A box plot analysis was applied to determine the high and low

statistical isotopic H/L ratio cutoffs. Neo-N-termini peptides with a H/L ratio above the high statistical ratio cutoff and contained an arginine at its C terminus (semi-tryptic; representing internal cleavages within the protein) were designated as high confidence candidate substrates. For poliovirus $3C^{pro}$, 72 high confidence candidate substrates were identified including a peptide from isoform 2 of PTB, a known substrate of $3C^{pro}$ (Figure 3.3B, Table 3.1). Moreover, the PTB peptide indicated that cleavage occurs between ^{311}AIPQ|AAGL^{318}, which is an identical cleavage site reported previously, and thus provided validation of the TAILS approach of $3C^{pro}$ (107). An additional 78 natural N-termini or neo-N-termini non-semi-tryptic peptides were identified with a H/L ratio above the statistical cut off. Furthermore, we identified 165 neo-N-termini and natural N-termini peptides with a H/L ratio below the low statistical ratio cutoff, which may also include candidate substrates whose unprocessed form was found in higher abundance in the mutant light-labeled sample. Alternatively, identified peptides either above or below the statistical ratio cutoffs may represent protein substrates that are indirectly affected by $3C^{pro}$.

The same approach of substrate winnowing was applied to identify 34 and 63 high confidence candidate substrates of CVB3 $3C^{pro}$ and $2A^{pro}$, respectively (Figure 3.3C and 3.3D, Table 3.2 and 3.3). An additional 10 and 162 natural N-termini or non semi-tryptic neo-N-termini peptide, and 36 and 265 significantly down-regulated neo-N-termini and natural N-termini peptides, for CVB3 $3C^{pro}$ and $2A^{pro}$, respectively, were identified. Three common peptides were found among both poliovirus and CVB3 $3C^{pro}$ list of high confidence substrates: hnRNP K, hnRNP M and phosphoribosylformylglycinamidine synthase (PFAS) (Figure 3.4A and Table 3.4). Furthermore, a peptide corresponding to hnRNP K was also identified among the list of high confidence substrates for CVB3 $2A^{pro}$; however, at a different putative cleavage site

A

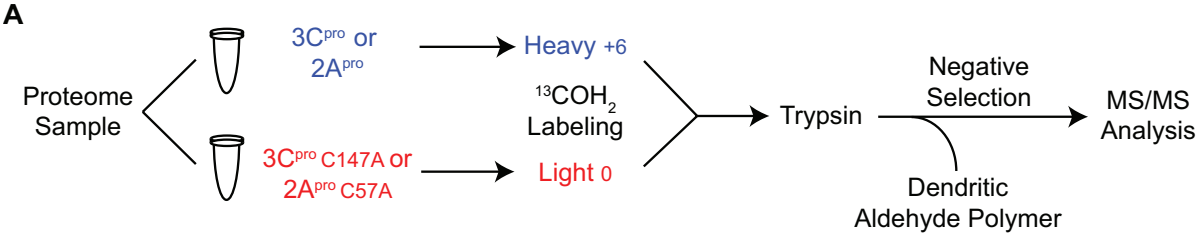

B

Poliovirus 3C^{pro}

Instrument	N	Total Peptides	Unique Peptides	Unique Proteins	High Confidence Substrates
OrbiXL	3	627	534	444	10
QExactive	2	1778	1741	1059	37
QToF	2	1077	759	614	10
OrbiXL+ QExactive	5	2253	2224	1239	15
Total	7	3482	3210	1965	72 Unique Peptides

C

CVB3 2A^{pro}

Instrument	N	Total Peptides	Unique Peptides	Unique Proteins	High Confidence Substrates
OrbiXL	3	333	268	227	6
QExactive	2	1360	1343	782	43
QToF	2	1964	999	805	9
OrbiXL+ QExactive	5	1564	1546	874	7
Total	7	5221	4156	2688	65 Unique Peptides

D

CVB3 3C^{pro}

Instrument	N	Total Peptides	Unique Peptides	Unique Proteins	High Confidence Substrates
QExactive	3	364	347	240	34

Figure 3.3 Summary of total peptides and proteins identified by TAILS analysis of poliovirus 3C^{pro}, CVB3 2A^{pro}, and CVB3 3C^{pro}. (A) A schematic of the TAILS workflow. Proteome samples were incubated with purified recombinant wild-type or mutant 3C^{pro} or 2A^{pro}, followed by isotopic dimethylation labeling and TAILS. Enriched N-terminal peptides were identified by LC-MS/MS and quantified. Total and unique peptide, total protein, and number of high confidence substrates are summarized for poliovirus 3C^{pro} (B), CVB3 2A^{pro} (C), and CVB3 3C^{pro} (D). High confidence substrates were determined by box plot analysis of quantified heavy:light (H/L) ratio of dimethylation-labeled semi-tryptic neo-N-termini peptides.

Table 3.1 Select poliovirus $3C^{pro}$ high confidence candidate substrates from HeLa cells

Protein Description	Gene	P4-P1	TAILS Peptide	Log2 H/L Ratio
Receptor-interacting serine/threonine-protein kinase 1	RIPK1	YKGR	IILEIIEGMCYL	5.22
ATP-citrate synthase	ACYL	AKNQ	ALKEAGVFVPR	5.54
Ataxin-2	PFAS	ASPQ	AGIIPTEAVAMPIPAASPTPASPASNR	2.75
Polypyrimidine tract-binding protein 1 isoform 2	PTBP1	AIPQ	AAGLSVPNVHGALAPLAIPSAAAAAAAAGR	4.39, 4.29
Programmed cell death 6-interacting protein	PDCD6IP	PAYQ	SSPAGGHAPTPPTPAPR	3.65
General vesicular transport factor p115	USO1	VEVQ	GETETIIATKTTDVEGR	3.45, 3.44
Ribonuclease inhibitor	RNH1	VLCQ	GLKDSPCQLEALKLESCGVTSDNCR	3.55

Table 3.2 Select CVB3 $2A^{pro}$ high confidence candidate substrates from HeLa cells

Protein Description	Gene	P4-P1	TAILS Peptide	Log2 H/L Ratio
Transcription elongation facot SPT6	SUPT6H	ELER	QGYGDKHITLYDIR	1.93
Cyclin-dependent kinases regulatory subunit 1	CKS1B	SDKY	DDEEFEYR	1.92
Exportin-1	XPO1	IKEF	AGEDTSDLFLEER	1.60
Seroin B6	EXOS9	QKFY	QAEMEELDFISAVEKSR	1.30
Hetergeneous nuclear ribonucleoprotein K	HNRNPK	WQMA	AYEPQGGSGYDYSYAAGR	0.36

Table 3.3 Select CVB3 $3C^{pro}$ high confidence candidate substrates from HL-1 cardiomyocyte cells

Protein Description	Gene	P4-P1	TAILS Peptide	Log2 H/L Ratio
Microtubule-associated protein 1B	MAP1B	AAHQ	ASSSPPIDAATAEPYGFR	2.80
Filamin-A	FLNA	NYPQ	GSQQTWIPER	4.24
Lysosomal alpha-glucosidase	LYAG	IPLQ	GPSLTTTESR	5.13
Exosome Complex Component RRP45	EXOS9	VSVQ	GEEVTLYTPEER	0.79
DNA-directed RNA polymerase II subunit RPB2	RPB2	IDLQ	AEAQHASGEVEEPPR	1.25

(Figure 3.4B and Table 3.5). This data suggests that these proteins may be strategic targets for enterovirus infection. One common protein, heat shock protein beta-1, was identified in both CVB3 $3C^{pro}$ and poliovirus $3C^{pro}$ high confidence substrate lists, and thus may also serve as a common enterovirus $3C^{pro}$ substrate but is cleaved at different sites (Figure 3.4B and Table 3.6). Interestingly, we identified five common peptides between poliovirus $3C^{pro}$ and CVB3 $2A^{pro}$ (Figure 3.4A and Table 3.5), and an additional three common proteins (Figure 3.4B and Table 3.7). No common peptides were identified between CVB3 $3C^{pro}$ and CVB3 $2A^{pro}$ (Figure 3.4A); however, one common high confidence substrate, Actin, was identified at the protein level (Table 3.8). Thus, there may be additional proteins that serve as substrates for both enterovirus $3C^{pro}$ and $2A^{pro}$.

An analysis of poliovirus $3C^{pro}$ high confidence substrate peptides revealed a strong preference for glutamine, proline and alanine at the P1, P2 and P4 position, respectively, which is consistent with the consensus cleavage sites within the polyprotein (Figure 3.5A) (5). However, there is flexibility at the P1' position, showing preferences for alanine, methionine, and glutamine, in addition to the preferred glycine. Similarly, CVB3 $3C^{pro}$ shows a strong preference for glutamine at the P1, as well as the small amino acid alanine, in addition to glycine, at P1', and hydrophobic amino acids at P4 (Figure 3.5B). The CVB3 $2A^{pro}$-identified peptides showed a more variable consensus cleavage site in contrast to its consensus cleavage site within the viral polyprotein (Figure 3.5C). In summary, the TAILS approach has identified several novel candidate substrates and revealed flexibility in the cleavage site of $3C^{pro}$ and $2A^{pro}$ beyond the previously reported consensus sequence.

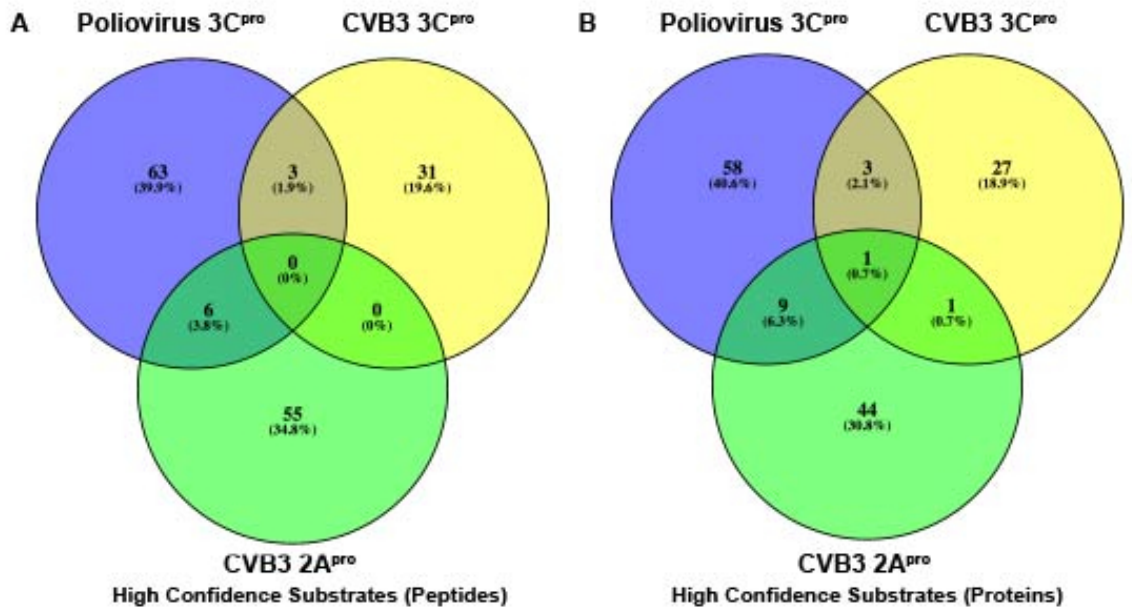

Figure 3.4 Venn diagram of high confidence substrates of poliovirus 3C^{pro}, CVB3 3C^{pro}, and CVB3 2A^{pro}.

Venn diagram illustrating the percentage of (A) common high confidence peptides and (B) common high confidence proteins between poliovirus 3C^{pro}, CVB3 3C^{pro}, and CVB3 2A^{pro}.

Table 3.4 Common high confidence poliovirus 3C^{pro} and CVB3 3C^{pro} peptides identified by TAILS

Protein Description	Gene	P4-P1	TAILS Peptide	Log2 H/L Ratio PV	Log2 H/L Ratio CVB3
Heterogeneous nuclear ribonucleoprotein K	HNRNPK	YEPQ	GGSGYDYSYAGGR	4.39, 4.29	3.35
Phosphoribosylformylglycinamidine synthase	PFAS	VQVQ	GDNTSDLDFGAVQR	4.94, 4.16, 3.62	3.81
hetergeneous nuclear ribonucleoprotein M	HNRNPM	IAKQ	GGGGAGGSVPGIER	4.75	3.35

Table 3.5 Common high confidence poliovirus $3C^{pro}$ and CVB3 $2A^{pro}$ peptides identified by TAILS

Protein Description	Gene	P4-P1	TAILS Peptide	Log2 H/L Ratio PV $3C^{pro}$	Log2 H/L Ratio CVB3 $2A^{pro}$
Beta-1,3-galactosyl-O-glycosyl-glycoprotein beta-1,6-N-acetylglucosaminyltransferase 7	GCNT7	KDAP	GATPNAGWEGNVR	4.74	272.81
Coiled-coil domain-containing protein 94	CCDC94	QEED	EQETAALLEEAR	0.56	1.21
Enoyl-CoA hydratase, mitochondrial	ECHS1	WRPF	ASGANFEYIIAEKR	0.64	1.21
Heat schock 70 kDa protein 1A/1B	HSPA1B	VGVF	QHGKVEIIANDQGNR	0.43	1.95
LIM and SH3 domain protein 1	LASP1	PVAQ	SYGGYKEPAAPVSIQR	1.22	1.16
Small acidic protein	SMAP	KINE	ELESQYQQSMDSLKSGR	4.75	4.69

Table 3.6 Common high confidence poliovirus $3C^{pro}$ and CVB3 $3C^{pro}$ proteins identified by TAILS

Protein Description	Gene	Virus	P4-P1	TAILS Peptide	Log2 H/L Ratio
Heat schock protein beta-1	HSPB1	CVB3	ATAE	GPAAVTLAAPAFSR	0.77
		PV	LATQ	SNEITIPVTFESR	4.99

Table 3.7 Common high confidence poliovirus $3C^{pro}$ and CVB3 $2A^{pro}$ proteins identified by TAILS

Protein Description	Gene	Proteinase	P4-P1	TAILS Peptide	Log2 H/L Ratio
Annexin A5	ANXA5	2A	KDAP	GATPNAGWEGNVR	4.74
		3C	DKYM	TISGFQIEETIDR	0.57
Tubulin alpha-1B chain	TUBA1B	2A	WRPF	ASGANFEYIIAEKR	0.64
		3C	AVCM	LSNTTAIAEAWAR	0.90
Fructose-bisphosphate aldolase A	ALDOA	2A	VPLA	TNGETTTQGLDGLSER	1.17
		3C	AGTN	GETTTQGLDGLSER	0.55

Table 3.8 Common high confidence CVB3 $3C^{pro}$ and CVB3 $2A^{pro}$ proteins identified by TAILS

Protein Description	Gene	Proteinase	P4-P1	TAILS Peptide	Log2 H/L Ratio
Actin, cytoplasmic 1	ACTB	2A	LTER	GYSFTTTAER	13.44
		2A	LSGG	TTMYPGIADR	1.29
		3C	MVGM	GQKDSYVGDEAQSKR	1.84
		3C	ELPD	GQVITGNER	1.60
		3C	PRHQ	GVMVGMGQKDSYVGDEAQKSR	282.36, 361.3, 168.98

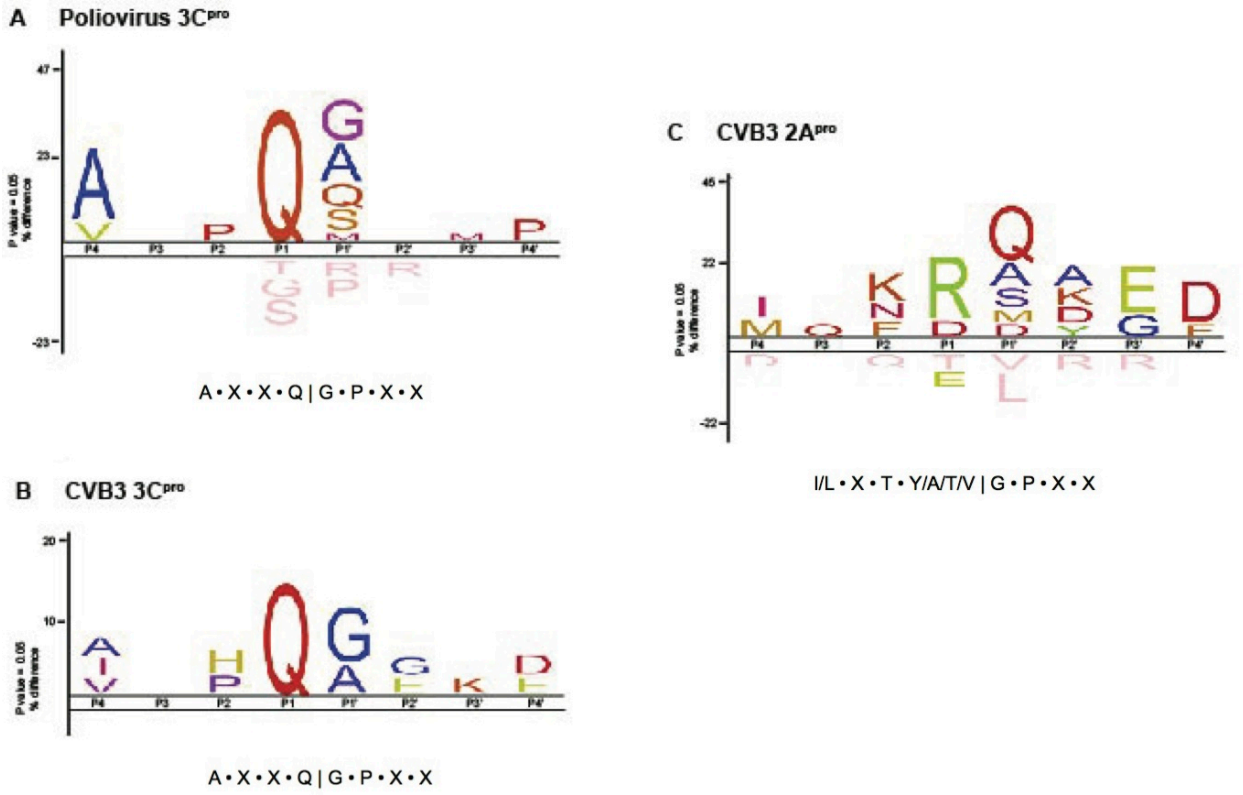

Figure 3.5 Consensus cleavage site analysis of $3C^{pro}$ and $2A^{pro}$ high confidence substrate peptides. Sequence logos of the four amino acids positioned directly upstream (P1 – P4) and downstream (P1' – P4') of the TAILS-identified peptides for (A) poliovirus $3C^{pro}$, (B) CVB3 $3C^{pro}$, and (C) CVB3 $2A^{pro}$. The consensus sequence derived from known polyprotein cleavage sites is depicted below, where X denotes any amino acid.

3.2.3 Validation of candidate substrates *in vitro*

To confirm whether TAILS-identified candidate substrates are bona fide targets of enterovirus proteinases, I performed a series of *in vitro* experiments using select high confidence candidate substrates of poliovirus $3C^{pro}$. The candidate substrates selected for validation were chosen based on a high H/L ratio, and whether the predicted cleavage site occurred between glutamine-glycine residues or the associated protein had previously characterized functions that may be relevant during virus infection. First, I monitored select candidate substrates by immunoblotting following an *in vitro* cleavage assay. Addition of recombinant poliovirus wild-type but not mutant $3C^{pro}$ in HeLa lysates resulted in cleavage of candidate substrates PFAS, hnRNP K, programmed cell death 6-interacting protein (ALIX), ATP-citrate synthase (ACLY), receptor-interacting serine/threonine-protein kinase 1 (RIPK1), and hnRNP M (Figure 3.6). Cleavage fragments of PFAS, hnRNP K, hnRNP M and ALIX were detected by immunoblotting consistent with the cleavage sites predicted by TAILS (Figure 3.6). For example, the TAILS-generated peptide of hnRNP K predicts cleavage between ^{364}Q|G^{365} to produce N- and C-terminal protein fragments of MW ~40.4 and 11.0 kDa, respectively.

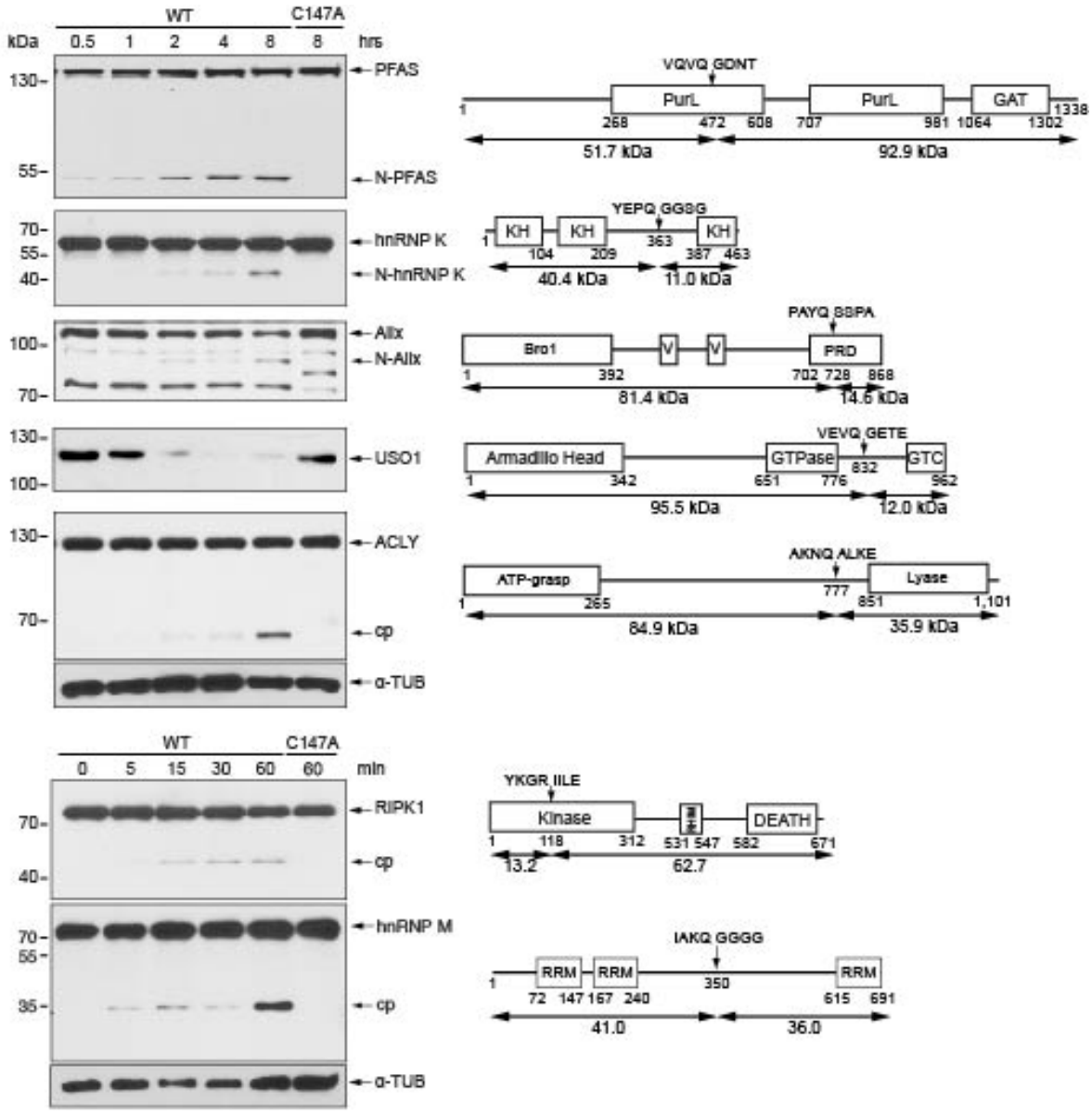

Figure 3.6 Validation of TAILS high confidence substrates by *in vitro* cleavage assay. *Left:* HeLa cell lysates were incubated with purified wild-type or mutant (C147A) poliovirus $3C^{pro}$ (100 ng/ul). Proteins were loaded on an SDS-PAGE and cleavage was assessed by immunobloting. *Right:* Schematics of corresponding high confidence candidate substrates, indicating key domains, the position of TAILS-predicted cleavage sites and the four amino acids position directly upstream (P1-P4) and downstream (P1'-P4') of the cleavage site. The predicted molecular weights of the cleavage protein fragments are shown below. cp, cleavage product; N, N-terminal cleavage product; TUB, tubulin.

Immunoblotting using the hnRNP K antibody detected an N-terminal cleavage fragment of ~40 kDa. The general vesicular transport factor p115 (USO1) antibody did not detect any cleavage products, but showed a loss of full-length protein in lysates incubated with wild-type $3C^{pro}$. In contrast, immunoblotting of ACLY and RIPK1 detected cleavage fragments that were inconsistent with the TAILS-predicted cleavage site, which suggests an alternative cleavage site or $3C^{pro}$-mediated cleavage at multiple sites. In summary, these results strongly suggest that the candidate substrates identified by TAILS are targets of poliovirus $3C^{pro}$.

To confirm the cleavage site identified by TAILS, I generated mutant candidate proteins that contain mutations at the P1 and P1` positions. I subcloned the wild-type or mutant genes into a cytomegalovirus promoter (CMV)-driven mammalian expression vector fused in frame with a 3xFLAG and 3xHA tag at the N- and C-termini, respectively (Figure 3.7A). Cell lysates from HeLa cells expressing either wild-type or mutant FLAG-HA constructs were subjected to the *in vitro* cleavage assay using wild-type or mutant poliovirus $3C^{pro}$. Incubation with poliovirus wild-type but not catalytically inactive $3C^{pro}$ resulted in cleavage of the FLAG-HA-tagged ALIX, hnRNP K, ACLY, PFAS, and hnRNP M (Figure 3.7B). In contrast, mutated versions of these proteins were resistant to cleavage by poliovirus $3C^{pro}$ (Figure 3.7B). The FLAG antibody detected two cleavage products of FLAG-ACLY-HA, at ~63 kDa and ~90 kDa (Figure 3.7B). The larger ~90 kDa cleavage product was not generated from the Q777E/A778P FLAG-ACLY-HA mutant, suggesting that poliovirus $3C^{pro}$ cleaves ACLY at two sites, one at $^{777}Q|A^{778}$, which is the predicted cleavage site from TAILS, and at an additional site that remains to be determined. Mutations at the TAILS-identified cleavage site for FLAG-RIPK1-HA failed to block cleavage, generating a single cleavage product of the same molecular weight as the wild-type version, which suggests that RIPK1 is cleaved at a different site or at multiple sites either

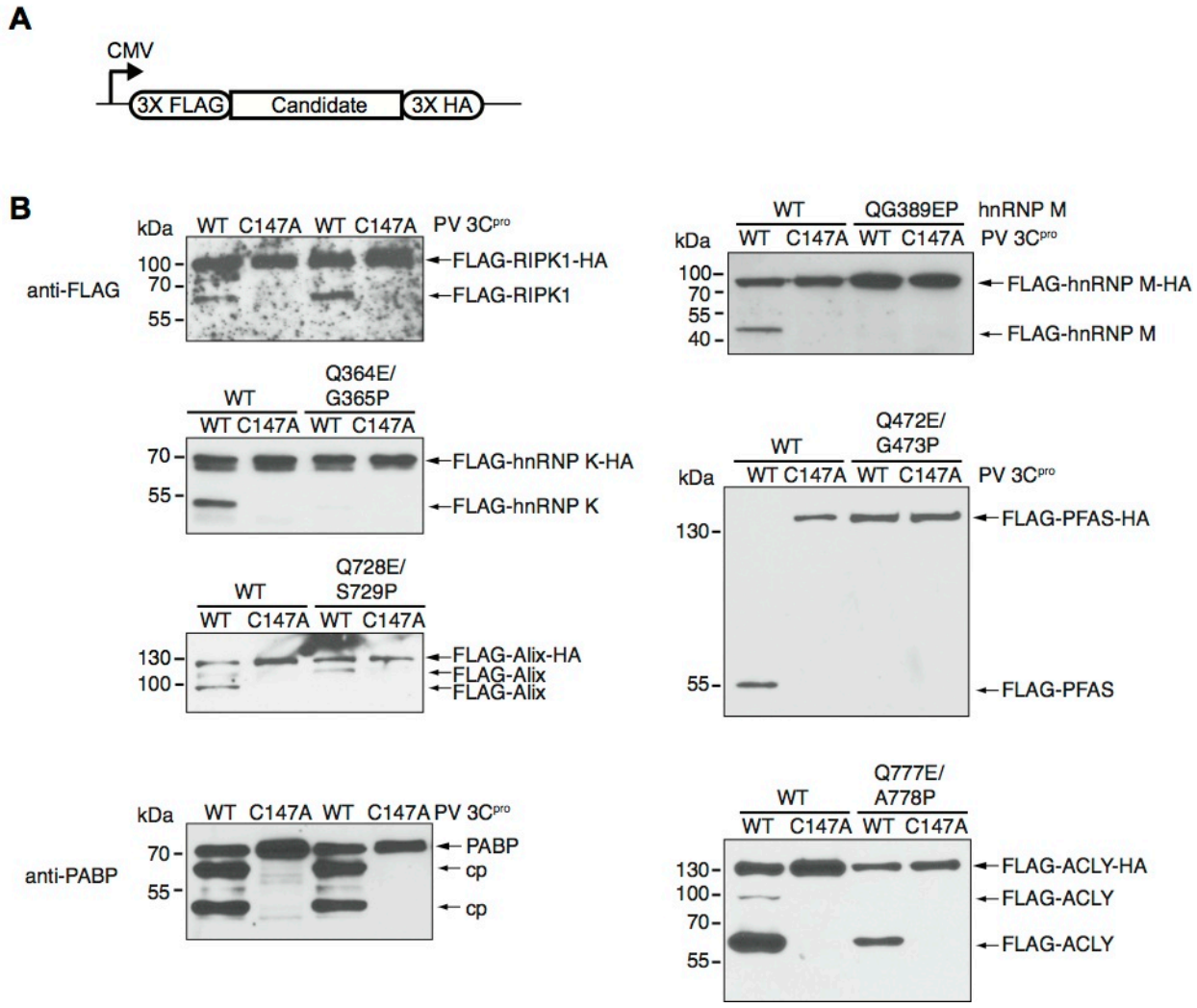

Figure 3.7 Validation of TAILS-predicted cleavage site by *in vitro* cleavage assay. (A) Schematic of cytomegolavirus (CMV) promoter-driven mammalian expression construct containing 3xFLAG and 3xHA fused in frame with the full-length candidate substrate. (B) Lysates from cells expressing the FLAG-HA-tagged wild-type or mutant candidate substrate were incubated with wild-type or mutant poliovirus $3C^{pro}$ and immuoblotted for FLAG or PABP. N, N-terminal cleavage product.

directly or indirectly by $3C^{pro}$. Cleavage of the known poliovirus $3C^{pro}$ PABP was detected in both samples incubated with wild-type $3C^{pro}$, indicating that $3C^{pro}$ was active in samples expressing the FLAG-HA mutant constructs. In summary, these results strongly indicate that most of the candidate substrates are bona fide targets of $3C^{pro}$ and that TAILS can predict their cleavage sites.

3.3 Discussion

Proteolytic cleavage of host substrates by enteroviral proteinases has been established as a key component of a successful virus infection (2, 252, 253). Several host proteins have already been identified as enterovirus $3C^{pro}$ and $2A^{pro}$ substrates that are targeted for cleavage during infection; however, the complete repertoire of their host protein targets still remains elusive. In this study, we applied TAILS using enterovirus $3C^{pro}$ and $2A^{pro}$ to enrich for N-termini peptides and identify novel candidate substrates using quantitative mass spectrometry. This is the first time that TAILS has been used to identify protein targets of a viral proteinase. We have established an *in vitro* cleavage assay using cell lysates to apply TAILS as we have successfully validated $3C^{pro}$-mediated cleavage of seven novel substrates identified by TAILS.

We identified a total of 72, 63 and 34 candidate substrates for poliovirus $3C^{pro}$, CVB3 $2A^{pro}$ and CVB3 $3C^{pro}$, respectively (Figure 3.3). A peptide corresponding to a known $3C^{pro}$ cleavage site for PTB was enriched in our HeLa cell lysates incubated with poliovirus $3C^{pro}$, validating TAILS as a means for identifying substrates of viral proteinases (Table 3.1). Indeed, this is only one of many known host substrates of poliovirus $3C^{pro}$, and no known substrates for CVB3 $3C^{pro}$ in HL-1 cells or CVB3 $2A^{pro}$ in HeLa cells were identified. While TAILS does provide a more comprehensive proteome analysis compared to conventional approaches for

identification of substrates, there are limitations in its ability to cover the entire N-terminal proteome. Protein N-termini may be subjected to post-translational modifications such as acetylation or cyclization, which render them insensitive to dimethylation labeling, and thus would not be detected using TAILS. Moreover, mass spectrometry-based identification of peptides must be of suitable length and be sufficiently ionizable, thus not all $2A^{pro}$- or $3C^{pro}$-derived peptides may be suitable for detection. Indeed, predicted trypsin-digested peptides generated from known $3C^{pro}$ substrates such as G3BP1, PABP, and AUF1 are either too short or too long for efficient ionization and fragmentation to be confidently detected by mass spectrometry (data not shown) (97, 108, 226). Nonetheless, TAILS provides greater proteome wide detection of protease substrates in an unbiased fashion compared to conventional approaches utilized to identify novel substrates of viral proteinases.

Our three-prong TAILS approach to identify candidate substrates of enterovirus proteinases was chosen to inventory common and distinct cleavage specificities. TAILS is a unique mass spectrometry-based approach for identification of protease substrates as it identifies substrates at its cleavage site, providing further insight into the protease active site specificity. Cleavage site analysis of the $3C^{pro}$ and $2A^{pro}$ TAILS-identified cleavage sites of the high confidence candidate substrates deviated from the consensus $3C^{pro}$ and $2A^{pro}$ sites derived from mutagenesis analysis of known cleavage sites within the viral polyprotein (Figure 3.5). Although many of these substrate cleavage sites still need to be verified, these results suggest that $3C^{pro}$ and $2A^{pro}$ are capable of accepting a wider range of amino acids within its active site, allowing for cleavage of a broader range of substrates. Interestingly, we identified three identical peptides between $3C^{pro}$ and $2A^{pro}$ high confidence substrates (Table 3.4). Examples of known host proteins that serve as substrates for both $3C^{pro}$ and $2A^{pro}$ have been previously described;

however, a single cleavage site targeted by both proteases within a common substrates has yet to be identified (92, 161, 187, 200, 201).

Similar findings were observed following cleavage site analysis of CVB3 $3C^{pro}$ high confidence peptides in comparison to poliovirus $3C^{pro}$, suggesting that both viral proteinases possess a similar substrate specificity and may hijack similar cellular pathways through proteolytic cleavage to facilitate infection (Figure 3.5A and 3.5B). Indeed, we have identified common peptides from three proteins among CVB3 and poliovirus $3C^{pro}$ high confidence substrates, whereby the TAILS-identified cleavage site occurred between glutamine and glycine residues (Table 3.4). Several known host protein substrates have already been identified as common targets of both poliovirus and CVB3 $3C^{pro}$ (251); however, it is unclear to what extent all known host protein substrates are commonly cleaved substrates among all enteroviruses, and to what extent substrate specificity is retained among all common substrates. We identified one common protein between poliovirus $3C^{pro}$ and CVB3 $3C^{pro}$ by two different peptides, suggesting possible deviations in substrate specificity between poliovirus and CVB3 $3C^{pro}$ (Table 3.6). The complete degradome of host proteins targeted by enteroviral proteinases is also not always consistent among different cell types. For example, cleavage of PCBP2 and PTB has been characterized as key regulators of the switch between translation and replication during poliovirus infection in HeLa cells, and is also cleaved in CVB3-infected HeLa cells (124). In contrast, neither PTB nor PCBP2 is cleaved in HRV16/14-infected human lung fibroblast cells, suggesting that HRV16/14 utilizes a different mechanism to regulate the translation-replication switch in lung cells compared to HeLa cells.

Chapter 4: Characterizing the Functions of Novel 3C^{pro} Substrates during Picornavirus Infection

4.1 Background

In the previous chapter, we applied TAILS to identify novel substrates of enterovirus proteinases from poliovirus and CVB3 (Chapter 3). From the list of high confidence candidate substrates, I validated seven candidate substrates as novel targets of poliovirus 3C^{pro} cleaved *in vitro* from HeLa cell extracts (Figure 3.6). The challenge now is to examine whether these *in vitro* targets of 3C^{pro} are also targeted for cleavage during virus infection, and whether these substrates are physiologically important. Moreover, confirming cleavage of these substrates during infection will validate whether an *in vitro* assay for TAILS can be applied to reveal substrates of viral proteinases that are targeted for cleavage during virus infection. Characterizing these cleavage events during virus infection, as well as assessing the functional significance of cleavage, will provide initial insights into the roles these host proteins may play during infection. Furthermore, it may elucidate new mechanisms for how picornavirus infection may contribute to disease pathogenesis.

In this chapter, I continue to address Aims 2 and 3 for six of the poliovirus 3C^{pro} substrates that I validated *in vitro*: hnRNP K, PFAS, ALIX, ACLY, RIPK1, and USO1. Based on previously characterized functions of these proteins, they may potentially serve important roles during virus infection. For example, hnRNP K is a member of the heterogenous nuclear ribonucleoprotein family of RNA binding proteins, which include many other hnRNP proteins that have previously been shown to function in various aspects of the viral life cycle (107, 108, 125). Moreover, hnRNP K has already been established as a binding factor for the EV71 5'UTR

to facilitate viral replication, and undergoes a nuclear-cytoplasmic relocalization during poliovirus infection and binds to poliovirus genomic RNA (29, 111, 255). Also, USO1 primarily functions in Golgi body vesicle transport, a cellular process known to be disrupted during poliovirus infection (257, 256). I validated these six candidate substrates further by demonstrating cleavage of these substrates in poliovirus- and CVB3-infected cells. Furthermore, the mutated candidate substrates resistant to cleavage *in vitro* were also resistant during infection, and cleavage at these TAILS-identified sites were not a result of caspase activity. siRNA-mediated depletion studies reveal functional significance of these substrates in promoting enterovirus infection. Over-expression of cleavage-resistant forms of hnRNP K and USO1 resulted in an increase and decrease in viral titres, respectively, suggesting that the cleavage of these proteins is functionally important for infection. Cleavage of hnRNP K promotes IRES-driven translation, thus demonstrating a viral strategy used to hijack a nuclear RNA binding protein to direct virus infection. USO1 facilitates poliovirus infection as loss of USO1 attenuated viral protein synthesis. Furthermore, USO1 underwent subcellular relocalization and subsequent degradation during infection. In summary, the use of TAILS has provided further insights into the substrate specificity during virus infection, and of the network of cellular processes that modulate virus infection.

4.2 Results

4.2.1 TAILS- generated $3C^{pro}$ candidate substrates are cleaved during virus infection

In chapter 3, I identified a list of high confidence host substrates of poliovirus and CVB3 $3C^{pro}$ *in vitro* using TAILS. To examine whether the cleavage of these substrates occur during virus infection, HeLa cells were either mock- or poliovirus-infected, harvested at different times

after infection, followed by immunoblotting (Figure 4.1A). At an MOI of 10, VP1 expression increased during the course of poliovirus infection. Moreover, cleavage of G3BP1, a known substrate of $3C^{pro}$, was observed starting at 3 hours post infection (h.p.i.), producing the expected cleavage product (226). Similarly, cleavage fragments of ALIX, ACLY, hnRNP K, RIPK1 and PFAS were detected as early at 3 or 5 h.p.i. (Figure 4.1A). Unlike the decrease in full-length G3BP1 during infection, there was not a detectable decrease in full-length proteins, ALIX, ACLY, hnRNP K, RIPK1 and PFAS. The one exception is USO1 as its full-length version decreased dramatically and was barely detected at 7 h.p.i.. No cleavage fragments of USO1 were detected by this antibody, similar to that observed *in vitro* (Figure 3.6). Immunoblotting for RIPK1 detected a smaller protein fragment in infected cells compared to that *in vitro*, consistent with the idea that RIPK1 may have multiple cleavage sites (Figure 3.6 and 3.7B). I also assessed whether any of these candidate substrates were also cleaved in CVB3-infected HL-1 cardiomyocytes. By immunoblotting, I found that RIPK1 and hnRNP K are also cleaved in CVB3-infected HL-1 cells at 12 h.p.i. (Figure 4.1B). These results confirmed that a subset of TAILS-generated candidate targets are cleaved in both poliovirus-infected HeLa cells and CVB3-infected HL-1 cells.

I next assessed whether the mutant candidate substrates that are resistant to $3C^{pro}$ cleavage *in vitro* (Figure 3.7B) were also resistant to cleavage during virus infection. HeLa cells were transfected with either wild-type or mutant FLAG-HA expression constructs followed by poliovirus infection. The FLAG antibody detected stable cleavage fragments of ALIX and hnRNP K during infection, similar to that observed *in vitro*, which suggests that ALIX, PFAS and hnRNP K are only targeted by $3C^{pro}$ (Figure 4.1C). In contrast, several cleavage fragments of FLAG-ACLY were detected that were not observed in the *in vitro* cleavage assay, suggesting

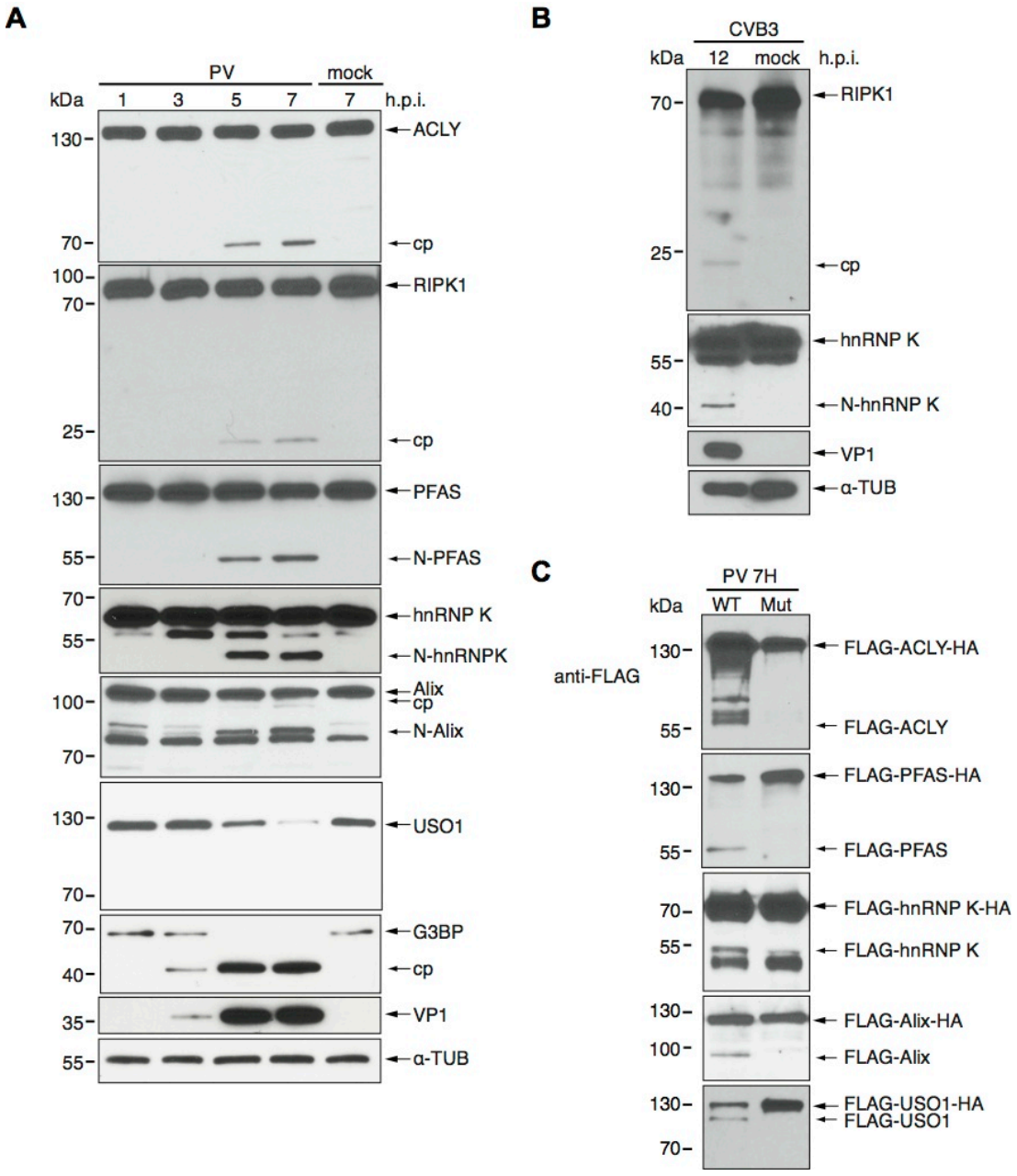

Figure 4.1 Cleavage of candidate substrates during virus infection. (A) HeLa cells were mock or poliovirus-infected (MOI 10) for the indicated times. (B) HL-1 cells were mock or CVB3-infected (MOI 50) for 12 hours. Candidate substrate, viral structural protein VP1, and α-tubulin were assessed by immunoblotting. (C) HeLa cells transfected with wild-type or mutant FLAG-HA constructs of candidate substrates were mock or poliovirus-infected (MOI 10) for 7 hours. Lysates were immunobloted with FLAG. h.p.i., hours post infection. cp, cleavage product; N, N-terminal cleavage product.

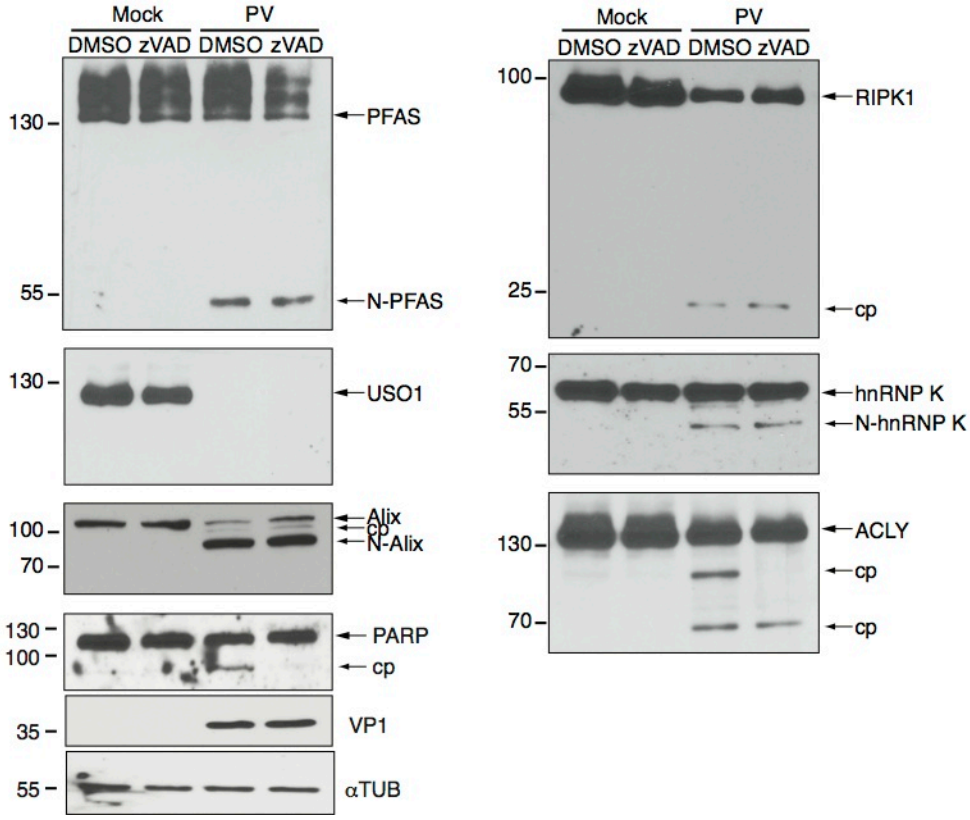

Figure 4.2 Cleavage of candidate substrates in poliovirus-infected HeLa cells in the presence of zVAD-FMK. HeLa cells were infected with poliovirus at an MOI of 10 in the presence or absence of 50 μM zVAD-FMK in poliovirus-infected cells. HeLa cells were infected with poliovirus at an MOI of 10 in the presence or absence of 50 uM zVAD-FMK (7 h.p.i.). Candidate proteins, poliovirus structural protein VP1, PARP and α-tubulin were assessed by immunoblotting.

that this protein is cleaved at multiple sites, by a cellular protease or $2A^{pro}$ during infection. The wild-type FLAG-USO1-HA decreased in expression during infection, similar to that observed using the USO1 antibody; however, here we were able to detect a faint ~100 kDa band, suggesting that the N-terminal cleavage product of USO1 is partially stable during infection. Interestingly, mutant ACLY, PFAS, hnRNP K, and ALIX that are resistant to $3C^{pro}$ cleavage *in vitro* (Figure 3.7) were also resistant to cleavage during infection, as well as the mutant USO1 (Figure 4.1C). Thus, this data demonstrates that these TAILS-generated proteins are targets of $3C^{pro}$-mediated cleavage during virus infection and further confirming that cleavage sites are identified.

To further assess whether the candidate substrates are direct targets of $3C^{pro}$, I subjected infected cells with zVAD-FMK, an inhibitor of pan-caspases, which can be activated during enterovirus infection (170, 171). As shown previously, caspases are activated during enterovirus infections and poly-ADP ribose polymerase (PARP) is cleaved in poliovirus-infected cells (170, 254). PARP cleavage was prevented by z-VAD treatment in poliovirus-infected cells (Figure 4.2). In all other cases, cleavage fragments of the candidate proteins at the TAILS-identified cleavage site were still detected in poliovirus-infected cells treated with zVAD-FMK (Figure 4.2), thus ruling out that cleavage occurs via caspases. Interestingly, a second cleavage product of approximately 90 kDa was observed for ACLY, in addition to the previously observed 65 kDa cleavage product. The 90 kDa cleavage product is of similar size to the TAILS-predicted cleavage product and was not previously observed in the previous experiment shown in Figure 4.1A. Cleavage of the FLAG-ACYL-HA during poliovirus infection revealed multiple N-terminal cleavage products, demonstrating that ACLY may be targeted for cleavage at multiple sites (Figure 4.1C). In addition, this data suggests that cleavage at these multiple sites may not

always occur consistently. Interestingly, while detection of this second cleavage product was still not observed in the presence of zVAD-FMK, the ~90 kDa cleavage product was not. This would suggest that cleavage at the TAILS-identified cleavage site may be caspase-dependent.

4.2.2 Depletion of $3C^{pro}$-targeted candidate substrates affect virus infection

I next explored the biological significance of the candidate substrates during virus infection using an siRNA knockdown approach. Following knockdown of each candidate substrate, the viral yields were measured by plaque assay following poliovirus infection for 7 hours at an MOI of 0.1 (Figure 4.3). Transfection of HeLa cells with substrate specific siRNAs for 24-72 hours led to >90% knockdown of each protein as compared to cells transfected with scrambled siRNAs. Knockdown of hnRNP K, USO1 and RIPK1 led to a 7-,5- and 3-fold decrease in extracellular viral yield, respectively. Similarly, knockdown of hnRNP K and USO1 resulted in a 2- and 5-fold decrease in intracellular viral yield, respectively, indicating a prominent role of these proteins in promoting virus infection. Intracellular viral yields for RIPK1 remained unchanged, indicating a possible role for RIPK1 in viral release. In contrast, knockdown of PFAS resulted in a 4- and 2-fold increase in extracellular and intracellular virus production, respectively suggesting that PFAS may be antiviral. Viral yields following either ALIX or ACLY knockdown resulted in a slight increase and decrease, respectively, in extracellular and intracellular viral titres but with no statistically significant difference. This would indicate that ALIX and ACLY play nonessential roles during infection. In summary, the *in vitro* TAILS approach has revealed novel $3C^{pro}$ substrates that can affect poliovirus infection.

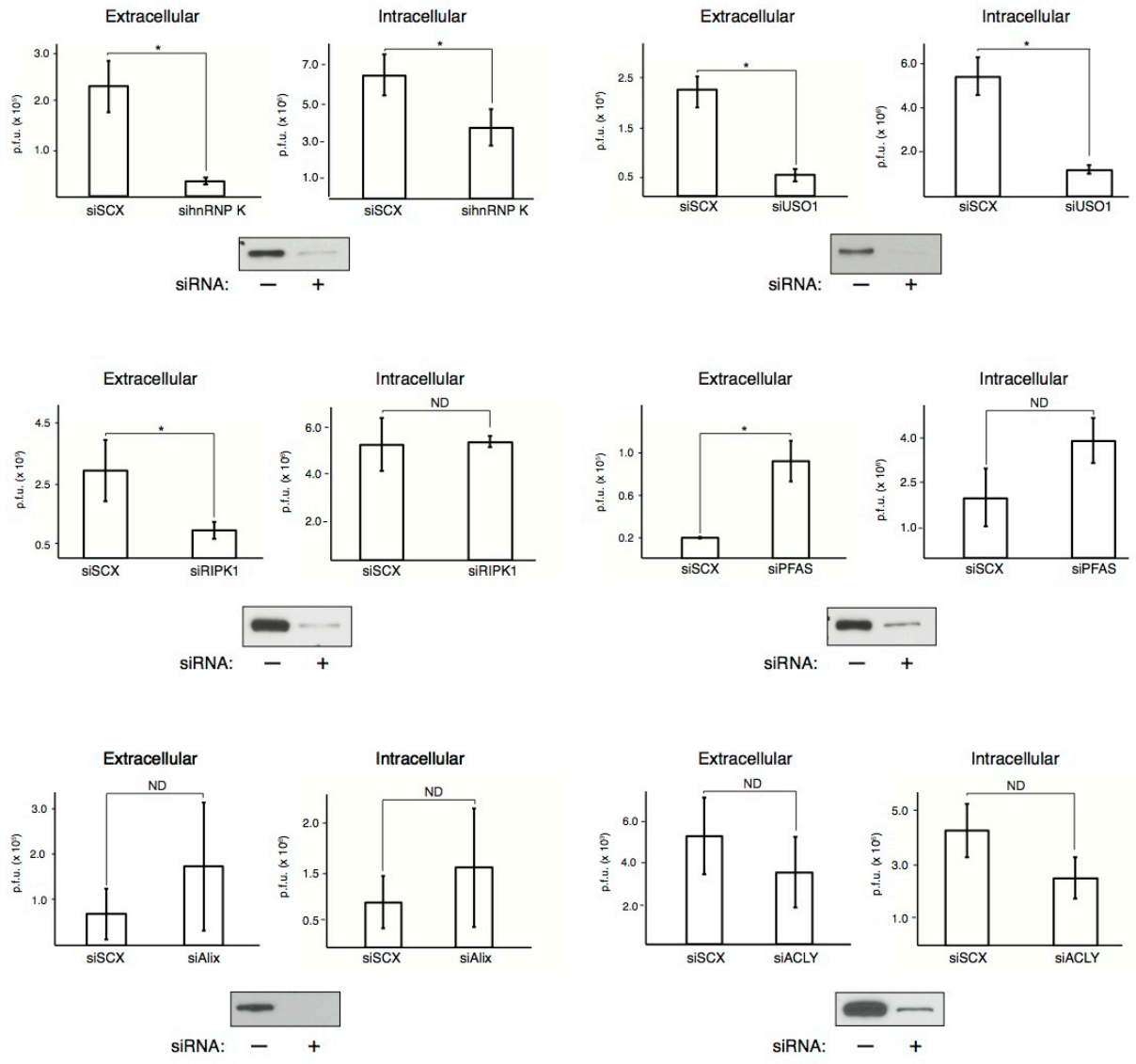

Figure 4.3 Candidate substrates identified by TAILS modulate poliovirus infection. HeLa cells were transfected with either scrambled (siSCX) or candidate specific siRNA for 24-72 hours, followed by poliovirus infection (MOI 0.1) for 7 hours. Extracellular and intracellular virus was titred by plaque assay and titres were calculated as plaque forming units (p.f.u/ml ± s.d., *$p<0.05$) from three independent experiments. ND, no statistical difference, $p<0.05$.

4.2.3 Expression of mutated cleavage-resistant hnRNP K and USO1 affect poliovirus infection

Loss of hnRNP K and USO1 by siRNA knockdown resulted in significant decreases in viral titres, suggesting that both proteins play a facilitative role during poliovirus infection. To determine whether cleavage is important for their putative roles during virus infection, I next measured viral titres by plaque assay following poliovirus infection of HeLa cells over-expressing either a wild-type or a cleavage-resistant form of USO1 or hnRNP K (Figure 4.4). HeLa cells were transfected with wild-type or Q364E/G365P mutant FLAG-hnRNP K-HA constructs for 48 hours, followed by poliovirus infection at MOI 1 for 7 hours (Figure 4.4A). Over-expression of the FLAG-hnRNP K-HA Q364E/G365P mutant led to a slight but not statistically significant 1.5-fold increase in viral titres, suggesting that full-length hnRNP K supports virus infection but not significantly.

The slight difference in viral titres observed for FLAG-hnRNP K-HA may be due to the low expression levels of FLAG-hnRNP K-HA relative to endogenous levels (Figure 4.4A). To increase abundance of recombinant protein relative to the endogenous protein, I subjected HeLa cells over-expressing either an N-terminal GFP-tagged wild-type or cleavage-resistant USO1 to FACS analysis prior to infection (Figure 4.4B). Over-expression of the GFP-USO1 Q832E/G833P mutant led to a consistent decrease in viral titres compared to wild-type GFP-USO1, with an approximate 4 fold decrease observed at 20 h.p.i. This would suggest that cleavage of USO1 is important for infection, and implicates a possible role for its cleavage products during infection. Altogether, this data demonstrates that expression of a cleavage-resistant form can affect virus production, and that cleavage may play a role in regulating the functions of hnRNP K and USO1 during virus infection.

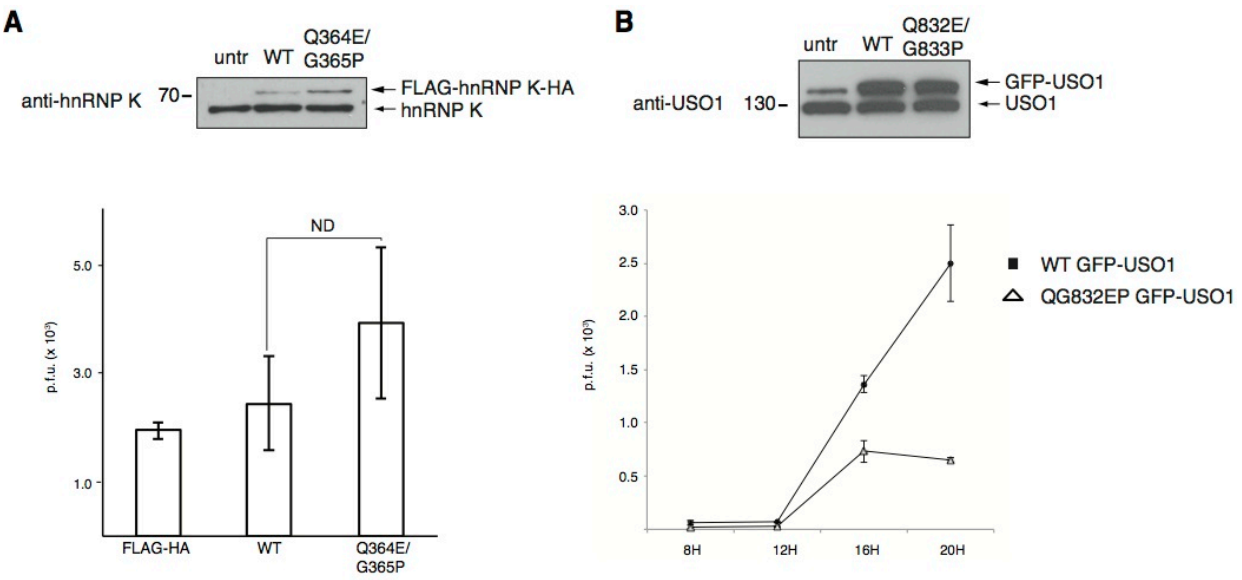

Figure 4.4 Over-expression of cleavage-resistant mutants modulate virus infection. (A) Expression of wild-type and cleavage resistant forms of FLAG-hnRNP K-HA *(top)* and extracellular viral titres following poliovirus infection at MOI 1 for 7 hours in HeLa cells transfected with wild-type or mutant FLAG-hnRNP K-HA *(bottom)*. (B) Expression of wild-type and cleavage resistant forms of GFP-USO1 *(top)* and intracellular viral titres following poliovirus infection at MOI 1 at 8, 12, 16, and 20 h.p.i. in FACS-sorted HeLa cells transfected with wild-type or mutant GFP-USO1 *(botton)*. Titres were measured by plaque assay and calculated as plaque forming units (p.f.u/ml ± s.d., *$p<0.05$) from three independent experiments. ND, no statistical difference, $p<0.05$.

4.2.4 Role of hnRNP K in poliovirus IRES translation

hnRNP M, hnRNP K and PFAS are common substrates of poliovirus and CVB3 $3C^{pro}$, suggesting that they may be strategic cleavage targets that facilitate enterovirus infection. I previously showed that hnRNP M is important for poliovirus infection and that one of its cleavage products may facilitate viral replication (251). hnRNP K has been shown to bind to the 5'UTR of EV71, a related picornavirus (111). Furthermore, hnRNP K has been identified as a putative binding protein for the poliovirus RNA genome (255). To examine more closely whether hnRNP K has a role in poliovirus translation, I monitored poliovirus IRES translation directly by using an IRES-containing reporter construct. The bicistronic reporter construct contains the poliovirus IRES within the intergenic region between the *Renilla* and firefly luciferase genes, which monitor cap-dependent and poliovirus IRES-mediated translation, respectively (Figure 4.5). Because hnRNP K redistributes to the cytoplasm during poliovirus infection (29), I monitored poliovirus IRES translation by transfecting the IRES-containing reporter construct into HeLa cells followed by poliovirus infection. Briefly, cells treated with scrambled or hnRNP K siRNAs for 48 h were transfected with the bicistronic construct for 1 h, followed by mock or poliovirus infection. Cells were then harvested 5 h.p.i., and the luciferase activities were measured.

In mock-infected cells, hnRNP siRNA treatment decreased *Renilla* luciferase activity by ~ 25% compared to scrambled siRNA treatment, indicating that depletion of hnRNP K had a moderate effect on cap-dependent translation using this transfection reporter approach (Figure 4.5). Similarly, firefly luciferase activity was detected at ~50% in hnRNP K siRNA transfected cells compared to scrambled siRNA cells, suggesting that hnRNP K promotes IRES translation. In poliovirus-infected cells, *Renilla* luciferase activity was inhibited more than that in mock-

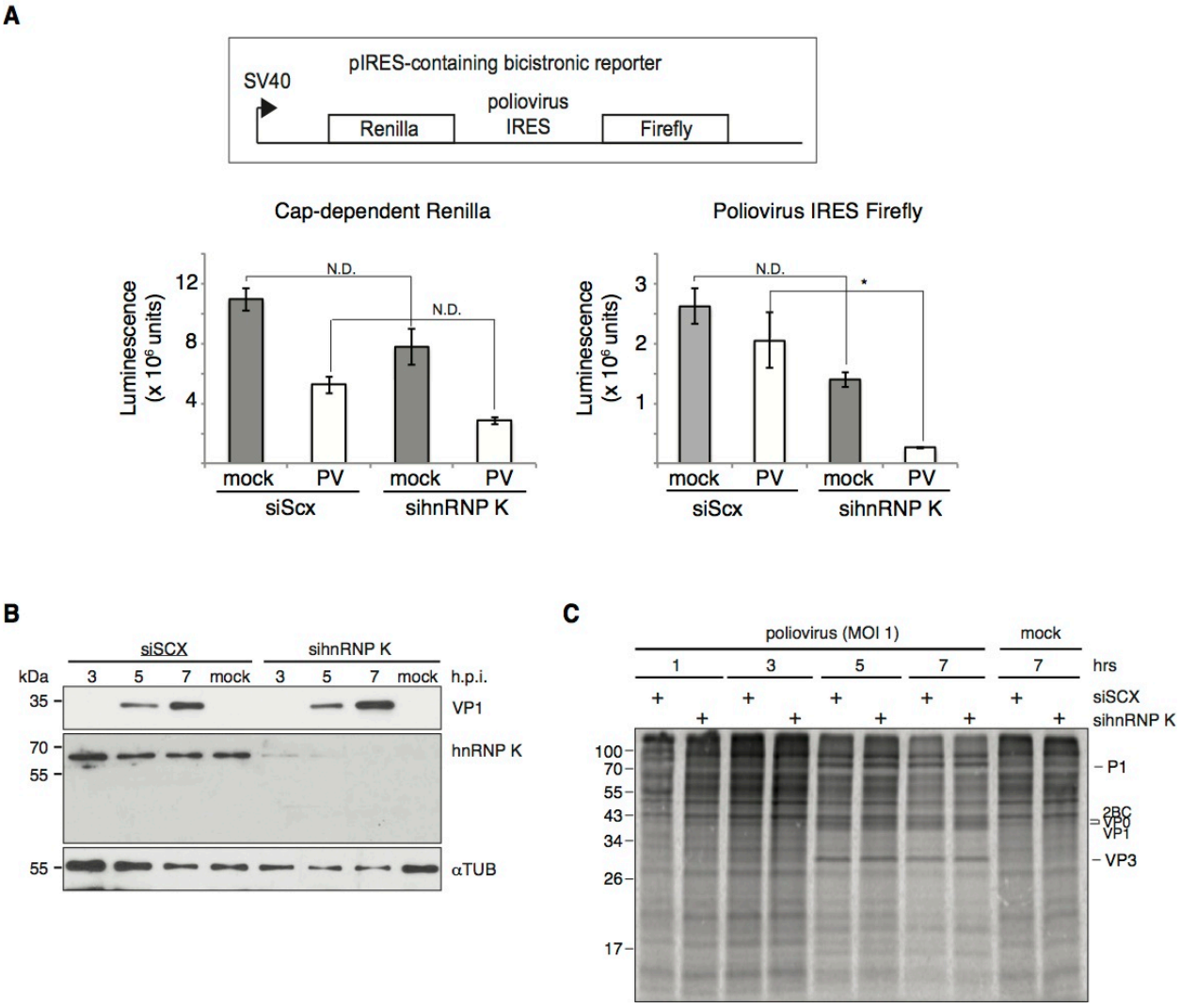

Figure 4.5 Role of hnRNP K in poliovirus IRES translation. (A) A schematic of the bicistronic reporter construct containing the poliovirus IRES within the intergenic region is shown above. Cap-dependent *Renilla* and IRES-mediated firefly luciferase activities of the PV IRES bicistronic reporter construction assessed by measuring luminescence production. Relative luminescence was calculated as a mean ± s.d. of three independent experiments. *p<0.001. (B) HeLa cells were transfected with either scrambled (siSCX) or hnRNP K (sihnRNP K) siRNAs for 48 hours, followed by poliovirus infection (MOI 1) for the indicated times. Immunoblots of hnRNP K, poliovirus structural protein VP1 and α-tubulin are shown. A representative gel is shown from two independent experiments. (C) Pulse-labeling using [S^{35}]-methionine/cysteine at the indicated times after poliovirus infection (MOI 1) in cells treated with siSCX or sihnRNP K for 48 hours prior to infection. A representative gel is shown from three independent experiments.

infected cells, ~50% in hnRNP K siRNA treatment compared to scrambled treatment, which is a reflection of shutoff of host translation during infection (Figure 4.5). In contrast, firefly luciferase activity was dramatically decreased (~10 fold less) in poliovirus-infected cells under hnRNP K siRNA treatment. Together, these results demonstrate that hnRNP K promotes poliovirus IRES translation.

Given that loss of hnRNP K decreases poliovirus IRES activity, I assessed whether loss of hnRNP K affects viral protein production by immunoblot analysis (Figure 4.5A). Scrambled or hnRNP K siRNA-treated HeLa cells were infected with poliovirus at an MOI 1, and synthesis of the viral structural protein VP1 was monitored over time by immunobloting. As previously observed, hnRNP K siRNA treated cells resulted in a significant loss of full-length hnRNP K. Interestingly, no significant difference was observed between VP1 levels in scrambled-treated cells in comparison to hnRNP K siRNA-treated cells. Similar results were observed in poliovirus infected cells (MOI 1) pre-treated with hnRNP K siRNAs that were pulse-labeled with [S^{35}]-methionine/cysteine for 30 minutes prior to harvesting at the times indicated (Figure 4.5B). Similar to hnRNP M, loss of hnRNP K did not significantly affect overall protein synthesis as compared to scrambled siRNA-treated cells during mock infection. No difference in synthesis of viral proteins P1, VP0, VP3, VP1 and 2BC was observed between scrambled and hnRNP K-siRNA treated cells, which is consistent with the result observed in Figure 4.5B. Thus, while hnRNP K does alter poliovirus IRES activity, it does not significantly affect viral protein synthesis.

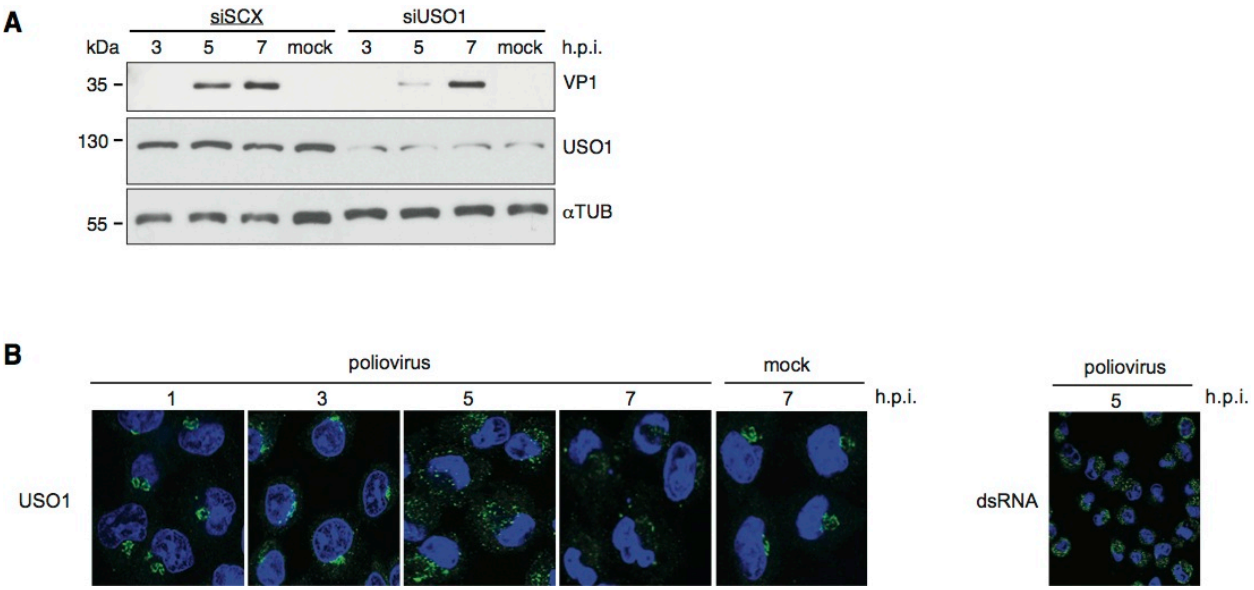

Figure 4.6 USO1 facilitates viral protein synthesis and relocalizes during poliovirus infection. (A) HeLa cells were transfected with either scrambled (siSCX) or USO1 (siUSO1) siRNAs for 48 hours, followed by poliovirus infection (MOI 1) for the indicated times. Immunoblots of USO1, poliovirus structural protein VP1 and α-tubulin are shown. A representative gel is shown from three independent experiments. (B) HeLa cells were mock- or PV-infected (MOI 10) for the indicated times (left). Cells were permeabilized, fixed and co-stained for USO1 (green) and DNA (Hoescht). An image of HeLa cells stained for viral RNA using an anti-dsRNA antibody at 5 h.p.i. is shown to demonstrate the efficiency of infection at an MOI of 10 (right). Representative confocal images are shown from at least three independent experiments.

4.2.5 Subcellular rearrangement of USO1 during poliovirus infections

USO1 is a Golgi-associated protein that functions in vesicle transport from and within the Golgi body, as well as functions in Golgi biogenesis (256, 257). I have previously demonstrated that USO1 is cleaved to near completion during poliovirus infection (Figure 4.1) and that loss of USO1 by siRNA knockdown results in a decrease in viral production (Figure 4.3), while over-expression of a cleavage resistant form increases viral titres (Figure 4.4). This data suggests that the full-length USO1 plays a facilitative role during poliovirus infection. To support this data, I next assessed whether loss of USO1 decreases viral protein production by immunoblot analysis (Figure 4.6). Synthesis of VP1 was monitored over time throughout poliovirus infection in HeLa cells pre-treated with either scrambled or USO1 siRNA. Loss of USO1 showed a delay in VP1 synthesis, most noticeably at 5 h.p.i. This demonstrates that loss of USO1 attenuates viral protein accumulation, and further supports our hypothesis that USO1 facilitates poliovirus infection.

To further characterize USO1 during poliovirus infection, I next assessed whether its subcellular localization as a Golgi-associated protein changes during poliovirus infection by immunofluorescence (Figure 4.6B). In mock-infected cells, USO1 was predominantly localized in a single cluster adjacent to the nucleus, similar to the subcellular localization of known Golgi-associated proteins GM130 and Goglin-97 (258, 259). Upon infection, USO1 disperses into the cytoplasm, beginning at 3 h.p.i. to near complete dissociation at 5 h.p.i. At 7 h.p.i., detection of USO1 is decreased, which correlates with the significant loss in full-length USO1 I observed at 7 h.p.i. by immunobloting (Figure 4.1). Thus, this data demonstrates that USO1 is displaced from its subcellular location and subsequently becomes undetectable during poliovirus infection.

4.2.6 Role for ALIX in autophagy during poliovirus infection

The most well characterized role for ALIX is within the endosomal sorting complexes required for transport (ESRCRT) for the formation of multivesicular bodies for intracellular or extracellular transport; however, recent studies have implicated a role for ALIX in basal autophagy (283, 284). Infection of many picornaviruses leads to the induction of autophagic signals, with the generation of autophagosome-like vesicles late during infection that are visable by electron microscopy (260). These autophagosome-like vesicles have recently been implicated in the vesicle release of a subpopulation of enteroviruses and in the maturation of poliovirus particles into infectious virus (287-9). To explore whether ALIX may function in autophagy during poliovirus infection, I monitored p62 degradation during poliovirus infection following siRNA knockdown of ALIX in HeLa cells (Figure 4.7). Degradation of p62 is a hallmark of autophagic induction and is induced during poliovirus infection (284). Preliminary experiments showed a significant decrease in p62 accumulation at 6 h.p.i.in HeLa cells pretreated with ALIX siRNA compared to SCX control, suggesting that loss of ALIX may enhance autophagic induction. Moreover, this role may not specific to poliovirus infection, as a loss in p62 accumulation was also observed in the mock infected samples (Figure 4.7). However, these results could not be repeated, thus a role for ALIX in autophagy during poliovirus infection still remains unclear.

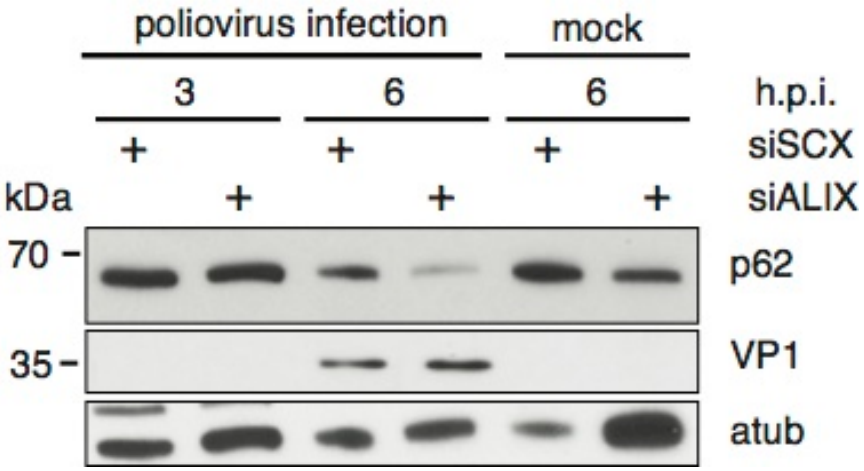

Figure 4.7 Effects on p62 degradation following loss of ALIX during poliovirus infection. HeLa cells were transfected with either scrambled (siSCX) or ALIX (siALIX) siRNAs for 48 hours, followed by poliovirus infection (MOI 50) for the times indicated. Immunoblots of p62, VP1 and α-tubulin are shown.

4.2.7 Role for PFAS in NFκB activation during poliovirus infection

Identical peptides representing PFAS were identified in both poliovirus and CVB3 $3C^{pro}$ TAILS analyses, suggesting that cleavage of PFAS may facilitate a conserved function important for enterovirus infection. PFAS is primarily known as a component of the purine synthesis pathway; however, PFAS has recently been implicated the promotion of gamma herpesviral infections through the inhibition of NFκB-mediated cytokine production (261). I have demonstrated that loss of PFAS leads to a 4-fold increase in poliovirus, which would indicate a possible antiviral role for PFAS during poliovirus infection. To further assess whether PFAS may mediate its antiviral functions through NFκB signalling, I monitored for changes in expression of NFκB signalling proteins IκBα, a negative regulator of NFκB, and p65, a subunit of the NFκB transcription factor complex (Figure 4.8). Upon activation, p65 becomes phosphorylated to promote the formation of additional protein-protein interactions necessary for its transcriptional activity. Preliminary experiments suggested that loss of PFAS during poliovirus infection could modulate expression of IκBα and the phosphorylation of p65 (Figure 4.8). These alterations were also observed during mock-infected conditions, indicating that PFAS function in NFκB activation may not be specific to virus infection. These results; however, could not be repeated, and thus it remains unclear whether PFAS does mediate its antiviral properties through NFκB signalling.

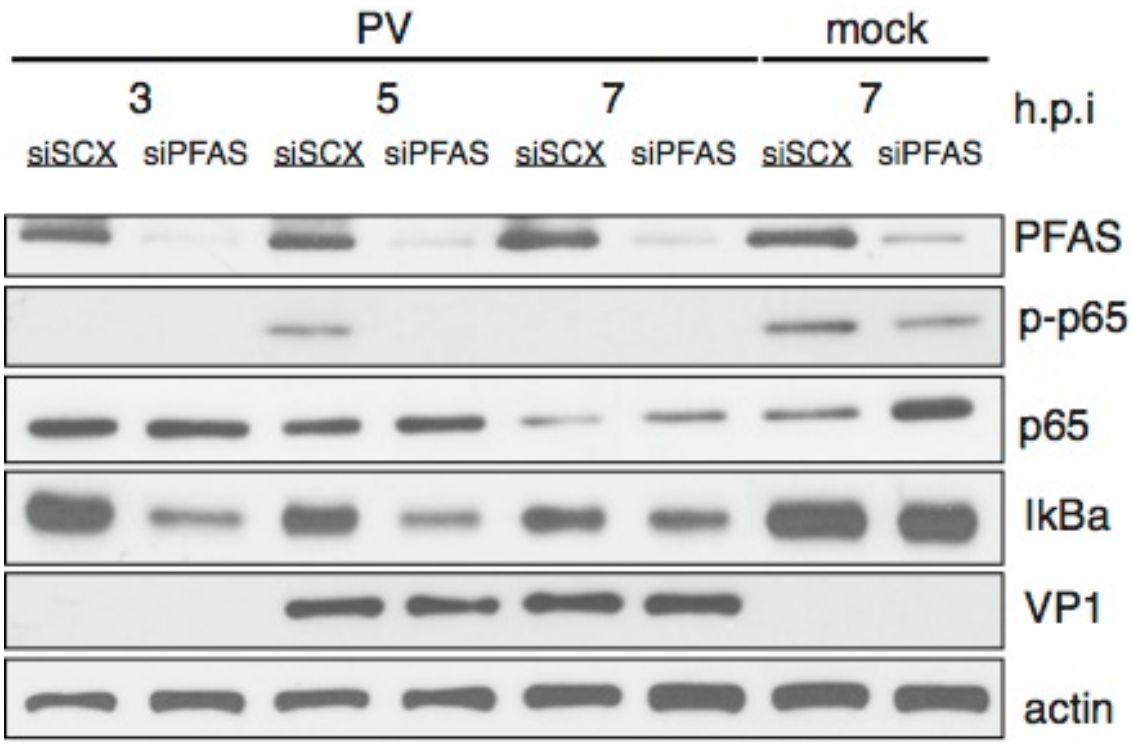

Figure 4.8 Effects on NFκB signalling proteins following loss of PFAS during poliovirus infection. HeLa cells were transfected with either scrambled (siSCX) or PFAS (siPFAS) siRNAs for 48 hours, followed by poliovirus infection (MOI 10) for the times indicated. Immunoblots of PFAS, p65, phosphorylated p65 (p-p65), IκBα, VP1 and Actin are shown.

4.3 Discussion

Although an *in vitro* cleavage assay using cell lysates was used to perform TAILS, I have now demonstrated that this approach can identify several bona fide substrates of $3C^{pro}$ that are targeted for cleavage during virus infection. Importantly, I showed that knockdown of some of these candidate proteins have an affect on viral titres, thus reflecting the power of the TAILS approach in identifying substrates that are important for virus infection. I next aimed to address why these host proteins are targeted for cleavage during infection.

Through validation of select candidate substrates PFAS, hnRNP K, hnRNP M and ALIX, the cleavage products produced by *in vitro* cleavage assays and during virus infection were similar, thus demonstrating 1) the power of TAILS to identify bona fide protein substrates using an *in vitro* cleavage assay from lysates, 2) the substrates are likely mainly cleaved by the viral $3C^{pro}$ and 3) at least some of the cleavage products are stable enough throughout infection to be detected by immunoblotting. In contrast, although showing cleavage by $3C^{pro}$, the cleavage products of RIPK1 and ACLY were not of similar mass *in vitro* compared to during infection. These results suggest that $3C^{pro}$ may cleave at multiple sites within the substrate, or by $2A^{pro}$ or another cellular proteinase. Nevertheless, the *in vitro* cleavage assays indicate that cleavage of these substrates is directed by $3C^{pro}$, again validating the TAILS approach.

I identified hnRNP K, PFAS and hnRNP M as common substrates of poliovirus and CVB3 $3C^{pro}$ among HeLa and HL-1 cardiomyocyte cells using TAILS, and I have shown cleavage of hnRNP K and RIPK1 in poliovirus-infected HeLa cells and CVB3-infected cardiomyocyte. These results support the idea that these proteins play key general roles in enterovirus infection, and that TAILS can be utilized to reveal common substrates among similar viruses.

An outstanding question is why these host proteins are targeted for cleavage by $3C^{pro}$. I have provided some insight into the possible roles of cleavage of candidate substrates in virus infection. Many hnRNPs are targeted by enterovirus proteinases (103, 104, 120, 121, 128, 132). Despite being a cytoplasmic virus, poliovirus infection can lead to redistribution of some hnRNPs from the nucleus to cytoplasm, which then directly or indirectly contribute to virus translation and replication. hnRNP K is an RNA-binding protein that interacts with stem loops I-II and IV of the 5' UTR of EV71 through its KH1, KH2 and proline-rich domains (111, 255). I now reveal that hnRNP K is cleaved during poliovirus infection and acts as a positive regulator of poliovirus IRES translation (Figure 4.5A). Furthermore, over-expression of a cleavage-resistant form of hnRNP K resulted in a slight increase in viral titres compared to wild-type, suggesting that the full-length form may be required for its function. Thus, cleavage of hnRNP K may regulate its ability to facilitate IRES activity, possibly by inhibiting IRES activity mediated by the full-length protein, to promote the switch from viral translation to replication.

Surprisingly, loss of hnRNP K did not result in a similar loss in viral protein synthesis (Figure 4.5B and 4.5C). Previous studies have reported discrepancies among ITAF requirements for IRES activity across picornavirus species. For example, immunodepletion of PTB reduces poliovirus and EMCV IRES activity *in vitro*; however, addition of recombinant PTB into depleted extracts did not restore IRES activity (128). Furthermore, *in vitro* reconstitution of translation initiation for poliovirus, EV71, and bovine enteroviruses IRES activity have shown that PTB had minor stimulatory effects, whereas the presence of PCBP2 was essential (262). Discrepancies among the functional importance of La on HAV IRES translation have also been reported (263, 264). Thus, it is possible that in the context of poliovirus-infected HeLa cells, hnRNP K may only enhance translation efficiency but is not essential for its activity.

Examples of hnRNP K as both a positive and a negative regulator of cellular mRNA translation have been described (265). One of the more well characterized examples of this is the c-src-mediated phosphorylation of hnRNP K to inhibit translational repression of 15-lipoxygenase mRNA, an enzyme required for erythroid cell differentiation, by disrupting hnRNP K binding affinity for its 3'UTR (266-268). Functions for hnRNP K have also been implicated in cell cycle regulation, transcription regulation, and apoptosis (269-272).Thus, it is also possible that cleavage of hnRNP K may disrupt other cellular functions, and disruption of these alternate functions may have varying effects on the viral life cycle.

It is important to note that these observations of hnRNP K-mediated IRES activity are solely based on a bicistronic reporter construct. ITAF requirements for EMCV IRES activity have been show to vary between IRES reporter constructs due to sequence variations (273). Thus, it is important that these results be verified utilizing a different reporter construct with a poliovirus 5'UTR that most closely mimics its most natural and complete sequence, such as a poliovirus minigenome reporter construct that drives luciferase expression utilizing an authentic poliovirus 5' and 3'UTR.

Enterovirus infection induces reorganization of cellular membranes, in part to facilitate the assembly of replication organelles (274). Formation of replication organelles requires recruitment of membrane components such as cholesterol and phosphatidylinositol-4 phosphate from the Golgi body and plasma membrane, as well as enhance synthesis of phosphatidylcholine (275). ACLY functions as the primary enzyme responsible for synthesis of acetyl CoA, which is a precursor for de novo lipid synthesis (276). Thus, cleavage of ACLY may facilitate the hijacking of lipid synthesis pathways to promote formation of replication organelles. However,

its role may be minor as no significant difference in viral titres was observed during poliovirus infection following siRNA-mediated knockdown of ACLY.

Similarly, poliovirus may hijack USO1 function to support formation of replication complexes, as USO1 primarily functions in COPII vesicle transport to the Golgi (256, 277). Previous studies have shown that COPII vesicle budding is increased during poliovirus infection, and that COPII complex proteins associated with the viral protein 2B, which is capable of inducing membrane remodeling when expressed alone in its precursor form as 2BC (278-280). USO1 may also mediate its functions in poliovirus infection through its ability to associate with the COPI protein subunit βCOP during Gogli body biogenesis (281). More recently, COPI-associated proteins have been shown to colocalize more closely with poliovirus replication complexes compared to COPII proteins, suggesting that COPI complex proteins are more likely to be the source of poliovirus replication complex components (282). I have demonstrated that USO1 plays a facilitative role during poliovirus as loss of USO1 decreases viral titres and reduces viral protein accumulation (Figure 4.3 and 4.6A). Moreover, I also demonstrate that USO1 becomes dispersed within the cytoplasm throughout infection (Figure 4.6B). Given that the USO1 detected by immunofluorence was done utilizing the same antibody that only detected the full-length USO1 by immunoblot, the USO1 observed within the cytoplasm at 3, 5 and 7 h.p.i. is the full-length form. At 7 h.p.i, full-length USO1 becomes undetectable by immunoblot and immunofluorescence, which may indicate that USO1 is cleaved to near-completion during poliovirus infection. I hypothesis that USO1 function in its full-length form is subverted into the cytoplasm during virus infection to support viral replication, possibly through facilitating the formation viral replication complexes. The decrease in viral titres I observed following over-expression of a cleavage resistant form would indeed support this hypothesis (Figure 4.4B).

ALIX has been extensively studied for its role in assembly of the ESCRT complex (283). More recently, ALIX has been identified as a binding partner for ATG proteins to promote basal autophagy (284). During virus infection, ALIX function has been predominantly associated with the budding release of enveloped viruses, including HIV and HAV (34, 285, 286). While enteroviruses are considered non-enveloped viruses, a sub population of poliovirus and CVB3 virions have recently been shown to exit the cells in autophagosome-like vesicles prior to cell lysis (287-289). Furthermore, poliovirus induces autophagy, to promote maturation of capsid particles and generate infectious virus particles (290). Thus, ALIX may be acting to promote autophagy during infection, to possibly support the formation of these autophagosome-like vesicles for viral maturation or viral release. Preliminary results suggested that ALIX may inhibit autophagic induction, as noted by an increase in p62 degradation; however, these results could not be repeated (Figure 4.7). Additional experiments can be utilized to assess autophagic activity following loss of ALIX under poliovirus infection, including the post-translational modification of autophagic protein LC3-I into LC3-II and the localization of LAMP-1 and LC3-II to autophagosomic vesicles upon autophagic induction (290, (291).

Enteroviruses utilize proteolytic cleavage to block host antiviral responses (100, 101, 186, 191-196, 203). Cleavage of pathogen recognition receptors, as well as their downstream signalling component, is capable of inhibiting induction of type I interferon responses. RIPK1, a serine/threonine kinase that regulates processes of apoptosis, necrosis, cell survival and innate immune signalling, has recently been characterized as a promoter of pro-inflammatory cytokines (292). NLRP3, a major inflammasome promoter, is cleaved by $2A^{pro}$ and $3C^{pro}$ during EV71 infection, resulting in inhibition of inflammasome activation and a reduction in IL-1β production (196). A similar mechanism of inflammasome inhibition may be occurring in other

enteroviruses, including poliovirus and CVB3. In our studies, I showed that RIPK1 is cleaved during poliovirus infection; however, the cleavage site remains to be determined. Inflammasome inhibition may enhance activation of apoptosis, which has been shown to support coxsackievirus infection (168-169).

Interestingly, the amidotransferase activity of PFAS has recently been shown to promote gamma herpesviral infection by usurping PFAS enzymatic activity to deaminate RIG-I, a pathogen recognition receptor, which ultimately leads to inhibition of antiviral NFκB-dependent cytokine production (293). Cleavage of PFAS during enterovirus infection (this study) could modulate PFAS enzymatic function for similar antiviral purposes. Preliminary experiments suggested that loss of PFAS during poliovirus infection could modulate expression of IκBα and the phosphorylation of p65; however, these results could not be repeated (Figure 4.8). Thus it remains unclear how PFAS may mediate its antiviral properties during poliovirus infection through NFκB, or other antiviral signalling pathways.

Chapter 5: Heterogeneous Nuclear Ribonucleoprotein M Facilitates Enterovirus Infection

5.1 Background

hnRNPs are a family of nucleo-cytoplasmic shuttling RNA-binding proteins that were originally identified based on their association with pre-mRNAs (294). There are approximately 20 hnRNPs, named hnRNP A to U, that all contain at least one RNA-binding domain, either an RNA recognition motif (RRM) or an hnRNP K-homologues (KH) domain. Most hnRNPs are primarily involved in pre-mRNA splicing but they also aid in diverse aspects of RNA metabolism, including translational control, telomere biogenesis, mRNA stability and trafficking (294, 295). hnRNP activity also contributes to different steps of the picornavirus life cycle. For example, hnRNPs A1, I (more commonly known as the PTB) and K interact with the 5'UTR IRES of several picornaviruses to facilitate viral translation and replication (107, 111, 296). Moreover, viral proteinases target a subset of hnRNPs to regulate specific steps of virus infection. PCBP2, also known as hnRNP E2, binds to the poliovirus IRES to facilitate translation initiation; however, at late times of infection, cleavage of PCBP2 by $3C^{pro}$ modifies its association with the 5' UTR to inhibit viral translation and thereby switches to viral replication (125, 297). Thus, poliovirus has evolved a strategy to regulate PCBP2 function via cleavage by $3C^{pro}$ in order to temporally regulate viral translation and replication. Not all hnRNPs are pro-viral, as some hnRNPs have anti-viral effects; hnRNP D, also known as AUF1, binds directly to stem-loop IV of the poliovirus IRES to inhibit viral translation and/or targets the AU-rich region within the 3'UTR for degradation (109, 132, 133). However, in poliovirus- and CVB3-infected cells, this antiviral activity is inhibited through $3C^{pro}$-mediated cleavage of AUF1 (132, 133).

In this chapter, I address Aims 2 and 3 for another candidate substrate identified by TAILS, hnRNP M. I have validated hnRNP M as a novel substrate of both poliovirus and CVB3 $3C^{pro}$. hnRNP M was cleaved in both poliovirus- and CVB3 infected cells and mouse tissues, producing two cleavage products that persisted during infection. I demonstrated that endogenous hnRNP M relocalizes from the nucleus to the cytoplasm during poliovirus infection and that hnRNP M promoted poliovirus and CVB3 infection. Depletion of hnRNP M did not affect IRES translation nor viral RNA stability. In summary, this data reveals a strategy utilized by poliovirus and CVB3 to target hnRNP M by the $3C^{pro}$ to aid in virus infection.

5.2 Results

5.2.1 hnRNP M is targeted by poliovirus 3C proteinase

Using TAILS, we identified a spectra of a neo-N-termini peptide from hnRNP M with a cleavage site at position ^{389}Gln↓Gly (Table 3.1, Figure 5.1A and 5.1B). The ^{389}Q and ^{390}G at P1 and P1` positions, respectively, is consistent with the consensus cleavage site of poliovirus $3C^{pro}$ (68). hnRNP M is a nucleo-cytoplasmic shuttling protein primarily known for its role in pre-mRNA splicing and alternative splicing (298-303). There are 4 alternatively spliced isoforms of hnRNP M derived from a single pre-mRNA transcript, all of which contain three RRMs (304). All four isoforms are highly similar in size and typically migrate as a closely spaced doublet referred to as M1/2 and M3/4 (304). The M4 isoform encodes the longest isoform of 730 amino acids, with a predicted molecular weight of 77 kDa (Figure 5.1A) (304). The M1 isoform encodes a 690 amino acid variant of M4 of 74 kDa, containing a 39 amino acid deletion between RRM1 and RRM2 (304). Notably the same cleavage site sequence is found in all isoforms of

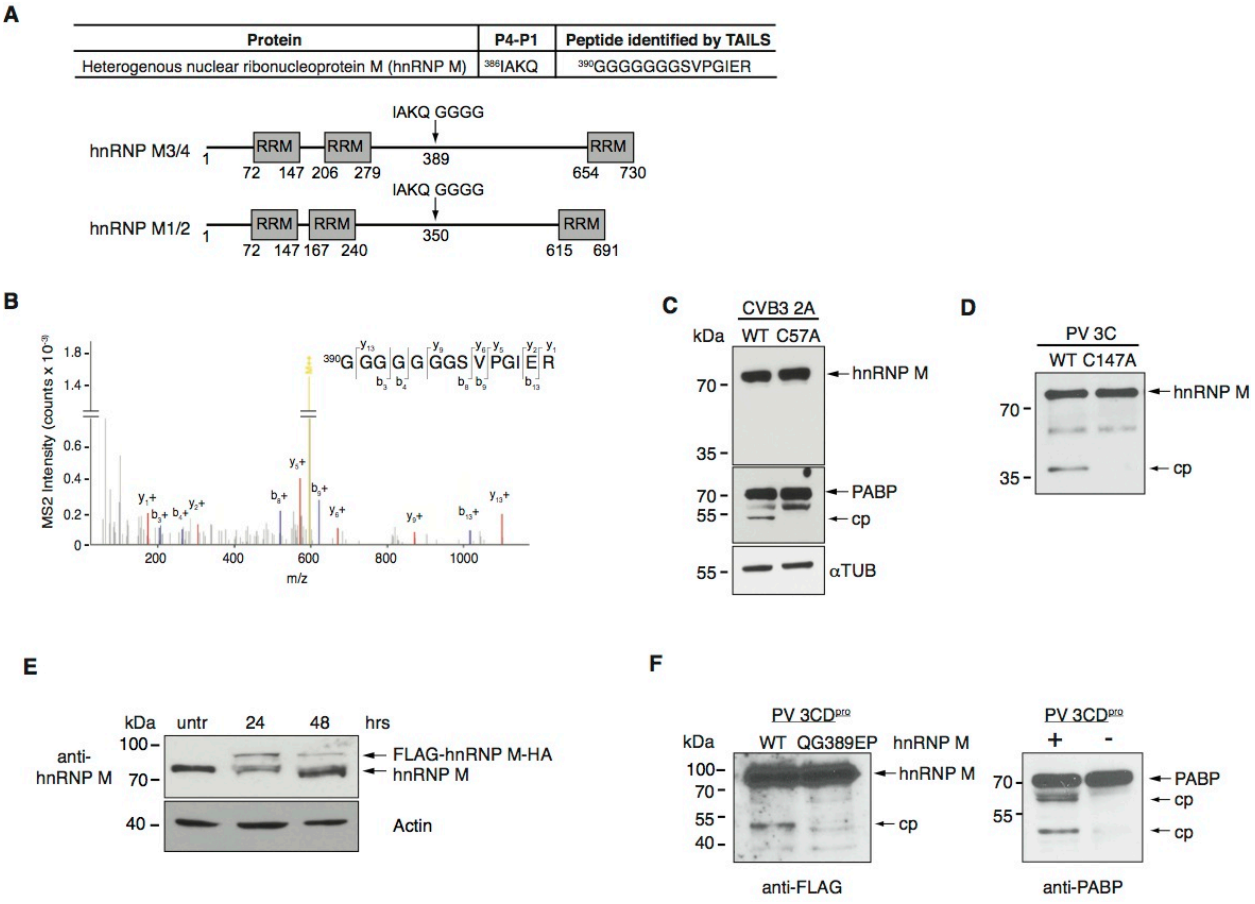

Figure 5.1 hnRNP M is cleaved by poliovirus 3C proteinase *in vitro*. (A) The hnRNP M peptide identified by TAILS is shown, including the four amino acids located directly upstream (P4-P1). Schematic of hnRNP M protein isoforms are shown. RRM - RNA recognition motifs. Arrow denotes the cleavage site of poliovirus $3C^{pro}$. (B) Fragmented spectra of the doubly charged GGGGGGGSVPGIER peptide identified following N-terminal enrichment by TAILS. HeLa cell lysates were incubated with purified wild type or mutant (C109A) CVB3 $2A^{pro}$ (100 ng/μl) for 1 hour (C). hnRNP M, PABP, and α-tubulin were detected by immunblot analysis. (D) Cleavage of recombinant hnRNP M by purified poliovirus $3C^{pro}$. Proteins were loaded on a SDS-PAGE and immunobloted for hnRNP M. (E) Expression of FLAG-hnRNP M-HA in HeLa cells. (F) Lysates from cells expressing the wild type or mutant (Q389E/G390P) tagged hnRNP M (FLAG-hnRNP M-HA) were incubated with wild type or mutant poliovirus $3CD^{pro}$ and immunoblotted for FLAG and PABP. cp - cleavage protein.

hnRNP M (Figure 5.1A). The cleavage site falls between RRM2 and RRM3 at amino acid 389 within the M4 isoform, which would result in two cleavage products of approximately 41 and 36 kDa.

To confirm that hnRNP M is targeted by poliovirus $3C^{pro}$, I used an *in vitro* cleavage assay to validate hnRNP M cleavage in HeLa cell lysates incubated with purified recombinant poliovirus $3C^{pro}$ (Figure 3.6). Incubation of wild-type but not mutant $3C^{pro}$ with lysates resulted in the expected cleavage products of PABP, a known substrate of $3C^{pro}$ (98). Immunoblotting using the hnRNP M (1D8) antibody detected a prominent band at approximately 77 kDa, which corresponds to the mass of the M4 isoform (Figure 5.1A). Addition of the wild-type poliovirus $3C^{pro}$ resulted in the accumulation of a cleavage product of approximately 36 kDa, which was detected as early as 5 minutes of incubation, whereas no cleavage was observed with the mutant $3C^{pro}$ after incubating for 60 minutes (Figure 3.6). Detection of the 36 kDa cleavage product is consistent with the predicted size of the C-terminal protein product generated from cleavage at the site identified by TAILS, suggesting that the 1D8 antibody recognizes the C-terminal half of hnRNP M. Addition of a recombinant CVB3 $2A^{pro}$ to HeLa cell lysates resulted in cleavage of PABP but not hnRNP M, suggesting that cleavage of hnRNP M is $3C^{pro}$-specific (Figure 5.1C). To further assess whether hnRNP M is a direct substrate for $3C^{pro}$, I incubated poliovirus $3C^{pro}$ with purified recombinant hnRNP M. Wild-type $3C^{pro}$, but not the mutant, generated a 36 kDa cleavage product similar to that observed from the *in vitro* cleavage assay (Figure 5.1D). Finally, I confirmed the TAILS-predicted cleavage site by expressing hnRNP M subcloned into a pCMV mammalian expression vector fused in-frame with a 3X FLAG-tag and 3X HA-tag at the N- and C-terminus, respectively (FLAG-hnRNP M-HA, Figure 3.7A and 5.1E). Using the 1D8 hnRNP M antibody, immunoblotting analysis detected two proteins in lysates of cells transfected with

FLAG-hnRNP M-HA, the endogenous hnRNP M at 77 kDa and the slower migrating tagged protein at approximately 84 kDa (Figure 5.1E). Moreover, expression of FLAG-hnRNP M-HA was also detected using a FLAG antibody (Figure 3.7B and 5.1F). The expected molecular weight of FLAG-hnRNP M-HA is approximately 84 kDa. Wild-type, but not the inactive $3C^{pro}$ generated a 43 kDa cleavage product that was detected by anti-FLAG antibody (Figure 3.7B). As predicted, the Q389E/G390P FLAG-hnRNP M-HA mutant was insensitive to $3C^{pro}$ cleavage (Figure 3.7B). Because $3C^{pro}$ is also expressed as 3CD (59), I determined whether $3CD^{pro}$ targets hnRNP M. As shown with $3C^{pro}$, recombinant $3CD^{pro}$ targeted wild-type but not mutant Q389E/G390P FLAG-hnRNP M-HA in the *in vitro* cleavage assay (Figure 5.1H). Taken together, these results demonstrate that hnRNP M is a *bona fide* substrate of poliovirus $3C^{pro}$ and $3CD^{pro}$ and is cleaved directly between amino acid pair ^{389}Q↓G.

5.2.2 hnRNP M is cleaved in poliovirus-infected HeLa cells

To examine whether cleavage of hnRNP M occurs during virus infection, HeLa cells were either mock- or poliovirus-infected, then harvested at different times after infection. Cleavage of PABP was observed beginning at 3 hours post infection, producing the expected cleavage products (Figure 5.2A) (97). Similar to the timing of PABP cleavage, the levels of full-length hnRNP M began to decrease at 3 hours post infection, which is concurrent with the appearance of two proteins at 36 and 39 kDa (Figure 5.2A). By 7 hours post infection, the full-length hnRNP M was completely degraded, whereas the two cleavage products remained detectable throughout infection (Figure 5.2A). The presence of two cleaved proteins suggests that hnRNP M may be cleaved more than once during infection.

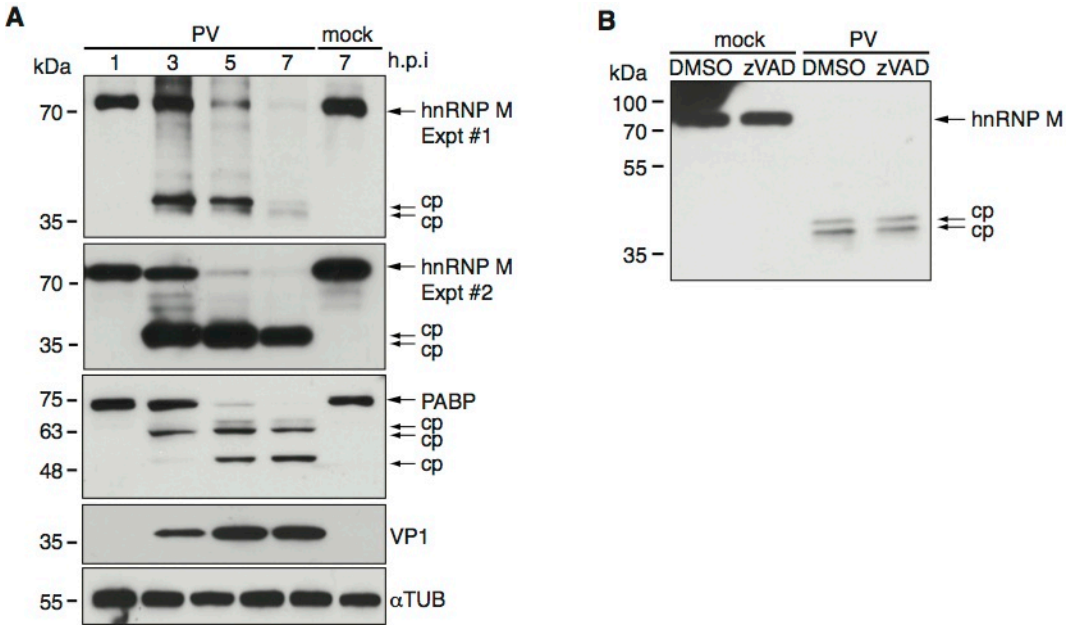

Figure 5.2 Cleavage of hnRNP M in poliovirus-infected HeLa cells. (A) HeLa cells were mock or poliovirus-infected (MOI 10) for the indicated times. (B) Cleavage of hnRNP M is insensitive to zVAD-FMK in poliovirus-infected cells. HeLa cells were infected with poliovirus at an MOI of 10 in the presence or absence of 50 μM zVAD-FMK (7 hours post infection, h.p.i.). hnRNP M was assessed by immunoblot analysis. cp- cleavage proteins. Representative gels are shown from at least two independent experiments.

Apoptosis-induced activation of caspases can occur in picornavirus infections (305, 306). To assess whether cleavage of hnRNP M is a result of caspase activation, poliovirus-infected HeLa cells were incubated in the presence or absence of the general caspase inhibitor, zVAD-FMK. Both hnRNP M cleavage products were still observed in poliovirus-infected cells in the presence of zVAD-FMK, whereas cleavage of poly(ADP) ribose polymerase (PARP), a known caspase-3 substrate, was inhibited (Figure 5.2B). Thus, I demonstrate that hnRNP M is cleaved to completion during poliovirus infection in a caspase-independent manner and that the cleavage products persist during infection.

5.2.3 Subcellular relocalization of hnRNP M in poliovirus-infected cells

hnRNP M is a predominantly nuclear localized protein (307). Thus, it is of interest to determine how hnRNP M is targeted by a cytoplasmic RNA virus. To address this, I monitored the localization of hnRNP M in mock- and poliovirus-infected cells by immunofluorescence confocal microscopy. In mock-infected cells, hnRNP M was predominantly localized to the nucleus, in agreement with its role as a nuclear protein involved in pre-mRNA splicing (Figure 5.3, mock-infected). However, upon infection, hnRNP M underwent a dramatic relocalization to the cytoplasm beginning at 3 hours post infection to near completion at 5 and 7 hours post infection (Figure 5.3, poliovirus-infected). This subcellular redistribution from the nucleus to the cytoplasm is similar to that observed with other hnRNPs such as hnRNP K and A1 during poliovirus infection (29). Given that hnRNP M is cleaved nearly to completion and that the cleaved fragments of hnRNP M persist in poliovirus-infected cells at 5 and 7 hours post infection (Figure 4.2A), the immunoflourescence signal detected in the cytoplasm most likely represents the cleaved forms of hnRNP M.

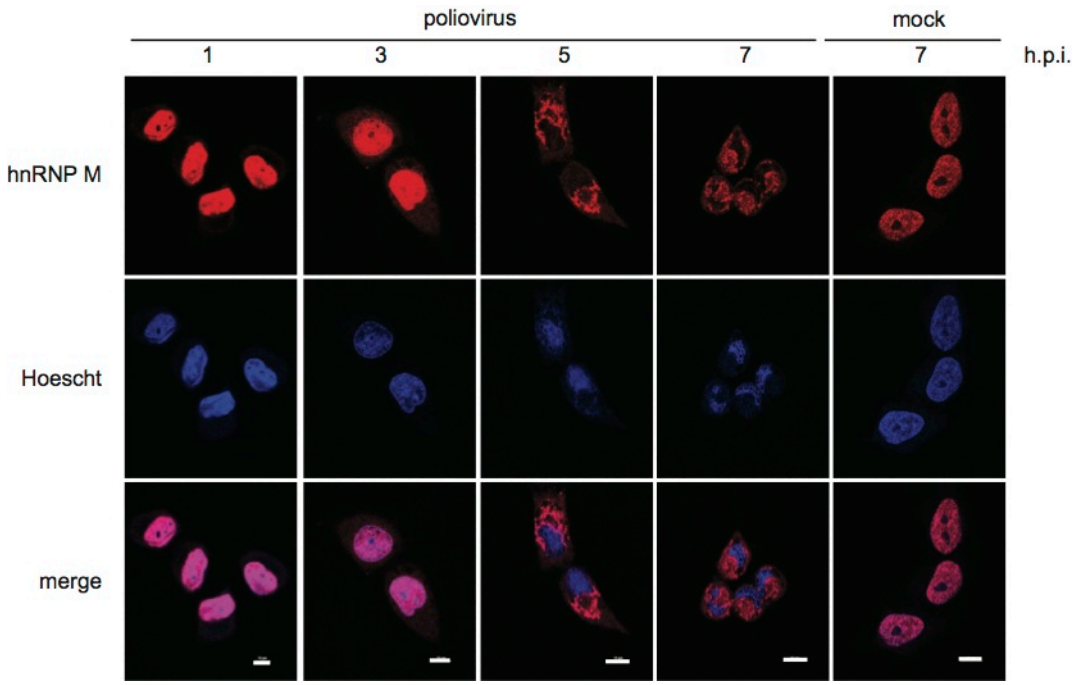

Figure 5.3 Subcellular Localization of hnRNP M in PV-infected HeLa cells. HeLa cells were mock- or PV-infected (MOI 10) for the indicated times. Cells were permeabilized, fixed and co-stained for hnRNP M (red) and DNA (Hoescht). Representative confocal images are shown from at least three independent experiments.

I next assessed the subcellular location of the N- and C-terminal hnRNP M cleavage products during infection. I expressed FLAG-hnRNP M-HA in HeLa cells and monitored the fate of N- and C-terminal cleavage products by FLAG and HA antibodies during infection. As shown in Figure 5.1G, a predominant 84 kDa protein was detected by FLAG and HA antibodies in transfected cells, indicative of FLAG-hnRNP M-HA expression (Figure 5.4B, mock-infected). Expression of FLAG-hnRNP M-HA had a reproducible moderate effect on cell viability in HeLa cells, suggesting that over-expression of hnRNP M is somewhat toxic (Figure 5.4A). When probed with the hnRNP M antibody, both the endogenous hnRNP M and the C-terminal HA-tagged fragment of hnRNP M were detected (Figure 5.4B, long exposure). I then subjected HeLa cells expressing FLAG-hnRNP M-HA to poliovirus infection. Immunoblotting for FLAG detected two N-terminal cleavage products of approximately 44 and 47 kDa at 5 and 7 hours post infection, which is slightly delayed compared to when endogenous hnRNP M is cleaved (Figure 5.4B). It is probable that the over-expression of the tagged hnRNP M delays infection. Interestingly, the HA antibody detected only a single protein at approximately 42 kDa (Figure 5.4B). It is noted that the full-length endogenous hnRNP M and FLAG-hnRNP M-HA were not cleaved to completion as observed in Figure 5.2. It is likely that over-expression of FLAG-hnRNP M-HA may affect the extent of protein processing of endogenous hnRNP M by the virus during infection. Similar to that of the endogenous hnRNP M, the tagged hnRNP M is cleaved and the N- and C-terminal cleavage products persist during poliovirus infection. However, it is noted that the C-terminal tagged HA-hnRNP M is less stable at 7 h.p.i. which is similar to that observed using the hnRNP M antibody for detection.

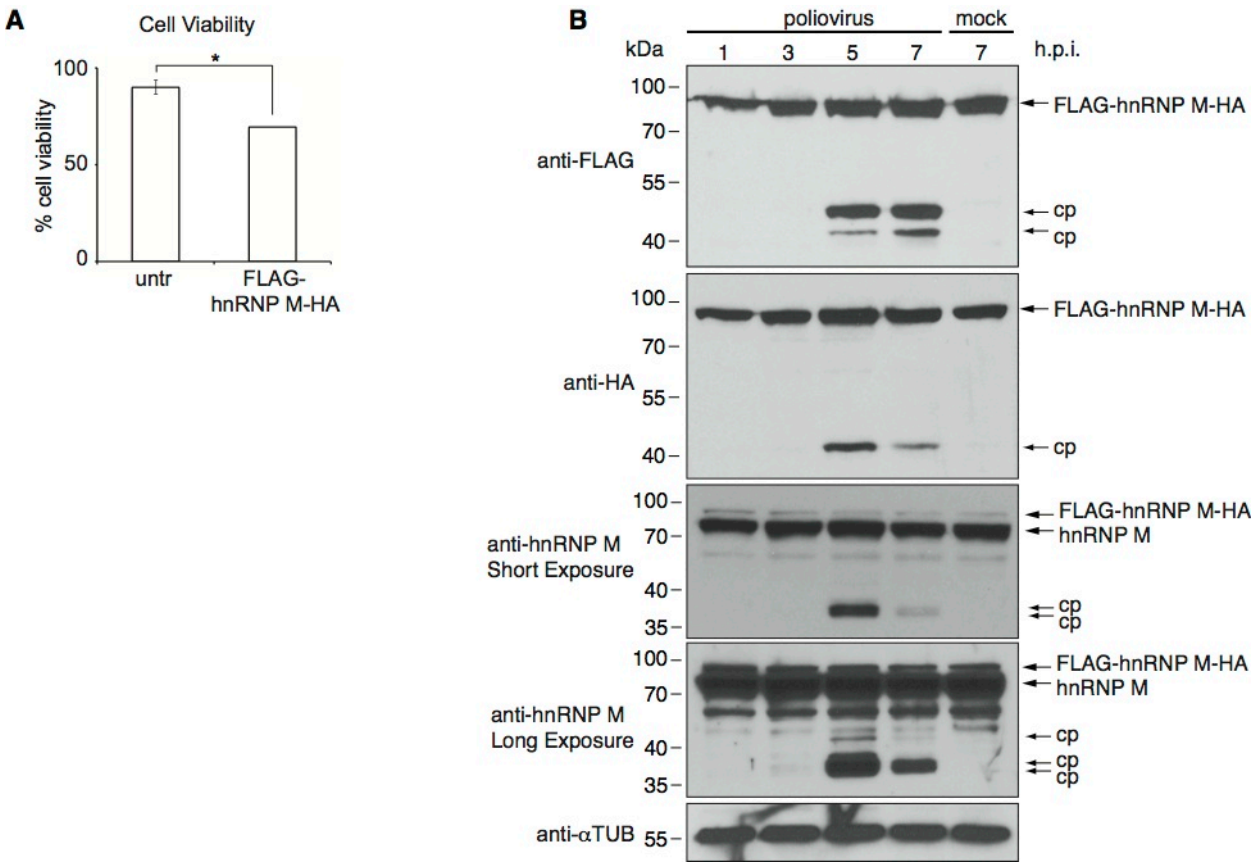

Figure 5.4 Cleavage of hnRNP M in poliovirus-infected cells. (A) Cell viability of cells transfected with FLAG-hnRNP M-HA for 48 hours. Cell viability was assessed by the percentage of cells that are not stained with trypan blue. Averages ± s.d. are shown, *$p<0.05$. (B) HeLa cells transfected with FLAG-hnRNP M-HA were either mock- or poliovirus-infected (MOI 10) for the indicated times. Lysates were immunoblotted for FLAG, HA, hnRNP M and α-tubulin.

I then monitored expression of FLAG-hnRNP M-HA in poliovirus-infected HeLa cells by immunofluoresence, to assess the N- and C-terminal cellular localization of hnRNP M. A dsRNA antibody was used to monitor the accumulation of viral replication intermediates. In mock-infected cells transfected with FLAG-hnRNP M-HA, HA and FLAG signals were detected primarily in the nucleus, similar to nuclear localization of the endogenous protein (Figure 5.5A and B, mock-infected). Beginning at 3 h.p.i., which is the time prior to cleavage of FLAG-hnRNP M-HA, staining for both FLAG and HA tags showed a diffuse cytoplasmic staining (Figure 5.5A and B). FLAG and HA signals accumulated in the cytoplasm at 5 and 7 h.p.i. (Figure 5.5A and B). As expected, dsRNA antibody staining was only detected in the cytoplasm of poliovirus-infected cells (Figure 5.5). Interestingly, no colocalization was observed between either FLAG or HA and dsRNA signals, which would suggest that hnRNP M does not have a direct effect on viral replication. In summary, FLAG-hnRNP M-HA recapitulates the subcellular localization and cleavage pattern of endogenous hnRNP M.

5.2.4 Expression of mutant hnRNP M Q389E/G390P in cells

Our results indicated that mutant Q389E/G390P hnRNP M is resistant to cleavage by poliovirus $3C^{pro}$ (Figure 5.1G). To determine whether this mutant is resistant to cleavage in poliovirus-infected HeLa cells, I transfected the FLAG-hnRNP M-HA construct that contains the Q389E/G390P mutations and followed the fate of the protein by immunoblot analysis. Surprisingly, despite being resistant to $3C^{pro}$ and $3CD^{pro}$ in the *in vitro* cleavage assay, the Q389E/G390P FLAG-hnRNP M-HA was still cleaved at roughly the same time and extent as the wild-type version in poliovirus-infected cells (Figure 5.6A). Furthermore, the cleavage products of mutant and wild-type hnRNP M in infected cells migrated similarly by immunoblot

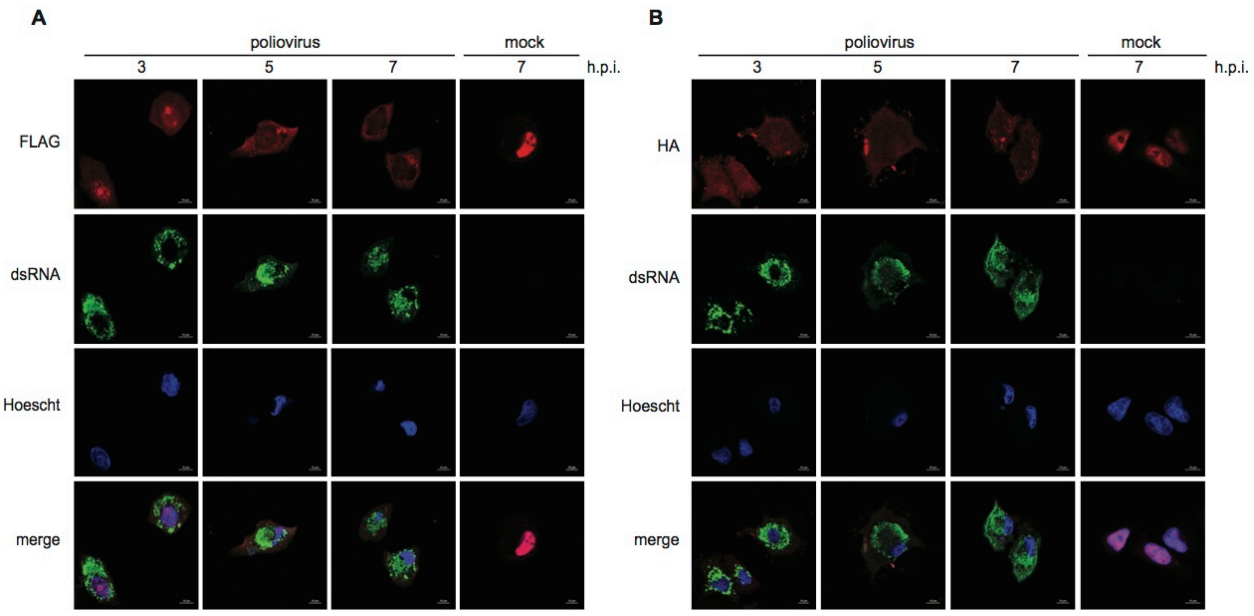

Figure 5.5 Subcellular localization of N- and C-terminal cleavage products of hnRNP M in poliovirus-infected HeLa cells. (A) Subcellular localization of N-terminal and C-terminal cleavage products of hnRNP M. HeLa cells transfected with FLAG-hnRNP M-HA for 48 hours, followed by either mock or poliovirus infection (MOI 10) for the times indicated. Cells were fixed and co-stained for FLAG (red in A) or HA (red in B), dsRNA (green) for detection of virus, and Hoescht (blue). Shown are representative images from at least three independent experiments.

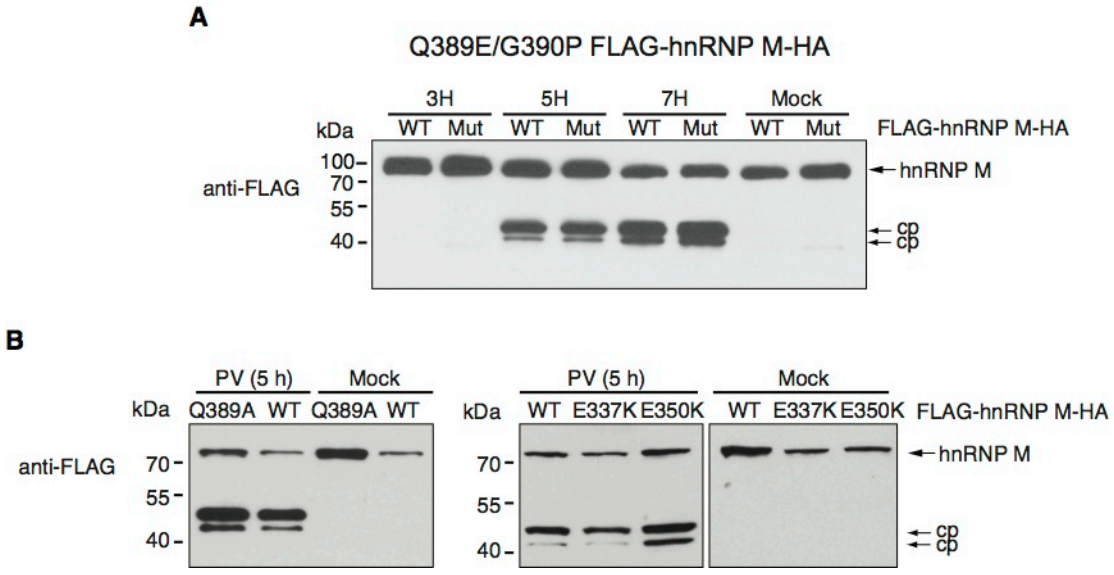

Figure 5.6 Expression of mutant FLAG-hnRNP M-HA in poliovirus infected cells. HeLa cells were transfected with either wild-type or mutant Q389E/G390P (A), or E337K, E350K FLAG-hnRNP M-HA expression plasmids for 48 hours (B), followed by mock- or poliovirus-infection (MOI 1) for the indicated times. Lysates were immunoblotted with anti-FLAG.

analysis. This result suggests that hnRNP M is cleaved at a distinct site(s), likely close to the $3C^{pro}$-sensitive Q389/G390 site. One possibility is that $3C^{pro}$ may cleave at multiple sites on hnRNP M. Surveying for putative 3C proteinase sites nearby, I found two sites at QE336-7 and QE349-50 that if cleaved by $3C^{pro}$ would result in cleavage products similar in mass as that observed during infection. However, expression of mutant FLAG-hnRNP M-HA containing mutations at these sites resulted in cleavage products during poliovirus infection (Figure 5.6B). Nevertheless, I next determined whether the Q389E/G390P FLAG-hnRNP M-HA localized to the same cellular compartments as the wild-type version during poliovirus infection. As observed with endogenous hnRNP M and the wild-type FLAG-hnRNP M-HA, the FLAG and HA signals were predominantly nuclear localized in mock-infected cells and were localized to the cytoplasm in poliovirus-infected cells to the same extent and time as the wild-type protein (data not shown). In summary, these results indicate that although $3C^{pro}$ cleaves between amino acid pair ^{389}Q↓G *in vitro*, hnRNP M is likely cleaved at another site nearby during poliovirus-infected cells. Currently, it is unclear whether the secondary site(s) is cleaved by $3C^{pro}$ or by another protease.

5.2.5 hnRNP M facilitates poliovirus infection

I next explored the significance of hnRNP M during poliovirus infection using a siRNA knockdown approach. Transfection of hnRNP M-specific siRNAs but not scrambled-siRNAs in HeLa cells resulted in loss of hnRNP M protein expression (Figure 5.7A) and did not significantly affect cell viability (Figure 5.7B). Cells transfected with scrambled or hnRNP M siRNAs for 72 hours were then mock- or poliovirus-infected, and virus production was monitored by immunoblot and Northern blot analysis. In scrambled-siRNA treated cells, cleavage of hnRNP M was detected in poliovirus-infected cells at 5 and 7 h.p.i.

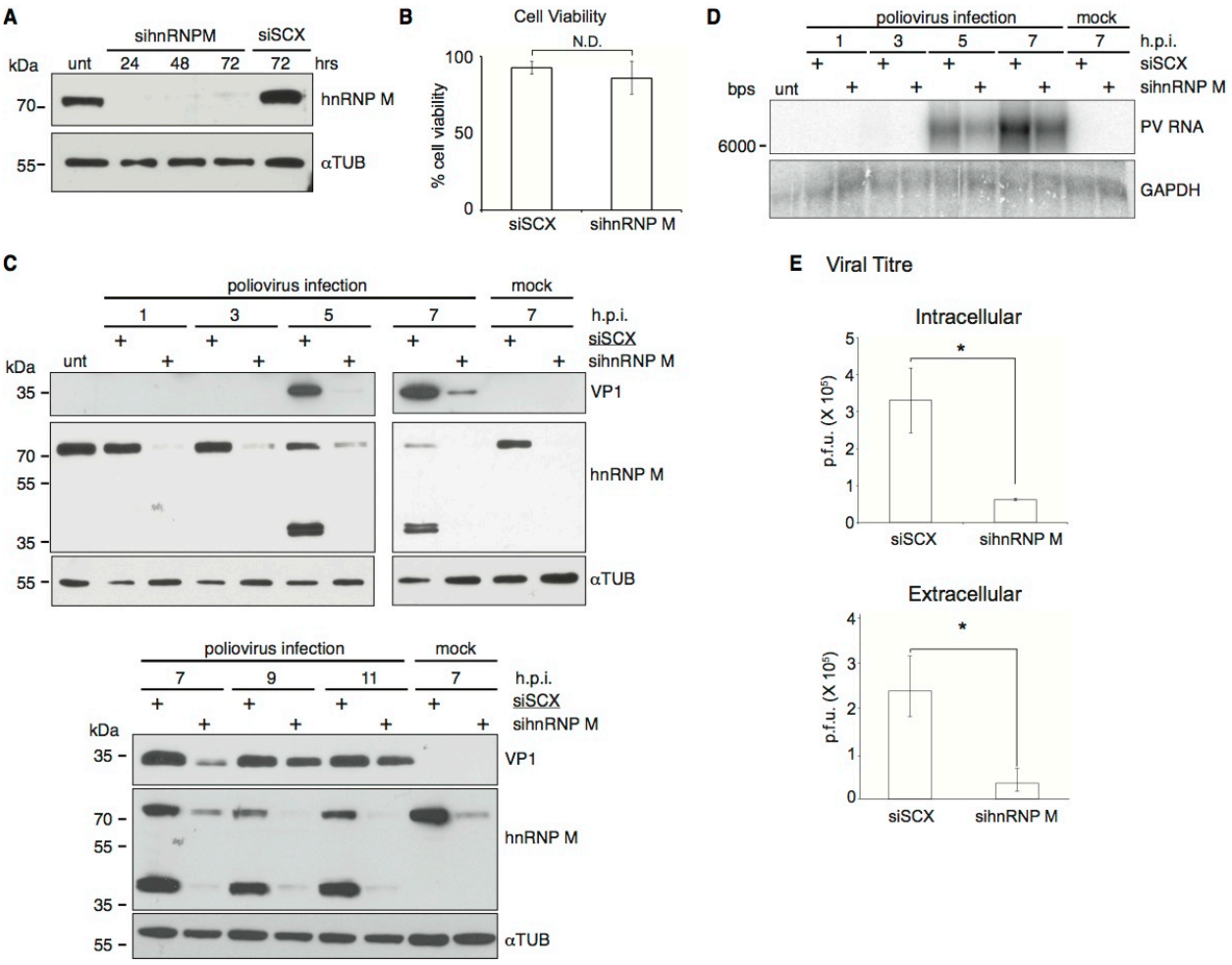

Figure 5.7 Poliovirus infection is inhibited in HeLa cells lacking hnRNP M. (A) hnRNP M knockdown by transfection of siRNA in HeLa cells. hnRNP M and α-tubulin were assessed by immunoblot. (B) Cell viability of cells treated with siRNAs for 72 hours was calculated by the percentage of cells that are not stained with trypan blue. Averages ± s.d. are shown. N.D., no statistical difference, $p<0.05$. (C) HeLa cells were transfected with either scrambled (siSCX) or hnRNP M (sihnRNP M) siRNA for 72 hours, followed by poliovirus infection (MOI 1) for the indicated times. Immunoblots of hnRNP M, poliovirus structural protein VP1 and α-tubulin are shown. (D) Northern blot analysis of poliovirus genomic RNA in poliovirus-infected HeLa cells (MOI 1) treated with siSCX or sihnRNP M. (E) Viral titres of intracellular (5 h.p.i.) and extracellular (7 h.p.i.) virus from poliovirus-infected cells (MOI 0.1) pre-treated with siSCX or sihnRNP M. Titres were calculated as plaque forming units (p.f.u./ml ± s.d., *$p<0.05$) from three independent experiments.

(Figure 5.7C). As expected, hnRNP M was barely detected in infected cells treated with hnRNP M siRNAs (Figure 5.7C). Interestingly, the viral structural protein VP1 was significantly reduced in poliovirus-infected cells treated with hnRNP M siRNAs compared to the scrambled control at 5 and 7 hours post infection (Figure 5.7C). By 9 and 11 hours post infection, VP1 expression in hnRNP siRNA-treated cells accumulated to similar levels as in scrambled treated cells (Figure 5.7C). These results suggest that loss of hnRNP M inhibits and delays poliovirus infection. Furthermore, knockdown of hnRNP M decreased the levels of poliovirus genomic RNA at 5 and 7 h.p.i. (Figure 5.7D) and resulted in a 5 to 6-fold decrease in viral titre of both intracellular (5 h.p.i.) and extracellular viral yield (7 h.p.i.) compared to the scrambled control (Figure 5.7E). These results collectively demonstrate that hnRNP M facilitates poliovirus infection in HeLa cells.

5.2.6 Role of hnRNP M in poliovirus IRES translation

I have shown that hnRNP M promotes poliovirus infection. Given that hnRNP M does not colocalize with replication complexes during infection, I next investigated a role for hnRNP M in viral translation. To examine this further, I investigated whether hnRNP M affects host translation and viral protein synthesis during infection. Mock- or poliovirus-infected cells that were pre-treated with hnRNP M siRNAs for 72 hours were pulse-labeled with [^{35}S]-methionine/cysteine for 30 minutes prior to harvesting at each time point. Knockdown of hnRNP M did not significantly affect (94% ± 11%) overall protein synthesis as compared to cells treated with scrambled siRNAs, which is in agreement with our observation that knockdown of hnRNP M does not affect cell viability (Figure 5.8A, mock infected lanes). Host translational shutoff

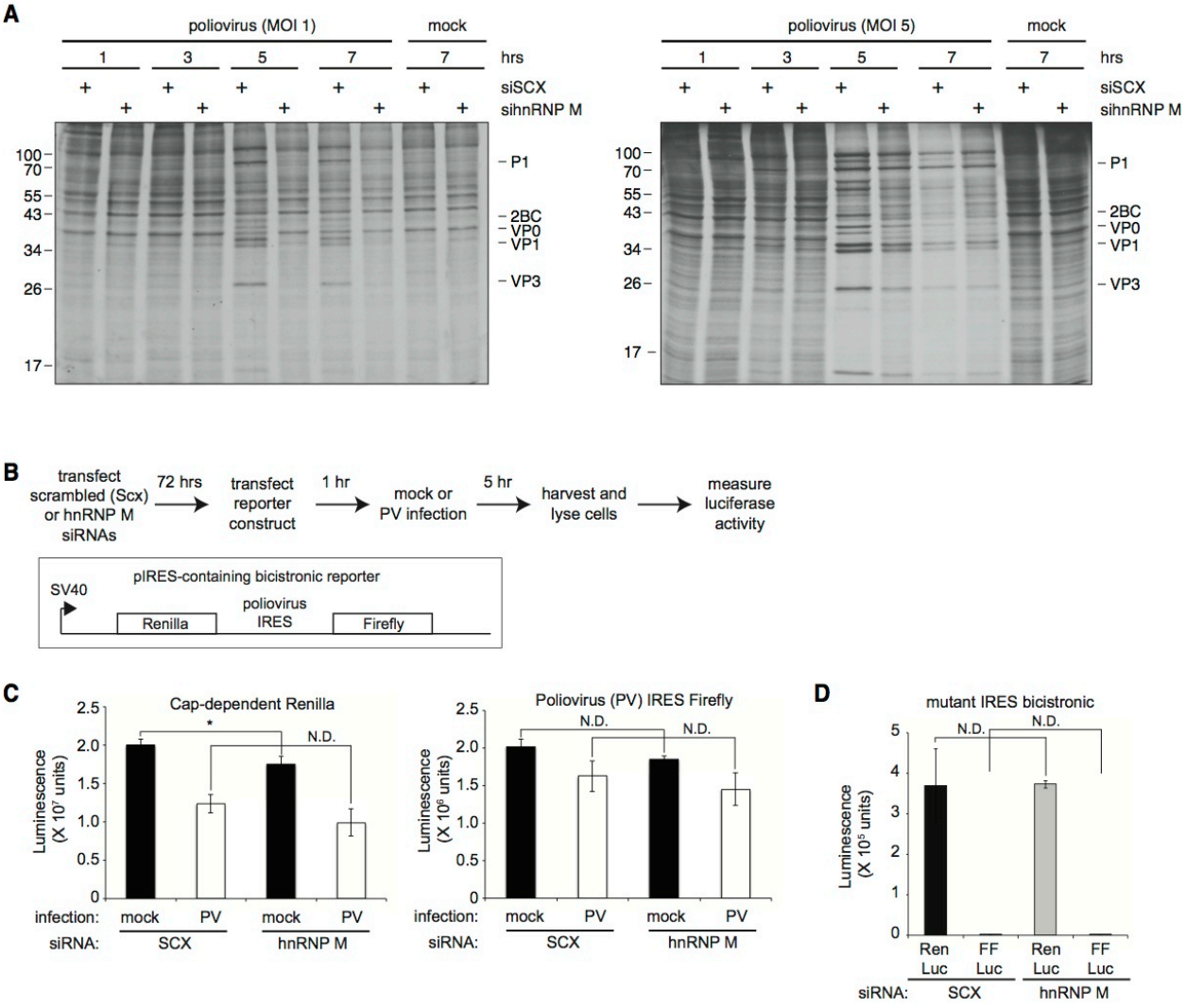

Figure 5.8 Role of hnRNP M in poliovirus IRES translation. (A) Pulse-labeling using [^{35}S]-methionine/cysteine at the indicated times after poliovirus infection (MOI 1 and 5) in cells treated with siSCX or sihnRNP M for 72 hours prior to infection. The cells were pulse-labeled for 30 minutes prior to harvesting at each time point. A representative gel is shown from at least two independent experiments. (B) Flowchart of the transfection protocol to monitor poliovirus IRES translation. A schematic of the bicistronic reporter construct containing the poliovirus IRES within the intergenic region is shown below. (C) and (D) Cap-dependent Renilla and IRES-mediated firefly luciferase activities of the (C) PV IRES bicistronic reporter construct and (D) mutant EMCV IRES bicistronic reporter construct. Relative luminescence was calculated as a mean ± s.d. of three independent experiments. N.D., no statistical difference, *p<0.05.

was observed beginning at 3-5 h.p.i. in poliovirus-infected scrambled siRNA-treated cells at an MOI of 5, which is concomitant with viral protein synthesis (Figure 5.8A). Synthesis of viral proteins such as P1, VP0, VP3, VP1 and 2BC was clearly observed in infected cells at an MOI of 1 and 5 at 5 h.p.i. (Figure 5.8A). By contrast, in cells depleted of hnRNP M, host translational shutoff was delayed at 5 and 7 h.p.i. in infected cells at an MOI of 5 (Figure 5.8A). Moreover, viral protein accumulation was reduced in these cells, which is consistent with the observation that VP1 expression is decreased in hnRNP M siRNA-treated, virus-infected cells (Figure 5.8A and Figure 5.7C). This result is most evident in infected cells at an MOI of 1 where viral protein synthesis is barely detected at 5 and 7 hours post infection (Figure 5.8A). Thus, depletion of hnRNP M results in a decrease in either viral protein accumulation or replication in infected HeLa cells.

To examine more closely whether hnRNP M has a role in viral translation, I monitored poliovirus IRES translation directly by using an IRES-containing reporter construct (Figure 5.8B). The bicistronic reporter construct contains the poliovirus IRES within the intergenic region between the Renilla and firefly luciferase genes, which monitor cap-dependent and poliovirus IRES-mediated translation, respectively (Figure 5.8B). Because hnRNP M redistributes to the cytoplasm during poliovirus infection, I monitored poliovirus IRES translation by transfecting the IRES-containing reporter construct in poliovirus-infected cells. Briefly, cells treated with scrambled or hnRNP M siRNAs for 72 hours were transfected with the bicistronic construct for 1 hour, followed by mock or poliovirus infection (Figure 5.8B, flowchart). Cells were then harvested 5 hours later and luciferase activities were measured.

In mock-infected cells, hnRNP M siRNA treatment decreased Renilla luciferase activity by approximately 12% as compared to scrambled siRNA treatment, indicating that depletion of

hnRNP M had a slight effect on cap-dependent translation using this transfection reporter approach (Figure 5.8C). In contrast, firefly luciferase activity was detected at similar levels in both the scrambled and hnRNP M siRNA treatments, suggesting that hnRNP M does not have a role in IRES-dependent translation under basal conditions (Figure 5.8C). In poliovirus-infected cells, Renilla luciferase activity was inhibited to the same extent in both the scrambled and hnRNP M siRNA treatments, which is a reflection of shutoff of host translation during infection (Figure 5.8C). In contrast, firefly luciferase activity was still detected at similar levels in the hnRNP M siRNA treated cells compared to the scrambled controls (Figure 5.8C), suggesting that hnRNP M is not required for poliovirus IRES translation. A bicistronic construct containing an inactive IRES did not result in firefly luciferase expression, indicating that IRES activity is being measured (Figure 5.8D). In summary, the results suggest that hnRNP M is not required for poliovirus IRES translation during infection, and likely participates in another step of the viral life cycle.

5.2.7 hnRNP M is not required for poliovirus genomic RNA stability

The decrease in viral RNA in poliovirus infected cells that are depleted of hnRNP M may be due to an effect on viral replication or viral RNA stability. To address whether hnRNP M is involved in viral RNA stability, I monitored the fate of viral RNA in scrambled or hnRNP M siRNA-transfected poliovirus-infected cells after treating the cells at 4 h.p.i. with 2 mM guanidine hydrochloride (GuHCL), a known inhibitor of poliovirus RNA synthesis (308). No significant difference was observed between the stabilities of viral RNA between the scrambled and hnRNP M siRNA-treated cells following the addition of guanidine hydrochloride (Figure 5.9). Thus, hnRNP M is not required for maintaining poliovirus RNA stability during infection.

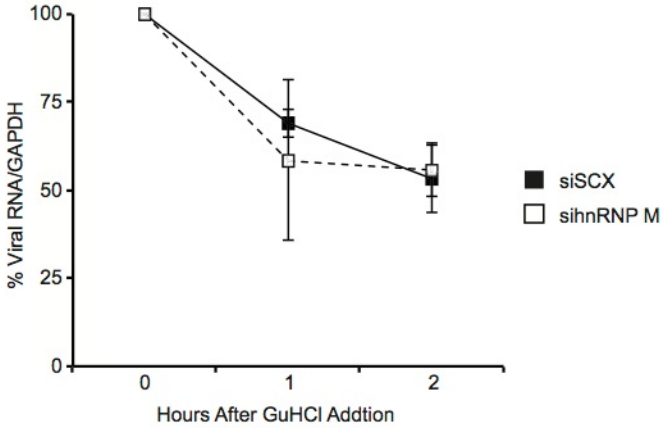

Figure 5.9 Stability of viral genomic RNA in poliovirus-infected cells. Hela cells pretreated with siSCX or sihnRNP M for 24 hours were infected with poliovirus (MOI 5) and at 4 hours post infection, treated with 2mM guanidine hydrochloride (GuHCL). Cells were harvested at the indicated times and the viral RNA and GAPDH mRNA assayed by Northern blot analysis. The ratio of viral RNA to GAPDH at 4 hours post infection was set as 100%. Shown are the averages of three independent experiments ± s.d.

5.2.8 Role of hnRNP M in CVB3 infection

Our results have established a novel role of hnRNP M in poliovirus infection. I next determined whether the requirement of hnRNP M is specific to poliovirus infection. To address this, I asked whether hnRNP M facilitates infection of another picornavirus, CVB3. Similar to that observed with poliovirus $3C^{pro}$, immunoblot analysis detected the accumulation of a cleavage product of approximately 34 kDa in HeLa lysates incubated with purified CVB3 $3C^{pro}$ but not a catalytically inactive CVB3 $3C^{pro}$ (Figure 5.10A). The cleavage product of hnRNP M by CVB3 $3C^{pro}$ appears to migrate slightly farther than the cleavage product produced by poliovirus $3C^{pro}$, suggesting the CVB3 $3C^{pro}$ may target another site within hnRNP M (Figure 5.10A). When monitored during CVB3 infection, a single cleavage 55 kDa protein was observed at 5 hours post infection followed by multiple cleavage products observed at 7 and 9 hours post infection, demonstrating the hnRNP M is cleaved at multiple sites during CVB3 infection (Figure 5.10B). Cleavage of hnRNP M was still observed during CVB3 infection in the presence of zVAD-FMK, demonstrating that targeting of hnRNP M is not due to caspase activity (data not shown). The significance of hnRNP M in CVB3 infection was also explored by measuring viral titres following siRNA-mediated knockdown of hnRNP M. I observed an approximately seven-fold decrease in CVB3 titre in hnRNP M siRNA-treated cells (Figure 5.10C).

CVB3 is a prevalent contributor to dilated cardiomyopathy among young children by targeting and ultimately destroying cardiomyocytes (250). To assess whether cleavage of hnRNP M occurs under more physiologically relevant conditions, I monitored hnRNP M in cardiomyocytes from mice infected with CVB3. Cleavage products of hnRNP M were detected in the CVB3 treated mice but not in the mock treated mice (Figure 5.10D). Altogether, this data

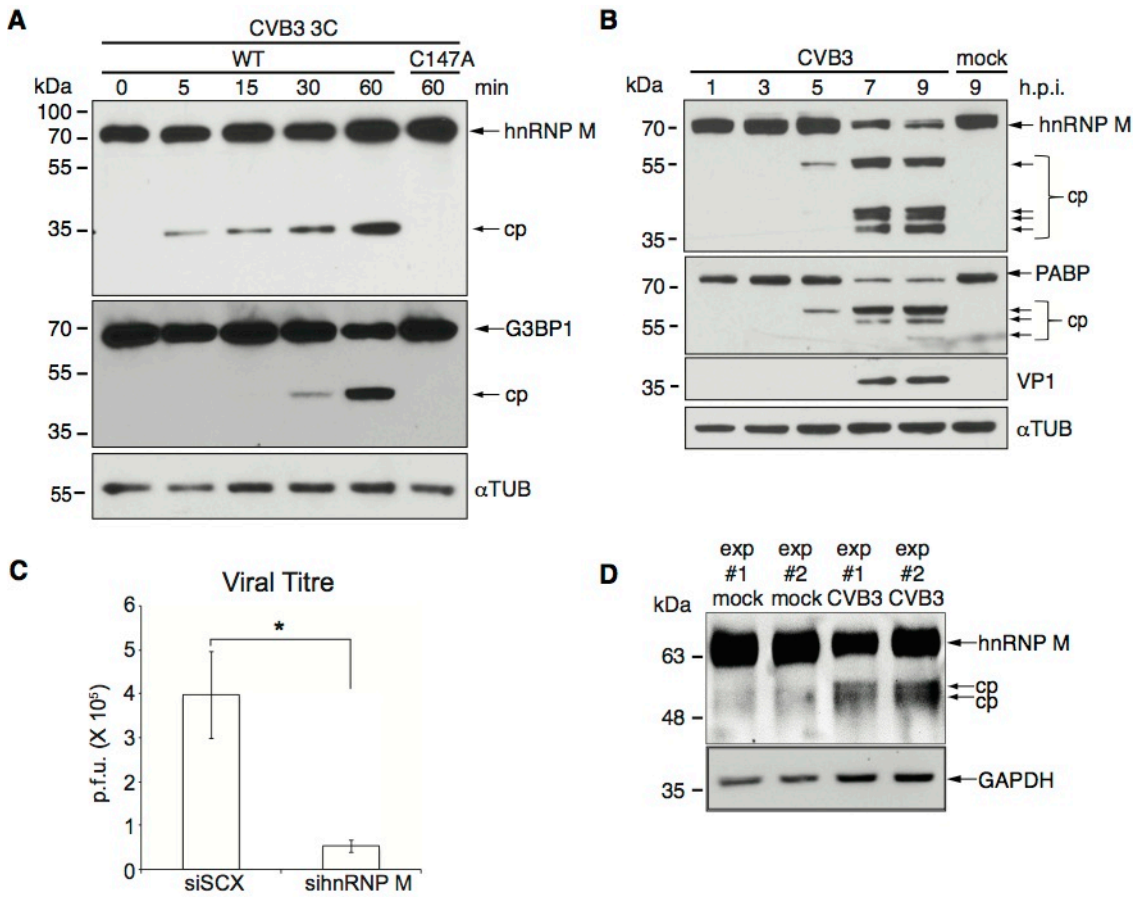

Figure 5.10 hnRNP M in CVB3-infected cells. (A) Cleavage of hnRNP M in CVB3-infected cells. (A) Immunoblots of HeLa lysates incubated with purified wild type or mutant (C147A) CVB3 3C proteinase. (B) Immunoblots of lysates from mock- or CVB3-infected HeLa cells (MOI 10) or (D) hearts of CVB3-infected mice (two independent experiments are shown). (C) Viral titers of CVB3-infected (MOI 1, 16 h.p.i.) HeLa cells that were pre-treated with siSCX or sihnRNP M (n=3, mean ± s.d, *$p<0.05$).

indicates that cleavage of hnRNP M and the requirement of this protein for infection may be a conserved strategy among picornaviruses to facilitate virus infection.

5.3 Discussion

I have identified hnRNP M as a direct substrate of poliovirus $3C^{pro}$ and $3CD^{pro}$ *in vitro,* and that hnRNP M is cleaved in both poliovirus and CVB3-infected cells. I also demonstrate that hnRNP M promotes both poliovirus and CVB3 infection. Several members of the hnRNP family, including hnRNP A1, PCBP1/2, AUF1, and PTB, are important host factors for picornavirus infection (107, 109, 111, 125, 132, 133, 296, 297). A subset of these hnRNPs are modified through cleavage by picornavirus proteinases in infected-cells and as a result, picornaviruses either can either inhibit or alter the function of these proteins, or exploit the function of their cleavage products. Our work suggests that cleavage of hnRNP M is a common strategy of picornavirus infections and that picornaviruses hijack hnRNP M to facilitate infection.

I demonstrate conclusively that hnRNP M is cleaved by poliovirus $3C^{pro}$ and $3CD^{pro}$ between $^{389}Q{\downarrow}G^{390}$ (M4 isoform numbering) *in vitro* to produce a 36 kDa cleavage protein that is detected by the 1D8 hnRNP M antibody (Figure 3.6). The 1D8 antibody recognizes an epitope within the C-terminal fragment of hnRNP M, which is based on the observation that both 1D8 and HA antibodies detect the same C-terminal cleavage product of the FLAG-hnRNP M-HA in poliovirus-infected cells (Figure 5.4B). I posit that all variants of hnRNP M are targeted as all isoforms harbor the region containing the identified cleavage site and thus cleavage by $3C^{pro}$ would produce the same C-terminal end of hnRNP M. Furthermore, hnRNP M is completely

cleaved by 7 hours post infection in poliovirus-infected HeLa cells, which suggests that all four isoforms are being targeted during infection (Figure 5.2A).

I detected a single 36 kDa cleavage product of hnRNP M *in vitro* (Figure 3.6); however, two cleavage products of approximately 36 and 39 kDa were consistently detected in poliovirus-infected cells (Figure 5.6). Accumulation of a second cleavage product during infection may occur through more than one mechanism. First, hnRNP M may be cleaved twice at a second site close in proximity to the ^{389}Q↓G^{390} cleavage site identified *in vitro*, through either 3C^{pro} or another protease. I have determined that the viral 2A^{pro} is unlikely involved and ruled out the possibility of caspase-induced cleavage (Figure 5.2B). Furthermore, while mutating Q389E/G390P prevented direct cleavage by 3C^{pro} *in vitro*, I still observed cleavage of this mutant during poliovirus infection (Figure 3.7 and 5.6A). These results suggest that hnRNP M is cleaved at one or more sites in close proximity to the 3C^{pro} ^{389}Q↓G^{390} *in vitro* cleavage site. Several candidate proteinase cleavage sites were tested but all failed to prevent cleavage (Figure 5.6B; data not shown). Further mapping of the cleavage sites will provide insights into the proteases that target hnRNP M during poliovirus infection. Interestingly, expression of FLAG-hnRNP M-HA generates two cleavage products detected by the FLAG epitope during poliovirus infection and only one cleavage product detected by the HA epitope. This may indicate that a second cleavage event is occurring on a cleavage product following destabilization of the hnRNP M structure following the initial cleavage. Alternatively, the two cleavage products may be due to two distinct isoforms that are cleaved during infection, or that the cleaved fragment is subject to post-translational modification. Further investigation is required to determine the cleavage activity of hnRNP M during infection.

During poliovirus and CVB3 infections, hnRNP M is relocalized to the cytoplasm, where it is cleaved by the viral $3C^{pro}$ (Figure 5.3, data not shown). The subcellular relocalization of hnRNP M is similar to that observed of other hnRNP proteins during poliovirus infection, thus suggesting a general strategy of picornaviruses to redistribute RNA-binding proteins (29). Poliovirus and CVB3 infections lead to remodeling of the nuclear pore complex by viral proteinases, which contributes to the inhibition of nuclear import of nucleo-cytoplasmic shuttling proteins (29, 116-118). Interestingly, it has previously been demonstrated that 3C in its precurser form as $3CD^{pro}$ is capable of entering the nucleus of virus-infected cells through a $3D^{pol}$ nuclear localization signal (137). While I demonstrate that hnRNP M can also serve as a substrate of $3CD^{pro}$ (Figure 5.1H), I observed that FLAG-hnRNP M-HA begins to redistribute from the nucleus to the cytoplasm at 3 hours post infection prior to being cleaved (Figure 5.4B and 5.5). It is likely that hnRNP M relocalizes to the cytoplasm due to blockage of nuclear import mediated by the 2A proteinase, and is then targeted by the 3C proteinase.

Like other hnRNPs, hnRNP M is a RNA-binding protein that associates with G-U rich regions of pre-mRNA (304). hnRNP M is part of pre-spliceosome assembly complexes and functions in splice-site recognition and alternative splicing (299-301, 307, 309, 310). In addition hnRNP M has also been implicated in transcriptional controls, heat shock stress responses and cell signalling (311-313). Our work shows for the first time that the function of hnRNP M is subverted during poliovirus infection and diverted towards a step in the viral life cycle. An indirect effect of relocalization of hnRNP M to the cytoplasm is that splicing will cease or be altered in the nucleus. Previous reports have shown that inhibition of splicing may be a strategy utilized by picornaviruses to subvert host antiviral responses (141, 142, 314). Thus, redistribution of hnRNP M could contribute to this effect.

Although hnRNP M is cleaved during infection, our study shows that hnRNP M is required for optimal picornavirus infection (Figure 5.7E and 5.20C), suggesting that hnRNP M and/or its cleavage products contribute to a specific step of the viral life cycle. Several hnRNPs are exploited by picornaviruses to aid in viral translation, replication or stability of the viral genome. For example, inhibition of nucleo-cytoplasmic transport of protein during picornavirus infection leads to relocalization of nuclear proteins, such as PTB and PCBP2, to the cytoplasm that then aid in viral translation (29, 117, 136). While several hnRNP proteins have been identified as mediators of poliovirus translation through direct interaction with the IRES (107, 111, 125, 296, 297), our translation assays in hnRNP M-depleted cells do not show an effect on poliovirus IRES-mediated translation (Figure 5.8B).

Given that viral RNA levels are reduced in hnRNP M siRNA treated cells, the simplest hypotheses are that the defect is at the step of RNA metabolism replication or viral RNA stability (Figure 5.7D). I showed that hnRNP M does not have role in maintaining viral RNA stability in infected HeLa cells treated with GuHCL (Figure 5.9). Previous studies have implicated a role for hnRNP M in replication of influenza A virus and Semiliki Forest virus (SFV) (315, 316). Moreover, depletion of hnRNP M enhances SFV gene expression and replication, suggesting that hnRNP M may be anti-viral. Both the N- and C-terminal cleavage proteins of hnRNP M contain at least one RRM and thus presumably have the ability to bind RNA. Moreover, because both the N- and C-terminal fragment persist at least until 5 h.p.i. (Figure 4.2 and 4.4), I hypothesized that the cleavage products of hnRNP M act in viral replication. However, quantitation of the confocal images showed no co-localization of the tagged hnRNP M and dsRNA antibody signals, which mark sites of replication (Figure 5.5; data not shown) (282). Moreover, viral RNA was not detected in hnRNP M immunoprecipitation experiments (data not shown). Thus, hnRNP M does

not have a direct role in poliovirus replication. It is still possible that hnRNP M has an indirect role in replication, possibly by interacting with and affecting the function of a specific protein or an mRNA that encodes a protein involved in viral replication. Alternatively, hnRNP M may interact with a protein or mRNA that encodes a protein that have a role in the innate immune response or in stress granules or P body formation, host processes that could affect poliovirus RNA accumulation during infection (226, 317, 318). Further experiments to identify the proteins and/or mRNAs that interact with the cleavage products of hnRNP M in infected cells will undoubtedly shed light into the functions of hnRNP M in infected cells.

Our findings are in line with the general theme that the RNA-binding family of hnRNPs is targeted by picornavirus infections. However, not all hnRNPs function similarly in infected cells. Depletion of a subset of hnRNPs does not have an effect on virus infection whereas depletion of others does, thus highlighting that each hnRNP has specific roles in picornavirus-host interactions (107, 109, 111, 125, 132, 133, 296, 297). Our work demonstrates that hnRNP M plays an important role in poliovirus and CVB3 infections. It will be important to determine how the cleavage products contribute to a specific step of the viral life cycle.

Chapter 6: Summary, Limitations and Future Directions

6.1 Thesis summary

Viruses are dependent on cellular proteins within the infected host cells to facilitate infection. Host proteins play roles in every step of the viral life cycle. Picornaviruses have evolved strategies of proteolysis by encoding viral proteinases to hijack the function of host proteins to support infection and block antiviral responses. Conventional methods for identifying substrates of picornaviral proteinases have uncovered approximately 45 host proteins targeted for cleavage, which ultimately affects a variety of cellular functions, including transcription and translation of host proteins, RNA metabolism, and innate immune responses. I hypothesized that viral proteinases target additional host proteins that have yet to be identified through conventional methods. To address this, I applied TAILS as an unbiased global proteomics approach to conduct a global analysis of protease generated N-terminal peptides and identify novel substrates of picornaviral proteinases.

In this thesis, I established an *in vitro* assay for TAILS using cellular extracts subjected to treatment with recombinant proteinases from model enteroviruses as a viable approach for identifying novel substrates of viral proteinases targeted for cleavage during infection. In **Chapter 3**, I identified 72, 63 and 34 high confidence substrates for poliovirus $3C^{pro}$, CVB3 $2A^{pro}$, and CVB3 $3C^{pro}$, respectively, including the known poliovirus $3C^{pro}$ substrate PTB at a recognized cleavage site. Three identical peptides encoding for hnRNP K, hnRNP M, and PFAS, were identified in both poliovirus and CVB3 $3C^{pro}$ lists of high confidence peptides, suggesting that these host proteins may serve as part of a general strategy for enterovirus infections. Analysis of the putative cleavage sites of the identified high confidence substrates for

both poliovirus and CVB3 $3C^{pro}$ revealed many consistencies with the known consensus cleavage site of $3C^{pro}$, as well as positions which may have more lenient substrate specificity than previously considered. Similarly, cleavage site analysis of identified CVB3 $2A^{pro}$ high confidence substrates showed greater variability at several positions, and thus may accept a broader range of cleavage sites within its catalytic core. I validated a total of seven high confidence substrates as novel substrates of poliovirus $3C^{pro}$ *in vitro*: hnRNP K, hnRNP M, PFAS, ALIX, ACLY, RIPK1, and USO1. Moreover, mutations in the TAILS-identified cleavage sites for several candidates blocked cleavage *in vitro*.

In **Chapter 4**, I confirmed that six of substrates I validated as novel poliovirus $3C^{pro}$ targets *in vitro* are also targeted for cleavage during poliovirus infection. Moreover, mutant substrates that were cleavage-resistant *in vitro*, were also cleavage-resistant during infection. I confirmed that the poliovirus $3C^{pros}$ TAILS-identified substrates hnRNP K and RIPK1, are also targeted for cleavage during CVB3 infection in HL-1 cardiomyocytes, demonstrating novel $3C^{pro}$ host substrates that are common between both enteroviruses. Depletion of these proteins by siRNAs modulated virus infection, suggesting that cleavage either promoted or inhibited virus infection. Over-expression of cleavage-resistant hnRNP K and USO1 increased and decreased viral titres, respectively suggesting that cleavage is important for their functions during infection. Loss of hnRNP K decreased poliovirus growth in infected HeLa cells and led to a reduction in poliovirus IRES-mediated translation, suggesting a role for hnRNP K in facilitating viral translation. USO1 underwent a significant subcellular relocalization during poliovirus infection, and loss of USO1 attenuates viral protein synthesis. In contrast, loss of PFAS enhanced poliovirus production, possibly through modulating expression of NFκB signalling proteins, indicative of an antiviral role for PFAS during poliovirus infection.

Finally, in **Chapter 5**, I further characterized the role of the novel substrate, hnRNP M, in enterovirus infection. hnRNP M is cleaved *in vitro* by poliovirus and CVB3 $3C^{pro}$, and is targeted in poliovirus- and CVB3-infected HeLa cells and in hearts of CVB3-infected mice. hnRNP M relocalizes from the nucleus to cytoplasm during poliovirus infection. Finally, depletion of hnRNP M using siRNA knockdown approaches decreases poliovirus and CVB3 growth in HeLa cells and does not affect poliovirus IRES translation and viral RNA stability. I propose that cleavage of hnRNP M to subvert its function is a general strategy utilized by picornaviruses to facilitate viral infection.

In summary, identification of common cleaved substrates of poliovirus and CVB3 $3C^{pro}$ using TAILS has provided further insight into the general strategies of enterovirus infections. Importantly, identification of distinct host substrates may be key to understanding the specific tropism and virus-host interactions of each picornavirus infection.

6.2 Limitations and future directions

Much information can be obtained from the identification of substrates for viral proteinases. Identification of viral proteinase substrates has provided insight into general mechanisms utilized by viruses for successful infection. For example, picornaviruses evade host antiviral responses in part through cleavage of type I interferon signalling proteins and the near-complete shutoff of host translation through cleavage of eIF4GI/II and PABP (87-90). In addition, viruses utilize proteolysis to strategically regulate progression of the viral life cycle. For example, the synthesis of new virion particles involves a switch from translation of viral proteins to viral RNA replication for viral packaging, which is mediated by cleavage of associated ITAFs such as PCBP2 and PTB (101, 119). Characterizing the function of viral

proteinase substrates can also provide insight into the pathogenesis of viral-associated diseases. Thus, identifying the complete repertoire of host proteins targets of viral proteinases can further our understanding of the viral life cycle and potentially facilitate the design of novel antiviral therapies. I have now established TAILS as a valuable tool for gaining further insight into this research.

This approach can now serve as a useful tool for identifying host cell substrates of less well-characterized viral proteinases, including the least characterized picornavirus proteinase, L^{pro}. A very small subset of host proteins have been identified as targets of L^{pro} (56, 88, 89, 137). Similar to enteroviruses and rhinoviruses, infection by the aphthoviruses that encode L^{pro} induces a dramatic shutoff of host protein translation and inhibits type I IFN anti-viral responses (96, 103, 319, 320). Since the 2A protein of aphthoviruses and erboviruses does not have proteolytic activity, one could presume that L^{pro} shares a similar repertoire of host protein targets as $2A^{pro}$ of enteroviruses and rhinoviruses; however, limitations in the techniques available to explore host substrate targets have made this hypothesis difficult to address. Other families of viruses also encode viral proteinases that have been less well-characterized compared to picornavirus proteinases. The dicistrovirus family of arthropod-infecting viruses, including cricket paralysis and Israeli acute paralysis viruses, express a 3C-like proteinase similar to $3C^{pro}$ found in other positive single-strand RNA viruses (321, 322). Currently, these proteinases have no known function other than the proteolytic processing of the viral polypeptide. TAILS could therefore be utilized to provide much necessary insight into the life cycle of viruses that we know relatively little about.

I chose to apply TAILS using an *in vitro* approach with extracts from HeLa or HL-1 cells incubated with purified recombinant proteinase from poliovirus and CVB3 for many reasons,

including minimizing the occurrence of secondary cleavage events initiated as a result of virus infection to increase the likelihood of identifying direct substrates of these viral proteinases (161, 162). Indeed, I have demonstrated that this *in vitro* approach can identify novel substrates targeted during virus infection. There are; however, caveats when utilizing this approach to identify viral proteinase substrates by attempting to conduct a global proteome analysis. The physiological setting for viral proteinase activity is during virus infection, whereby the cellular environment has been vastly modified in comparison to uninfected cells. For example, viral replication complexes are made up of components of ER-derived COPII vesicles, Golgi-associated COPI complex proteins, cholesterol and phosphoinositol-4-kinase IIIβ, which consequently disrupt membrane integrity, interfere with protein trafficking and modulate lipid metabolism (28). Cleavage of nuclear pore complex proteins block import of nuclear proteins, resulting in the cytoplasmic accumulation of several nuclear proteins (27, 95, 96). Host cells induce antiviral responses upon infection, while viral proteins shutoff host translation and transcription (70-75, 138). The proteome composition would therefore vary quite significantly during infection, with respect to cellular localization and availability compared cell lysates derived from uninfected cells. Thus, the next step in this study would be to apply TAILS *in vivo* and potentially generate a more comprehensive list of high confidence candidate substrates.

An interesting aspect of applying TAILS *in vivo* would be to explore what proteolytic networks are created during viral infection, and which networks are initiated as a result of viral proteinase activity. It is known that expression of $3C^{pro}$ or $2A^{pro}$ alone in cells can induce caspase activity, leading to activation of apoptosis to possibly facilitating cell lysis and viral spread during virus infection (165). Activation of other cellular proteases have also been described during other picornavirus infection, including HRV16 and CVB3, and associated with

picornaviral-associated disease progression (323-326). Thus, establishing the proteolytic networks created during virus infection would potentially uncover additional cellular pathways that support virus infection, and possibly provide further insight into the role that viral proteinases contribute to the pathogenesis of viral-associated diseases. Moreover, TAILS could be applied at various time points throughout infection to monitor how these proteolytic networks change over time, and could potentially provides clues in the roles that the identified proteins play in infection. One possible approach for exploring which proteolytic networks are initiated as a result of viral proteinase activity would be to apply TAILS to extracts from cells expressing $3C^{pro}$ and $2A^{pro}$ alone in parallel to applying TAILS to extracts for infected cells. This two-prong approach would presumably identify substrates that are more likely to be direct or indirect targets of either $3C^{pro}$ and $2A^{pro}$ during virus infection if they are identified within both TAILS experiments.

In this study, I validated seven host proteins as novel substrates of poliovirus $3C^{pro}$ using TAILS; however, I have yet to fully address why any of these substrates are cleaved and the functional significance of such cleavage. One major hurdle encountered when trying to address these questions is the presence of endogenous protein, following either siRNA transfection or over-expression of wild-type or cleavage resistance forms. The presence of residual endogenous protein could potentially mask the effects on the viral life cycle when over-expressing a cleavage resistant form, or when knocking down protein expression (as opposed to a complete knockout). One approach to overcome this hurdle would be to generate stable cell lines expressing a cleavage resistant substrate using CRISPR-mediated homologous recombination (327). Such a stable cell line would ensure that all cells exposed to virus are expressing a cleavage resistant form of the protein of interest. Moreover, generating a knock-in cell line whereby only one or

two amino acids have been mutated in the protein of interest, would minimally disrupt its natural state, thus reducing the potential for off target effects.

While it remains unclear why these seven substrates are targeted for cleavage during infection, I was able to demonstrate the functional significance of a few substrates in promoting enterovirus infection through siRNA-mediated depletion studies. It is clear that hnRNP M plays a facilitative role in enterovirus infection; however, it does not function as an ITAF and does not promote RNA stability. To further investigate what specific function hnRNP M plays during virus infection, one approach could be to identify its protein-interacting partners by co-immunoprecipitation using lysates from infected cells coupled with mass spectrometry. This would be performed using both the full-length and cleaved forms, once the *in vivo* cleavage site for hnRNP M is identified. Identifying binding partners for hnRNP M from infected lysates could provide clues to the function of hnRNP M during infection, based on the functions of its binding partners. Methods for identifying protein-protein interactions *in vivo* based on proximity ligation may also be explored to identify hnRNP M binding proteins during virus infection. Such techniques involve expression of fusion of a protein of interest (ex. hnRNP M) to a promiscuous biotin-labeling enzyme that will biotinylate other proteins within close proximity within live cells (328). Biotinylated proteins are then isolated from cells by streptavidin affinity purification and identified by mass spectrometry. These approaches would also be useful for exploring the functions of other substrates, including hnRNP K, USO1, RIPK1 and PFAS.

I have provided evidence to suggest that hnRNP K supports poliovirus IRES activity during virus infection; however, loss of hnRNP K had no effect on viral protein synthesis. Loss of hnRNP K resulted in a 5-fold decrease in poliovirus titres, demonstrates that hnRNP K is indeed biologically important for viral infection. However, additional experiments will be

necessary in order to verify whether hnRNP K is a bona fide ITAF for poliovirus. For example, a poliovirus minigenome reporter construct whereby a luciferase gene is flanked by the native poliovirus 5' and 3'UTR can be utilized to provide a more accurate measure of IRES-mediated luciferase expression (93). Luciferase expression can then be measured during virus infection following transfection of a poliovirus minigenome reporter construct into cells pretreated with hnRNP K siRNAs. Monitoring accumulation of poliovirus genomic RNA by Northern blot would also provide additional clues for hnRNP K function. If hnRNP K does function in IRES-mediated translation, then a decrease in viral RNA accumulation would be expected following loss of hnRNP K during infection.

Based on the evidence I have demonstrated for USO1 function during poliovirus infection, and considering its previously characterized functions in Golgi vesicle transport, I hypothesis that full-length USO1 supports viral replication through a direct or indirect function in the formation of viral replication complexes (235, 254, 258). This would further be supported by performing a Northern blot or quantitative real-time polymerase chain reaction showing a reduction in viral genomic RNA accumulation following loss of USO1 during infection. We have demonstrated that endogenous USO1 disperses into the cytoplasm upon poliovirus infection. It would be interesting to explore whether expression of its cleavage resistant form would prevent this relocalization. Furthermore, does over-expression of either a wild-type or cleavage resistant form alter the number of replication complexes formed? A recently developed antibody that recognizes double stranded forms of RNA, which are not present in uninfected cells, has been used to visualize viral replication complexes during infection (275). It would also be interesting to utilize this antibody to explore whether cells over-expressing a wild-type or cleavage resistant form alter the number of replications formed in that cell. If USO1 does affect

viral RNA synthesis and influence the formation of replication complexes, through what pathway does it mediate its functions? Exploring what interacting partners USO1 may have during infection (COPI- or COPII- associated proteins, or even directly with the replication complexes themselves) would help address this question.

PFAS is the only candidate substrate identified in this study that showed an increase in viral titres following siRNA knockdown, suggesting a possible anti-viral role for PFAS during poliovirus infection. As previously mentioned, a recent paper described the ability for the gamma herpesvirus to hijack PFAS enzymatic activity to deaminate RIG-I, which ultimately resulted in the inhibition of antiviral NFκB-dependent cytokine production (329). While preliminary experiments I have performed to monitor changes in NFκB signalling protein accumulation during poliovirus infection following loss of PFAS were inconclusive, there are other approaches that can be used to investigate this further. The type I interferon response can also be monitored by changes in transcription of type I interferon response genes, such as IFN-β, by real-time quantitative polymerase chain reaction (330). Performing RNAseq in poliovirus-infected cells depleted of PFAS could also be utilized to provide a more global assessment of the role of PFAS on transcription. In both experiments described above, use of a stable cell line expressing either a wild type or cleavage resistant form of PFAS would help decrease the variability between experiments. Further exploring the function of PFAS during CVB3 infection would also be of interest, given that PFAS was detected in both poliovirus and CVB3 $3C^{pro}$-TAILS experiments at the same cleavage site.

It is possible that not all cleavage events mediated by viral proteinases are essential for the viral life cycle. For example, RIG-I is cleaved by many picornaviral $3C^{pro}$; however, loss of RIG-I has no effect on viral production (188, 190). Further studies have demonstrate that

MDA5, which recognizes long fragments of dsRNA, is the primary PRR responsible for recognizing picornaviral RNA; however, cleavage of RIG-I is still observed upon infection of several picornaviruses (171, 172). It is also possible that cleavage of some substrates may still contribute to the disease pathogenesis while playing no significant role within the viral life cycle. Thus, assessing cleavage in animal models would be important to fully address the biological significance of targeting these substrates for cleavage during virus infection. In this study, I observed no significant difference in viral production following knockdown of two candidate proteins, ALIX and ACLY. One possibility of why cleavage of a non-essential protein may still occur is due to the lack of selective pressure throughout evolution to forgo such an event during infection, which may have at one point been important. It is also possible that viral proteinases may target multiple proteins that collectively contribute to inhibit a given pathway, rather than rely on one or a few cleavage events. Lastly, I cannot rule out the possibility of some cleavage events occurring simply due to the presence of an accessible $3C^{pro}$-preferred consensus cleavage site. Only until the complete repertoire of host substrates of picornavirus proteinases targeted for cleavage during infection has been identified can we begin to address these outstanding questions.

The picornavirus $3C^{pro}$ has been recognized as an attractive target for antiviral therapies as it plays an essential role within the viral life cycle and it is expressed by all picornaviruses. Moreover, few vaccines have been developed to protect against picornavirus infections, thus the development of antivirals therapies is still desirable. One picornavirus $3C^{pro}$ inhibitor, rupintrivir, has progressed to clinical trails; however, it failed to show efficacy in natural infection studies (331, 332). Many antiviral therapies developed towards $3C^{pro}$ have been variations of peptide inhibitors targeting that mimic substrate binding within the active site (333-336). Given that

TAILS identifies cellular substrates at their cleavage site, TAILS serves as useful tool for the design of peptide inhibitors. Moreover, TAILS provides insight into substrate conservation among proteinases from different viral family members, which could help establish better broad-spectrum therapies. Thus, an interesting follow-up study would be to design modified peptides based on the TAILS-identified cleavage sites to further characterize the optimal consensus cleavage site for $3C^{pro}$. Highly selective peptide sequences can then be further modified to carry inhibitor compounds of $3C^{pro}$ activity. For example, the pan-caspase inhibitor zVAD-FMK harbours a C-terminal fluoromethly ketone (FMK) that covalently binds to the catalytic cysteines of caspases (337).

Validating TAILS as an approach for identifying substrates of viral proteinases also provides new opportunities to improve on existing therapies for many current clinically relevant virus, such as HIV-1 and hepatitis C virus (HCV). Highly-active antiretroviral therapy (HAART) is a cocktail of antiviral drugs commonly used for treatment of HIV, which include inhibitors that target the aspartyl protease encoded by HIV-1 (338). However, the high mutational rates during HIV-1 replication contribute to development towards resistance of antiretroviral drugs, including resistance towards protease inhibitors (339). Similarly, HCV encodes the NS3/4A chymotrypsin-like serine protease, for which there are four NS3/4A inhibitors currently used for treating HCV-associated diseases (340-343). Development of drug resistance towards these current inhibitors, as well as reduced efficiency across other HCV genotypes, has also been reported (344-346). TAILS can serve as a useful tool for assessing why certain viral proteases develop resistance towards treatment by analyzing changes in substrate specificity between sensitive and drug-resistant viral protease, and can contribute to the development of new antiviral therapies. TAILS could also identify host protein targets that may serve as antiviral therapies,

such as interferon-mediated antiviral therapies that are typically inhibited by viruses, as a means of circumventing drug resistance. A recent study applied COFRADIC to identify 120 candidate substrates for the HIV-1 protease from Jurkat cell lysates (238). Host protein substrates for the HCV protease have been described; however, a global proteomic approach has yet to be utilized to identify novel substrates (347, 348).

Altogether, this study has provided further insight into the function of picornavirus proteinases to support virus infection, and has opened new avenues of research to better characterize the role of novel host protein substrates during infection.

Bibliography

1. **Turk B, Turk D, Turk V.** 2012. Protease signalling: the cutting edge. EMBO J **31:**1630-1643.
2. **Sun D, Chen S, Cheng A, Wang M.** 2016. Roles of the Picornaviral 3C Proteinase in the Viral Life Cycle and Host Cells. Viruses **8:**82.
3. **Morikawa K, Gouttenoire J, Hernandez C, Dao Thi VL, Tran HT, Lange CM, Dill MT, Heim MH, Donze O, Penin F, Quadroni M, Moradpour D.** 2014. Quantitative proteomics identifies the membrane-associated peroxidase GPx8 as a cellular substrate of the hepatitis C virus NS3-4A protease. Hepatology **59:**423-433.
4. **Seipelt J, Liebig HD, Sommergruber W, Gerner C, Kuechler E.** 2000. 2A proteinase of human rhinovirus cleaves cytokeratin 8 in infected HeLa cells. J Biol Chem **275:**20084-20089.
5. **Blom N, Hansen J, Blaas D, Brunak S.** 1996. Cleavage site analysis in picornaviral polyproteins: discovering cellular targets by neural networks. Protein Sci **5:**2203-2216.
6. **Wilson CH, Indarto D, Doucet A, Pogson LD, Pitman MR, McNicholas K, Menz RI, Overall CM, Abbott CA.** 2013. Identifying natural substrates for dipeptidyl peptidases 8 and 9 using terminal amine isotopic labeling of substrates (TAILS) reveals in vivo roles in cellular homeostasis and energy metabolism. J Biol Chem **288:**13936-13949.
7. **Starr AE, Bellac CL, Dufour A, Goebeler V, Overall CM.** 2012. Biochemical characterization and N-terminomics analysis of leukolysin, the membrane-type 6 matrix metalloprotease (MMP25): chemokine and vimentin cleavages enhance cell migration and macrophage phagocytic activities. J Biol Chem **287:**13382-13395.
8. **Prudova A, auf dem Keller U, Butler GS, Overall CM.** 2010. Multiplex N-terminome analysis of MMP-2 and MMP-9 substrate degradomes by iTRAQ-TAILS quantitative proteomics. Mol Cell Proteomics **9:**894-911.
9. **Pelletier J, Sonenberg N.** 1988. Internal initiation of translation of eukaryotic mRNA directed by a sequence derived from poliovirus RNA. Nature **334:**320-325.
10. **Jang SK, Krausslich HG, Nicklin MJ, Duke GM, Palmenberg AC, Wimmer E.** 1988. A segment of the 5' nontranslated region of encephalomyocarditis virus RNA directs internal entry of ribosomes during in vitro translation. J Virol **62:**2636-2643.
11. **Spector DH, Baltimore D.** 1974. Requirement of 3'-terminal poly(adenylic acid) for the infectivity of poliovirus RNA. Proc Natl Acad Sci U S A **71:**2983-2987.
12. **Sarnow P.** 1989. Role of 3'-end sequences in infectivity of poliovirus transcripts made in vitro. J Virol **63:**467-470.
13. **Lawrence C, Thach RE.** 1975. Identification of a viral protein involved in post-translational maturation of the encephalomyocarditis virus capsid precursor. J Virol **15:**918-928.
14. **Strebel K, Beck E.** 1986. A second protease of foot-and-mouth disease virus. J Virol **58:**893-899.
15. **Toyoda H, Koide N, Kamiyama M, Tobita K, Mizumoto K, Imura N.** 1994. Host factors required for internal initiation of translation on poliovirus RNA. Arch Virol **138:**1-15.

16. **Lee YF, Nomoto A, Detjen BM, Wimmer E.** 1977. A protein covalently linked to poliovirus genome RNA. Proc Natl Acad Sci U S A **74:**59-63.
17. **Sweeney TR, Cisnetto V, Bose D, Bailey M, Wilson JR, Zhang X, Belsham GJ, Curry S.** 2010. Foot-and-mouth disease virus 2C is a hexameric AAA+ protein with a coordinated ATP hydrolysis mechanism. J Biol Chem **285:**24347-24359.
18. **Samuilova O, Krogerus C, Fabrichniy I, Hyypia T.** 2006. ATP hydrolysis and AMP kinase activities of nonstructural protein 2C of human parechovirus 1. J Virol **80:**1053-1058.
19. **Staunton DE, Merluzzi VJ, Rothlein R, Barton R, Marlin SD, Springer TA.** 1989. A cell adhesion molecule, ICAM-1, is the major surface receptor for rhinoviruses. Cell **56:**849-853.
20. **Mendelsohn CL, Wimmer E, Racaniello VR.** 1989. Cellular receptor for poliovirus: molecular cloning, nucleotide sequence, and expression of a new member of the immunoglobulin superfamily. Cell **56:**855-865.
21. **Coyne CB, Bergelson JM.** 2006. Virus-induced Abl and Fyn kinase signals permit coxsackievirus entry through epithelial tight junctions. Cell **124:**119-131.
22. **Bergelson JM, Cunningham JA, Droguett G, Kurt-Jones EA, Krithivas A, Hong JS, Horwitz MS, Crowell RL, Finberg RW.** 1997. Isolation of a common receptor for Coxsackie B viruses and adenoviruses 2 and 5. Science **275:**1320-1323.
23. **Tomko RP, Xu R, Philipson L.** 1997. HCAR and MCAR: the human and mouse cellular receptors for subgroup C adenoviruses and group B coxsackieviruses. Proc Natl Acad Sci U S A **94:**3352-3356.
24. **Milstone AM, Petrella J, Sanchez MD, Mahmud M, Whitbeck JC, Bergelson JM.** 2005. Interaction with coxsackievirus and adenovirus receptor, but not with decay-accelerating factor (DAF), induces A-particle formation in a DAF-binding coxsackievirus B3 isolate. J Virol **79:**655-660.
25. **Butan C, Filman DJ, Hogle JM.** 2014. Cryo-electron microscopy reconstruction shows poliovirus 135S particles poised for membrane interaction and RNA release. J Virol **88:**1758-1770.
26. **De Sena J, Mandel B.** 1977. Studies on the in vitro uncoating of poliovirus. II. Characteristics of the membrane-modified particle. Virology **78:**554-566.
27. **Andreev DE, Hirnet J, Terenin IM, Dmitriev SE, Niepmann M, Shatsky IN.** 2012. Glycyl-tRNA synthetase specifically binds to the poliovirus IRES to activate translation initiation. Nucleic Acids Res **40:**5602-5614.
28. **Hunt SL, Hsuan JJ, Totty N, Jackson RJ.** 1999. unr, a cellular cytoplasmic RNA-binding protein with five cold-shock domains, is required for internal initiation of translation of human rhinovirus RNA. Genes Dev **13:**437-448.
29. **Gustin KE, Sarnow P.** 2001. Effects of poliovirus infection on nucleo-cytoplasmic trafficking and nuclear pore complex composition. EMBO J **20:**240-249.
30. **Jackson WT.** 2014. Poliovirus-induced changes in cellular membranes throughout infection. Curr Opin Virol **9:**67-73.
31. **Cho MW, Teterina N, Egger D, Bienz K, Ehrenfeld E.** 1994. Membrane rearrangement and vesicle induction by recombinant poliovirus 2C and 2BC in human cells. Virology **202:**129-145.

32. **McKnight KL, Lemon SM.** 1998. The rhinovirus type 14 genome contains an internally located RNA structure that is required for viral replication. RNA **4:**1569-1584.
33. **Paul AV, Rieder E, Kim DW, van Boom JH, Wimmer E.** 2000. Identification of an RNA hairpin in poliovirus RNA that serves as the primary template in the in vitro uridylylation of VPg. J Virol **74:**10359-10370.
34. **Feng Z, Hensley L, McKnight KL, Hu F, Madden V, Ping L, Jeong SH, Walker C, Lanford RE, Lemon SM.** 2013. A pathogenic picornavirus acquires an envelope by hijacking cellular membranes. Nature **496:**367-371.
35. **Chen YH, Du W, Hagemeijer MC, Takvorian PM, Pau C, Cali A, Brantner CA, Stempinski ES, Connelly PS, Ma HC, Jiang P, Wimmer E, Altan-Bonnet G, Altan-Bonnet N.** 2015. Phosphatidylserine vesicles enable efficient en bloc transmission of enteroviruses. Cell **160:**619-630.
36. **Mueller S, Wimmer E, Cello J.** 2005. Poliovirus and poliomyelitis: a tale of guts, brains, and an accidental event. Virus Res **111:**175-193.
37. **Grubman MJ, Baxt B.** 2004. Foot-and-mouth disease. Clin Microbiol Rev **17:**465-493.
38. **Esfandiarei M, McManus BM.** 2008. Molecular biology and pathogenesis of viral myocarditis. Annu Rev Pathol **3:**127-155.
39. **Summers DF, Maizel JV, Jr.** 1968. Evidence for large precursor proteins in poliovirus synthesis. Proc Natl Acad Sci U S A **59:**966-971.
40. **Jacobson MF, Baltimore D.** 1968. Polypeptide cleavages in the formation of poliovirus proteins. Proc Natl Acad Sci U S A **61:**77-84.
41. **Toyoda H, Nicklin MJ, Murray MG, Anderson CW, Dunn JJ, Studier FW, Wimmer E.** 1986. A second virus-encoded proteinase involved in proteolytic processing of poliovirus polyprotein. Cell **45:**761-770.
42. **Hogle JM.** 2002. Poliovirus cell entry: common structural themes in viral cell entry pathways. Annu Rev Microbiol **56:**677-702.
43. **Baxter NJ, Roetzer A, Liebig HD, Sedelnikova SE, Hounslow AM, Skern T, Waltho JP.** 2006. Structure and dynamics of coxsackievirus B4 2A proteinase, an enyzme involved in the etiology of heart disease. J Virol **80:**1451-1462.
44. **Bazan JF, Fletterick RJ.** 1988. Viral cysteine proteases are homologous to the trypsin-like family of serine proteases: structural and functional implications. Proc Natl Acad Sci U S A **85:**7872-7876.
45. **Blinov VM, Gorbalenia AE, Donchenko AP.** 1984. [Structural similarity of poliovirus cysteine proteinase P3-7c and cellular serine proteinase of trypsin]. Dokl Akad Nauk SSSR **279:**502-505.
46. **Gorbalenya AE, Donchenko AP, Blinov VM, Koonin EV.** 1989. Cysteine proteases of positive strand RNA viruses and chymotrypsin-like serine proteases. A distinct protein superfamily with a common structural fold. FEBS Lett **243:**103-114.
47. **Mosimann SC, Cherney MM, Sia S, Plotch S, James MN.** 1997. Refined X-ray crystallographic structure of the poliovirus 3C gene product. J Mol Biol **273:**1032-1047.
48. **Lawson MA, Semler BL.** 1991. Poliovirus thiol proteinase 3C can utilize a serine nucleophile within the putative catalytic triad. Proc Natl Acad Sci U S A **88:**9919-9923.
49. **Cheah KC, Leong LE, Porter AG.** 1990. Site-directed mutagenesis suggests close functional relationship between a human rhinovirus 3C cysteine protease and cellular trypsin-like serine proteases. J Biol Chem **265:**7180-7187.

50. **Grubman MJ, Zellner M, Bablanian G, Mason PW, Piccone ME.** 1995. Identification of the active-site residues of the 3C proteinase of foot-and-mouth disease virus. Virology **213:**581-589.
51. **Hammerle T, Hellen CU, Wimmer E.** 1991. Site-directed mutagenesis of the putative catalytic triad of poliovirus 3C proteinase. J Biol Chem **266:**5412-5416.
52. **Hellen CU, Facke M, Krausslich HG, Lee CK, Wimmer E.** 1991. Characterization of poliovirus 2A proteinase by mutational analysis: residues required for autocatalytic activity are essential for induction of cleavage of eukaryotic initiation factor 4F polypeptide p220. J Virol **65:**4226-4231.
53. **Kean KM, Howell MT, Grunert S, Girard M, Jackson RJ.** 1993. Substitution mutations at the putative catalytic triad of the poliovirus 3C protease have differential effects on cleavage at different sites. Virology **194:**360-364.
54. **Kean KM, Teterina NL, Marc D, Girard M.** 1991. Analysis of putative active site residues of the poliovirus 3C protease. Virology **181:**609-619.
55. **Miyashita K, Kusumi M, Utsumi R, Katayama S, Noda M, Komano T, Satoh N.** 1993. Site-directed mutagenesis of the putative active site residues of 3C proteinase of coxsackievirus B3: evidence of a functional relationship with trypsin-like serine proteinases. Protein Eng **6:**189-193.
56. **Yu SF, Lloyd RE.** 1991. Identification of essential amino acid residues in the functional activity of poliovirus 2A protease. Virology **182:**615-625.
57. **Yu SF, Lloyd RE.** 1992. Characterization of the roles of conserved cysteine and histidine residues in poliovirus 2A protease. Virology **186:**725-735.
58. **Harris KS, Reddigari SR, Nicklin MJ, Hammerle T, Wimmer E.** 1992. Purification and characterization of poliovirus polypeptide 3CD, a proteinase and a precursor for RNA polymerase. J Virol **66:**7481-7489.
59. **Ypma-Wong MF, Dewalt PG, Johnson VH, Lamb JG, Semler BL.** 1988. Protein 3CD is the major poliovirus proteinase responsible for cleavage of the P1 capsid precursor. Virology **166:**265-270.
60. **Parsley TB, Cornell CT, Semler BL.** 1999. Modulation of the RNA binding and protein processing activities of poliovirus polypeptide 3CD by the viral RNA polymerase domain. J Biol Chem **274:**12867-12876.
61. **Marcotte LL, Wass AB, Gohara DW, Pathak HB, Arnold JJ, Filman DJ, Cameron CE, Hogle JM.** 2007. Crystal structure of poliovirus 3CD protein: virally encoded protease and precursor to the RNA-dependent RNA polymerase. J Virol **81:**3583-3596.
62. **Gorbalenya AE, Koonin EV, Lai MM.** 1991. Putative papain-related thiol proteases of positive-strand RNA viruses. Identification of rubi- and aphthovirus proteases and delineation of a novel conserved domain associated with proteases of rubi-, alpha- and coronaviruses. FEBS Lett **288:**201-205.
63. **Piccone ME, Zellner M, Kumosinski TF, Mason PW, Grubman MJ.** 1995. Identification of the active-site residues of the L proteinase of foot-and-mouth disease virus. J Virol **69:**4950-4956.
64. **Roberts PJ, Belsham GJ.** 1995. Identification of critical amino acids within the foot-and-mouth disease virus leader protein, a cysteine protease. Virology **213:**140-146.

65. **Guarne A, Tormo J, Kirchweger R, Pfistermueller D, Fita I, Skern T.** 1998. Structure of the foot-and-mouth disease virus leader protease: a papain-like fold adapted for self-processing and eIF4G recognition. EMBO J **17:**7469-7479.
66. **Guarne A, Hampoelz B, Glaser W, Carpena X, Tormo J, Fita I, Skern T.** 2000. Structural and biochemical features distinguish the foot-and-mouth disease virus leader proteinase from other papain-like enzymes. J Mol Biol **302:**1227-1240.
67. **Skern T, Fita I, Guarne A.** 1998. A structural model of picornavirus leader proteinases based on papain and bleomycin hydrolase. J Gen Virol **79 (Pt 2):**301-307.
68. **Hanecak R, Semler BL, Anderson CW, Wimmer E.** 1982. Proteolytic processing of poliovirus polypeptides: antibodies to polypeptide P3-7c inhibit cleavage at glutamine-glycine pairs. Proc Natl Acad Sci U S A **79:**3973-3977.
69. **Semler BL, Hanecak R, Anderson CW, Wimmer E.** 1981. Cleavage sites in the polypeptide precursors of poliovirus protein P2-X. Virology **114:**589-594.
70. **Ypma-Wong MF, Filman DJ, Hogle JM, Semler BL.** 1988. Structural domains of the poliovirus polyprotein are major determinants for proteolytic cleavage at Gln-Gly pairs. J Biol Chem **263:**17846-17856.
71. **Pallai PV, Burkhardt F, Skoog M, Schreiner K, Bax P, Cohen KA, Hansen G, Palladino DE, Harris KS, Nicklin MJ, et al.** 1989. Cleavage of synthetic peptides by purified poliovirus 3C proteinase. J Biol Chem **264:**9738-9741.
72. **Weidner JR, Dunn BM.** 1991. Development of synthetic peptide substrates for the poliovirus 3C proteinase. Arch Biochem Biophys **286:**402-408.
73. **Wang J, Fan T, Yao X, Wu Z, Guo L, Lei X, Wang J, Wang M, Jin Q, Cui S.** 2011. Crystal structures of enterovirus 71 3C protease complexed with rupintrivir reveal the roles of catalytically important residues. J Virol **85:**10021-10030.
74. **Santos JA, Gouvea IE, Judice WA, Izidoro MA, Alves FM, Melo RL, Juliano MA, Skern T, Juliano L.** 2009. Hydrolytic properties and substrate specificity of the foot-and-mouth disease leader protease. Biochemistry **48:**7948-7958.
75. **Nogueira Santos JA, Assis DM, Gouvea IE, Judice WA, Izidoro MA, Juliano MA, Skern T, Juliano L.** 2012. Foot and mouth disease leader protease (Lbpro): Investigation of prime side specificity allows the synthesis of a potent inhibitor. Biochimie **94:**711-718.
76. **Kuehnel E, Cencic R, Foeger N, Skern T.** 2004. Foot-and-mouth disease virus leader proteinase: specificity at the P2 and P3 positions and comparison with other papain-like enzymes. Biochemistry **43:**11482-11490.
77. **Martin EM, Work TS.** 1961. Studies on protein and nucleic acid metabolism in virus-infected mammalian cells. IV. The localization of metabolic changes within subcellular fractions of Krebs II mouse-ascites-tumour cells infected with encephalomyocarditis virus. Biochem J **81:**514-520.
78. **Franklin RM, Baltimore D.** 1962. Patterns of macromolecular synthesis in normal and virus-infected mammalian cells. Cold Spring Harb Symp Quant Biol **27:**175-198.
79. **Darnell JE, Jr., Levintow L.** 1960. Poliovirus protein: source of amino acids and time course of synthesis. J Biol Chem **235:**74-77.
80. **Holland JJ, Peterson JA.** 1964. Nucleic Acid and Protein Synthesis during Poliovirus Infection of Human Cells. J Mol Biol **8:**556-575.

81. **Penman S, Scherrer K, Becker Y, Darnell JE.** 1963. Polyribosomes in Normal and Poliovirus-Infected Hela Cells and Their Relationship to Messenger-Rna. Proc Natl Acad Sci U S A **49:**654-662.
82. **Willems M, Penman S.** 1966. The mechanism of host cell protein synthesis inhibition by poliovirus. Virology **30:**355-367.
83. **Barco A, Carrasco L.** 1998. Co-expression of human eIF-4G and poliovirus 2Apro in Saccharomyces cerevisiae: effects on gene expression. J Gen Virol **79 (Pt 11):**2651-2660.
84. **Davies MV, Pelletier J, Meerovitch K, Sonenberg N, Kaufman RJ.** 1991. The effect of poliovirus proteinase 2Apro expression on cellular metabolism. Inhibition of DNA replication, RNA polymerase II transcription, and translation. J Biol Chem **266:**14714-14720.
85. **Kuyumcu-Martinez NM, Van Eden ME, Younan P, Lloyd RE.** 2004. Cleavage of poly(A)-binding protein by poliovirus 3C protease inhibits host cell translation: a novel mechanism for host translation shutoff. Mol Cell Biol **24:**1779-1790.
86. **Sun XH, Baltimore D.** 1989. Human immunodeficiency virus tat-activated expression of poliovirus protein 2A inhibits mRNA translation. Proc Natl Acad Sci U S A **86:**2143-2146.
87. **Liebig HD, Ziegler E, Yan R, Hartmuth K, Klump H, Kowalski H, Blaas D, Sommergruber W, Frasel L, Lamphear B, et al.** 1993. Purification of two picornaviral 2A proteinases: interaction with eIF-4 gamma and influence on in vitro translation. Biochemistry **32:**7581-7588.
88. **Lamphear BJ, Yan R, Yang F, Waters D, Liebig HD, Klump H, Kuechler E, Skern T, Rhoads RE.** 1993. Mapping the cleavage site in protein synthesis initiation factor eIF-4 gamma of the 2A proteases from human Coxsackievirus and rhinovirus. J Biol Chem **268:**19200-19203.
89. **Etchison D, Milburn SC, Edery I, Sonenberg N, Hershey JW.** 1982. Inhibition of HeLa cell protein synthesis following poliovirus infection correlates with the proteolysis of a 220,000-dalton polypeptide associated with eucaryotic initiation factor 3 and a cap binding protein complex. J Biol Chem **257:**14806-14810.
90. **Haghighat A, Svitkin Y, Novoa I, Kuechler E, Skern T, Sonenberg N.** 1996. The eIF4G-eIF4E complex is the target for direct cleavage by the rhinovirus 2A proteinase. J Virol **70:**8444-8450.
91. **Lamphear BJ, Rhoads RE.** 1996. A single amino acid change in protein synthesis initiation factor 4G renders cap-dependent translation resistant to picornaviral 2A proteases. Biochemistry **35:**15726-15733.
92. **Gradi A, Svitkin YV, Sommergruber W, Imataka H, Morino S, Skern T, Sonenberg N.** 2003. Human rhinovirus 2A proteinase cleavage sites in eukaryotic initiation factors (eIF) 4GI and eIF4GII are different. J Virol **77:**5026-5029.
93. **Gradi A, Svitkin YV, Imataka H, Sonenberg N.** 1998. Proteolysis of human eukaryotic translation initiation factor eIF4GII, but not eIF4GI, coincides with the shutoff of host protein synthesis after poliovirus infection. Proc Natl Acad Sci U S A **95:**11089-11094.
94. **Hanson PJ, Ye X, Qiu Y, Zhang HM, Hemida MG, Wang F, Lim T, Gu A, Cho B, Kim H, Fung G, Granville DJ, Yang D.** 2016. Cleavage of DAP5 by coxsackievirus B3

2A protease facilitates viral replication and enhances apoptosis by altering translation of IRES-containing genes. Cell Death Differ **23:**828-840.
95. **Glaser W, Skern T.** 2000. Extremely efficient cleavage of eIF4G by picornaviral proteinases L and 2A in vitro. FEBS Lett **480:**151-155.
96. **Devaney MA, Vakharia VN, Lloyd RE, Ehrenfeld E, Grubman MJ.** 1988. Leader protein of foot-and-mouth disease virus is required for cleavage of the p220 component of the cap-binding protein complex. J Virol **62:**4407-4409.
97. **Kuyumcu-Martinez NM, Joachims M, Lloyd RE.** 2002. Efficient cleavage of ribosome-associated poly(A)-binding protein by enterovirus 3C protease. J Virol **76:**2062-2074.
98. **Joachims M, Van Breugel PC, Lloyd RE.** 1999. Cleavage of poly(A)-binding protein by enterovirus proteases concurrent with inhibition of translation in vitro. J Virol **73:**718-727.
99. **de Breyne S, Bonderoff JM, Chumakov KM, Lloyd RE, Hellen CU.** 2008. Cleavage of eukaryotic initiation factor eIF5B by enterovirus 3C proteases. Virology **378:**118-122.
100. **Kobayashi M, Arias C, Garabedian A, Palmenberg AC, Mohr I.** 2012. Site-Specific Cleavage of the Host Poly(A) Binding Protein by the Encephalomyocarditis Virus 3C Proteinase Stimulates Viral Replication. Journal of Virology **86:**10686-10694.
101. **Belov GA, Lidsky PV, Mikitas OV, Egger D, Lukyanov KA, Bienz K, Agol VI.** 2004. Bidirectional increase in permeability of nuclear envelope upon poliovirus infection and accompanying alterations of nuclear pores. J Virol **78:**10166-10177.
102. **Belov GA, Evstafieva AG, Rubtsov YP, Mikitas OV, Vartapetian AB, Agol VI.** 2000. Early alteration of nucleocytoplasmic traffic induced by some RNA viruses. Virology **275:**244-248.
103. **de Los Santos T, Diaz-San Segundo F, Grubman MJ.** 2007. Degradation of nuclear factor kappa B during foot-and-mouth disease virus infection. J Virol **81:**12803-12815.
104. **Mukherjee A, Morosky SA, Delorme-Axford E, Dybdahl-Sissoko N, Oberste MS, Wang T, Coyne CB.** 2011. The coxsackievirus B 3C protease cleaves MAVS and TRIF to attenuate host type I interferon and apoptotic signaling. PLoS Pathog **7:**e1001311.
105. **Neznanov N, Chumakov KM, Neznanova L, Almasan A, Banerjee AK, Gudkov AV.** 2005. Proteolytic cleavage of the p65-RelA subunit of NF-kappaB during poliovirus infection. J Biol Chem **280:**24153-24158.
106. **Zaragoza C, Saura M, Padalko EY, Lopez-Rivera E, Lizarbe TR, Lamas S, Lowenstein CJ.** 2006. Viral protease cleavage of inhibitor of kappaBalpha triggers host cell apoptosis. Proc Natl Acad Sci U S A **103:**19051-19056.
107. **Back SH, Kim YK, Kim WJ, Cho S, Oh HR, Kim JE, Jang SK.** 2002. Translation of polioviral mRNA is inhibited by cleavage of polypyrimidine tract-binding proteins executed by polioviral 3C(pro). J Virol **76:**2529-2542.
108. **Cathcart AL, Rozovics JM, Semler BL.** 2013. Cellular mRNA decay protein AUF1 negatively regulates enterovirus and human rhinovirus infections. J Virol **87:**10423-10434.
109. **Cathcart AL, Semler BL.** 2014. Differential restriction patterns of mRNA decay factor AUF1 during picornavirus infections. J Gen Virol **95:**1488-1492.
110. **Gamarnik AV, Andino R.** 1997. Two functional complexes formed by KH domain containing proteins with the 5' noncoding region of poliovirus RNA. RNA **3:**882-892.

111. **Lin JY, Li ML, Huang PN, Chien KY, Horng JT, Shih SR.** 2008. Heterogeneous nuclear ribonuclear protein K interacts with the enterovirus 71 5' untranslated region and participates in virus replication. J Gen Virol **89:**2540-2549.
112. **Meerovitch K, Svitkin YV, Lee HS, Lejbkowicz F, Kenan DJ, Chan EK, Agol VI, Keene JD, Sonenberg N.** 1993. La autoantigen enhances and corrects aberrant translation of poliovirus RNA in reticulocyte lysate. J Virol **67:**3798-3807.
113. **Fitzgerald KD, Semler BL.** 2011. Re-localization of cellular protein SRp20 during poliovirus infection: bridging a viral IRES to the host cell translation apparatus. PLoS Pathog **7:**e1002127.
114. **Watters K, Palmenberg AC.** 2011. Differential processing of nuclear pore complex proteins by rhinovirus 2A proteases from different species and serotypes. J Virol **85:**10874-10883.
115. **Park N, Schweers NJ, Gustin KE.** 2015. Selective Removal of FG Repeat Domains from the Nuclear Pore Complex by Enterovirus 2A(pro). J Virol **89:**11069-11079.
116. **Park N, Skern T, Gustin KE.** 2010. Specific cleavage of the nuclear pore complex protein Nup62 by a viral protease. J Biol Chem **285:**28796-28805.
117. **Park N, Katikaneni P, Skern T, Gustin KE.** 2008. Differential targeting of nuclear pore complex proteins in poliovirus-infected cells. J Virol **82:**1647-1655.
118. **Castello A, Izquierdo JM, Welnowska E, Carrasco L.** 2009. RNA nuclear export is blocked by poliovirus 2A protease and is concomitant with nucleoporin cleavage. J Cell Sci **122:**3799-3809.
119. **Panda D, Gold B, Tartell MA, Rausch K, Casas-Tinto S, Cherry S.** 2015. The transcription factor FoxK participates with Nup98 to regulate antiviral gene expression. MBio **6**.
120. **Porter FW, Palmenberg AC.** 2009. Leader-induced phosphorylation of nucleoporins correlates with nuclear trafficking inhibition by cardioviruses. J Virol **83:**1941-1951.
121. **Porter FW, Bochkov YA, Albee AJ, Wiese C, Palmenberg AC.** 2006. A picornavirus protein interacts with Ran-GTPase and disrupts nucleocytoplasmic transport. Proc Natl Acad Sci U S A **103:**12417-12422.
122. **Delhaye S, van Pesch V, Michiels T.** 2004. The leader protein of Theiler's virus interferes with nucleocytoplasmic trafficking of cellular proteins. J Virol **78:**4357-4362.
123. **Blyn LB, Swiderek KM, Richards O, Stahl DC, Semler BL, Ehrenfeld E.** 1996. Poly(rC) binding protein 2 binds to stem-loop IV of the poliovirus RNA 5' noncoding region: identification by automated liquid chromatography-tandem mass spectrometry. Proc Natl Acad Sci U S A **93:**11115-11120.
124. **Chase AJ, Semler BL.** 2014. Differential cleavage of IRES trans-acting factors (ITAFs) in cells infected by human rhinovirus. Virology **449:**35-44.
125. **Perera R, Daijogo S, Walter BL, Nguyen JH, Semler BL.** 2007. Cellular protein modification by poliovirus: the two faces of poly(rC)-binding protein. J Virol **81:**8919-8932.
126. **Gamarnik AV, Andino R.** 2000. Interactions of viral protein 3CD and poly(rC) binding protein with the 5' untranslated region of the poliovirus genome. J Virol **74:**2219-2226.
127. **Borman A, Howell MT, Patton JG, Jackson RJ.** 1993. The involvement of a spliceosome component in internal initiation of human rhinovirus RNA translation. J Gen Virol **74 (Pt 9):**1775-1788.

128. **Hellen CU, Witherell GW, Schmid M, Shin SH, Pestova TV, Gil A, Wimmer E.** 1993. A cytoplasmic 57-kDa protein that is required for translation of picornavirus RNA by internal ribosomal entry is identical to the nuclear pyrimidine tract-binding protein. Proc Natl Acad Sci U S A **90:**7642-7646.
129. **Kolupaeva VG, Hellen CU, Shatsky IN.** 1996. Structural analysis of the interaction of the pyrimidine tract-binding protein with the internal ribosomal entry site of encephalomyocarditis virus and foot-and-mouth disease virus RNAs. RNA **2:**1199-1212.
130. **Borovjagin A, Pestova T, Shatsky I.** 1994. Pyrimidine tract binding protein strongly stimulates in vitro encephalomyocarditis virus RNA translation at the level of preinitiation complex formation. FEBS Lett **351:**299-302.
131. **Andreev DE, Fernandez-Miragall O, Ramajo J, Dmitriev SE, Terenin IM, Martinez-Salas E, Shatsky IN.** 2007. Differential factor requirement to assemble translation initiation complexes at the alternative start codons of foot-and-mouth disease virus RNA. RNA **13:**1366-1374.
132. **Wong J, Si X, Angeles A, Zhang J, Shi J, Fung G, Jagdeo J, Wang T, Zhong Z, Jan E, Luo H.** 2013. Cytoplasmic redistribution and cleavage of AUF1 during coxsackievirus infection enhance the stability of its viral genome. FASEB J **27:**2777-2787.
133. **Rozovics JM, Chase AJ, Cathcart AL, Chou W, Gershon PD, Palusa S, Wilusz J, Semler BL.** 2012. Picornavirus modification of a host mRNA decay protein. MBio **3:**e00431-00412.
134. **Brewer G.** 1991. An A + U-rich element RNA-binding factor regulates c-myc mRNA stability in vitro. Mol Cell Biol **11:**2460-2466.
135. **Laroia G, Sarkar B, Schneider RJ.** 2002. Ubiquitin-dependent mechanism regulates rapid turnover of AU-rich cytokine mRNAs. Proc Natl Acad Sci U S A **99:**1842-1846.
136. **Shiroki K, Isoyama T, Kuge S, Ishii T, Ohmi S, Hata S, Suzuki K, Takasaki Y, Nomoto A.** 1999. Intracellular redistribution of truncated La protein produced by poliovirus 3Cpro-mediated cleavage. J Virol **73:**2193-2200.
137. **Sharma R, Raychaudhuri S, Dasgupta A.** 2004. Nuclear entry of poliovirus protease-polymerase precursor 3CD: implications for host cell transcription shut-off. Virology **320:**195-205.
138. **Bhattacharyya S, Das S.** 2006. An apical GAGA loop within 5' UTR of the coxsackievirus B3 RNA maintains structural organization of the IRES element required for efficient ribosome entry. RNA Biol **3:**60-68.
139. **Craig AW, Svitkin YV, Lee HS, Belsham GJ, Sonenberg N.** 1997. The La autoantigen contains a dimerization domain that is essential for enhancing translation. Mol Cell Biol **17:**163-169.
140. **Costa-Mattioli M, Svitkin Y, Sonenberg N.** 2004. La autoantigen is necessary for optimal function of the poliovirus and hepatitis C virus internal ribosome entry site in vivo and in vitro. Mol Cell Biol **24:**6861-6870.
141. **Alvarez E, Castello A, Carrasco L, Izquierdo JM.** 2011. Alternative splicing, a new target to block cellular gene expression by poliovirus 2A protease. Biochem Biophys Res Commun **414:**142-147.
142. **Almstead LL, Sarnow P.** 2007. Inhibition of U snRNP assembly by a virus-encoded proteinase. Genes Dev **21:**1086-1097.

143. **Pacheco A, Lopez de Quinto S, Ramajo J, Fernandez N, Martinez-Salas E.** 2009. A novel role for Gemin5 in mRNA translation. Nucleic Acids Res **37:**582-590.
144. **Flather D, Semler BL.** 2015. Picornaviruses and nuclear functions: targeting a cellular compartment distinct from the replication site of a positive-strand RNA virus. Front Microbiol **6:**594.
145. **Aminev AG, Amineva SP, Palmenberg AC.** 2003. Encephalomyocarditis virus (EMCV) proteins 2A and 3BCD localize to nuclei and inhibit cellular mRNA transcription but not rRNA transcription. Virus Res **95:**59-73.
146. **Sanchez-Aparicio MT, Rosas MF, Sobrino F.** 2013. Characterization of a nuclear localization signal in the foot-and-mouth disease virus polymerase. Virology **444:**203-210.
147. **Yalamanchili P, Harris K, Wimmer E, Dasgupta A.** 1996. Inhibition of basal transcription by poliovirus: a virus- encoded protease (3Cpro) inhibits formation of TBP-TATA box complex in vitro. J Virol **70:**2922-2929.
148. **Yalamanchili P, Banerjee R, Dasgupta A.** 1997. Poliovirus-encoded protease 2APro cleaves the TATA-binding protein but does not inhibit host cell RNA polymerase II transcription in vitro. J Virol **71:**6881-6886.
149. **Das S, Dasgupta A.** 1993. Identification of the cleavage site and determinants required for poliovirus 3CPro-catalyzed cleavage of human TATA-binding transcription factor TBP. J Virol **67:**3326-3331.
150. **Clark ME, Hammerle T, Wimmer E, Dasgupta A.** 1991. Poliovirus proteinase 3C converts an active form of transcription factor IIIC to an inactive form: a mechanism for inhibition of host cell polymerase III transcription by poliovirus. EMBO J **10:**2941-2947.
151. **Kundu P, Raychaudhuri S, Tsai W, Dasgupta A.** 2005. Shutoff of RNA polymerase II transcription by poliovirus involves 3C protease-mediated cleavage of the TATA-binding protein at an alternative site: incomplete shutoff of transcription interferes with efficient viral replication. J Virol **79:**9702-9713.
152. **Paulson M, Press C, Smith E, Tanese N, Levy DE.** 2002. IFN-Stimulated transcription through a TBP-free acetyltransferase complex escapes viral shutoff. Nat Cell Biol **4:**140-147.
153. **Yalamanchili P, Weidman K, Dasgupta A.** 1997. Cleavage of transcriptional activator Oct-1 by poliovirus encoded protease 3Cpro. Virology **239:**176-185.
154. **Yalamanchili P, Datta U, Dasgupta A.** 1997. Inhibition of host cell transcription by poliovirus: cleavage of transcription factor CREB by poliovirus-encoded protease 3Cpro. J Virol **71:**1220-1226.
155. **Wen AY, Sakamoto KM, Miller LS.** 2010. The role of the transcription factor CREB in immune function. J Immunol **185:**6413-6419.
156. **Tantin D, Schild-Poulter C, Wang V, Hache RJ, Sharp PA.** 2005. The octamer binding transcription factor Oct-1 is a stress sensor. Cancer Res **65:**10750-10758.
157. **Kang J, Gemberling M, Nakamura M, Whitby FG, Handa H, Fairbrother WG, Tantin D.** 2009. A general mechanism for transcription regulation by Oct1 and Oct4 in response to genotoxic and oxidative stress. Genes Dev **23:**208-222.
158. **Banerjee R, Weidman MK, Navarro S, Comai L, Dasgupta A.** 2005. Modifications of both selectivity factor and upstream binding factor contribute to poliovirus-mediated inhibition of RNA polymerase I transcription. J Gen Virol **86:**2315-2322.

159. **Joachims M, Harris KS, Etchison D.** 1995. Poliovirus protease 3C mediates cleavage of microtubule-associated protein 4. Virology **211:**451-461.
160. **Joachims M, Etchison D.** 1992. Poliovirus infection results in structural alteration of a microtubule-associated protein. J Virol **66:**5797-5804.
161. **Armer H, Moffat K, Wileman T, Belsham GJ, Jackson T, Duprex WP, Ryan M, Monaghan P.** 2008. Foot-and-mouth disease virus, but not bovine enterovirus, targets the host cell cytoskeleton via the nonstructural protein 3Cpro. J Virol **82:**10556-10566.
162. **Zhou Z, Mogensen MM, Powell PP, Curry S, Wileman T.** 2013. Foot-and-mouth disease virus 3C protease induces fragmentation of the Golgi compartment and blocks intra-Golgi transport. J Virol **87:**11721-11729.
163. **Badorff C, Lee GH, Lamphear BJ, Martone ME, Campbell KP, Rhoads RE, Knowlton KU.** 1999. Enteroviral protease 2A cleaves dystrophin: evidence of cytoskeletal disruption in an acquired cardiomyopathy. Nat Med **5:**320-326.
164. **Xiong D, Lee GH, Badorff C, Dorner A, Lee S, Wolf P, Knowlton KU.** 2002. Dystrophin deficiency markedly increases enterovirus-induced cardiomyopathy: a genetic predisposition to viral heart disease. Nat Med **8:**872-877.
165. **Xiong D, Yajima T, Lim BK, Stenbit A, Dublin A, Dalton ND, Summers-Torres D, Molkentin JD, Duplain H, Wessely R, Chen J, Knowlton KU.** 2007. Inducible cardiac-restricted expression of enteroviral protease 2A is sufficient to induce dilated cardiomyopathy. Circulation **115:**94-102.
166. **Lim BK, Peter AK, Xiong D, Narezkina A, Yung A, Dalton ND, Hwang KK, Yajima T, Chen J, Knowlton KU.** 2013. Inhibition of Coxsackievirus-associated dystrophin cleavage prevents cardiomyopathy. J Clin Invest **123:**5146-5151.
167. **Deconinck AE, Rafael JA, Skinner JA, Brown SC, Potter AC, Metzinger L, Watt DJ, Dickson JG, Tinsley JM, Davies KE.** 1997. Utrophin-dystrophin-deficient mice as a model for Duchenne muscular dystrophy. Cell **90:**717-727.
168. **Grady RM, Teng H, Nichol MC, Cunningham JC, Wilkinson RS, Sanes JR.** 1997. Skeletal and cardiac myopathies in mice lacking utrophin and dystrophin: a model for Duchenne muscular dystrophy. Cell **90:**729-738.
169. **Wang C, Wong J, Fung G, Shi J, Deng H, Zhang J, Bernatchez P, Luo H.** 2015. Dysferlin deficiency confers increased susceptibility to coxsackievirus-induced cardiomyopathy. Cell Microbiol **17:**1423-1430.
170. **Carthy CM, Granville DJ, Watson KA, Anderson DR, Wilson JE, Yang D, Hunt DW, McManus BM.** 1998. Caspase activation and specific cleavage of substrates after coxsackievirus B3-induced cytopathic effect in HeLa cells. J Virol **72:**7669-7675.
171. **Ammendolia MG, Tinari A, Calcabrini A, Superti F.** 1999. Poliovirus infection induces apoptosis in CaCo-2 cells. J Med Virol **59:**122-129.
172. **Agol VI, Belov GA, Bienz K, Egger D, Kolesnikova MS, Raikhlin NT, Romanova LI, Smirnova EA, Tolskaya EA.** 1998. Two types of death of poliovirus-infected cells: caspase involvement in the apoptosis but not cytopathic effect. Virology **252:**343-353.
173. **Girard S, Couderc T, Destombes J, Thiesson D, Delpeyroux F, Blondel B.** 1999. Poliovirus induces apoptosis in the mouse central nervous system. J Virol **73:**6066-6072.
174. **Venteo L, Bourlet T, Renois F, Douche-Aourik F, Mosnier JF, Maison GL, Pluot M, Pozzetto B, Andreoletti L.** 2010. Enterovirus-related activation of the cardiomyocyte

mitochondrial apoptotic pathway in patients with acute myocarditis. Eur Heart J **31:**728-736.
175. **Chau DH, Yuan J, Zhang H, Cheung P, Lim T, Liu Z, Sall A, Yang D.** 2007. Coxsackievirus B3 proteases 2A and 3C induce apoptotic cell death through mitochondrial injury and cleavage of eIF4GI but not DAP5/p97/NAT1. Apoptosis **12:**513-524.
176. **Jensen KJ, Garmaroudi FS, Zhang J, Lin J, Boroomand S, Zhang M, Luo Z, Yang D, Luo H, McManus BM, Janes KA.** 2013. An ERK-p38 subnetwork coordinates host cell apoptosis and necrosis during coxsackievirus B3 infection. Cell Host Microbe **13:**67-76.
177. **Gu H, Neel BG.** 2003. The "Gab" in signal transduction. Trends Cell Biol **13:**122-130.
178. **Nishida K, Hirano T.** 2003. The role of Gab family scaffolding adapter proteins in the signal transduction of cytokine and growth factor receptors. Cancer Sci **94:**1029-1033.
179. **Deng H, Fung G, Shi J, Xu S, Wang C, Yin M, Hou J, Zhang J, Jin ZG, Luo H.** 2015. Enhanced enteroviral infectivity via viral protease-mediated cleavage of Grb2-associated binder 1. FASEB J **29:**4523-4531.
180. **Huber M, Watson KA, Selinka HC, Carthy CM, Klingel K, McManus BM, Kandolf R.** 1999. Cleavage of RasGAP and phosphorylation of mitogen-activated protein kinase in the course of coxsackievirus B3 replication. J Virol **73:**3587-3594.
181. **Luo H, Yanagawa B, Zhang J, Luo Z, Zhang M, Esfandiarei M, Carthy C, Wilson JE, Yang D, McManus BM.** 2002. Coxsackievirus B3 replication is reduced by inhibition of the extracellular signal-regulated kinase (ERK) signaling pathway. J Virol **76:**3365-3373.
182. **Mogensen TH.** 2009. Pathogen recognition and inflammatory signaling in innate immune defenses. Clin Microbiol Rev **22:**240-273, Table of Contents.
183. **Hornung V, Ellegast J, Kim S, Brzozka K, Jung A, Kato H, Poeck H, Akira S, Conzelmann KK, Schlee M, Endres S, Hartmann G.** 2006. 5'-Triphosphate RNA is the ligand for RIG-I. Science **314:**994-997.
184. **Kato H, Takeuchi O, Sato S, Yoneyama M, Yamamoto M, Matsui K, Uematsu S, Jung A, Kawai T, Ishii KJ, Yamaguchi O, Otsu K, Tsujimura T, Koh CS, Reis e Sousa C, Matsuura Y, Fujita T, Akira S.** 2006. Differential roles of MDA5 and RIG-I helicases in the recognition of RNA viruses. Nature **441:**101-105.
185. **Saito T, Gale M, Jr.** 2008. Differential recognition of double-stranded RNA by RIG-I-like receptors in antiviral immunity. J Exp Med **205:**1523-1527.
186. **Kato H, Takeuchi O, Mikamo-Satoh E, Hirai R, Kawai T, Matsushita K, Hiiragi A, Dermody TS, Fujita T, Akira S.** 2008. Length-dependent recognition of double-stranded ribonucleic acids by retinoic acid-inducible gene-I and melanoma differentiation-associated gene 5. J Exp Med **205:**1601-1610.
187. **Pichlmair A, Schulz O, Tan CP, Naslund TI, Liljestrom P, Weber F, Reis e Sousa C.** 2006. RIG-I-mediated antiviral responses to single-stranded RNA bearing 5'-phosphates. Science **314:**997-1001.
188. **Wang Q, Miller DJ, Bowman ER, Nagarkar DR, Schneider D, Zhao Y, Linn MJ, Goldsmith AM, Bentley JK, Sajjan US, Hershenson MB.** 2011. MDA5 and TLR3 initiate pro-inflammatory signaling pathways leading to rhinovirus-induced airways inflammation and hyperresponsiveness. PLoS Pathog **7:**e1002070.

189. **Wang Q, Nagarkar DR, Bowman ER, Schneider D, Gosangi B, Lei J, Zhao Y, McHenry CL, Burgens RV, Miller DJ, Sajjan U, Hershenson MB.** 2009. Role of double-stranded RNA pattern recognition receptors in rhinovirus-induced airway epithelial cell responses. J Immunol **183:**6989-6997.
190. **Gitlin L, Barchet W, Gilfillan S, Cella M, Beutler B, Flavell RA, Diamond MS, Colonna M.** 2006. Essential role of mda-5 in type I IFN responses to polyriboinosinic:polyribocytidylic acid and encephalomyocarditis picornavirus. Proc Natl Acad Sci U S A **103:**8459-8464.
191. **Feng Q, Langereis MA, Lork M, Nguyen M, Hato SV, Lanke K, Emdad L, Bhoopathi P, Fisher PB, Lloyd RE, van Kuppeveld FJM.** 2014. Enterovirus 2A(Pro) Targets MDA5 and MAVS in Infected Cells. Journal of Virology **88:**3369-3378.
192. **Barral PM, Morrison JM, Drahos J, Gupta P, Sarkar D, Fisher PB, Racaniello VR.** 2007. MDA-5 is cleaved in poliovirus-infected cells. Journal of Virology **81:**3677-3684.
193. **Barral PM, Sarkar D, Fisher PB, Racaniello VR.** 2009. RIG-I is cleaved during picornavirus infection. Virology **391:**171-176.
194. **Lupfer C, Malik A, Kanneganti TD.** 2015. Inflammasome control of viral infection. Curr Opin Virol **12:**38-46.
195. **Kanneganti TD, Ozoren N, Body-Malapel M, Amer A, Park JH, Franchi L, Whitfield J, Barchet W, Colonna M, Vandenabeele P, Bertin J, Coyle A, Grant EP, Akira S, Nunez G.** 2006. Bacterial RNA and small antiviral compounds activate caspase-1 through cryopyrin/Nalp3. Nature **440:**233-236.
196. **Wang H, Lei X, Xiao X, Yang C, Lu W, Huang Z, Leng Q, Jin Q, He B, Meng G, Wang J.** 2015. Reciprocal Regulation between Enterovirus 71 and the NLRP3 Inflammasome. Cell Rep **12:**42-48.
197. **Qu L, Feng Z, Yamane D, Liang Y, Lanford RE, Li K, Lemon SM.** 2011. Disruption of TLR3 signaling due to cleavage of TRIF by the hepatitis A virus protease-polymerase processing intermediate, 3CD. PLoS Pathog **7:**e1002169.
198. **Lei X, Sun Z, Liu X, Jin Q, He B, Wang J.** 2011. Cleavage of the adaptor protein TRIF by enterovirus 71 3C inhibits antiviral responses mediated by Toll-like receptor 3. J Virol **85:**8811-8818.
199. **Xiang Z, Li L, Lei X, Zhou H, Zhou Z, He B, Wang J.** 2014. Enterovirus 68 3C protease cleaves TRIF to attenuate antiviral responses mediated by Toll-like receptor 3. J Virol **88:**6650-6659.
200. **Wang D, Fang L, Li K, Zhong H, Fan J, Ouyang C, Zhang H, Duan E, Luo R, Zhang Z, Liu X, Chen H, Xiao S.** 2012. Foot-and-mouth disease virus 3C protease cleaves NEMO to impair innate immune signaling. J Virol **86:**9311-9322.
201. **Wang D, Fang L, Wei D, Zhang H, Luo R, Chen H, Li K, Xiao S.** 2014. Hepatitis A virus 3C protease cleaves NEMO to impair induction of beta interferon. J Virol **88:**10252-10258.
202. **Chu W, Gong X, Li Z, Takabayashi K, Ouyang H, Chen Y, Lois A, Chen DJ, Li GC, Karin M, Raz E.** 2000. DNA-PKcs is required for activation of innate immunity by immunostimulatory DNA. Cell **103:**909-918.
203. **Ferguson BJ, Mansur DS, Peters NE, Ren H, Smith GL.** 2012. DNA-PK is a DNA sensor for IRF-3-dependent innate immunity. Elife **1:**e00047.

204. **Graham KL, Gustin KE, Rivera C, Kuyumcu-Martinez NM, Choe SS, Lloyd RE, Sarnow P, Utz PJ.** 2004. Proteolytic cleavage of the catalytic subunit of DNA-dependent protein kinase during poliovirus infection. J Virol **78:**6313-6321.
205. **Xiang Z, Liu L, Lei X, Zhou Z, He B, Wang J.** 2016. 3C Protease of Enterovirus D68 Inhibits Cellular Defense Mediated by Interferon Regulatory Factor 7. J Virol **90:**1613-1621.
206. **Lei X, Xiao X, Xue Q, Jin Q, He B, Wang J.** 2013. Cleavage of interferon regulatory factor 7 by enterovirus 71 3C suppresses cellular responses. J Virol **87:**1690-1698.
207. **Saura M, Lizarbe TR, Rama-Pacheco C, Lowenstein CJ, Zaragoza C.** 2007. Inhibitor of NF kappa B alpha is a host sensor of coxsackievirus infection. Cell Cycle **6:**503-506.
208. **Lei X, Han N, Xiao X, Jin Q, He B, Wang J.** 2014. Enterovirus 71 3C inhibits cytokine expression through cleavage of the TAK1/TAB1/TAB2/TAB3 complex. J Virol **88:**9830-9841.
209. **Schneider WM, Chevillotte MD, Rice CM.** 2014. Interferon-stimulated genes: a complex web of host defenses. Annu Rev Immunol **32:**513-545.
210. **Lu J, Yi L, Zhao J, Yu J, Chen Y, Lin MC, Kung HF, He ML.** 2012. Enterovirus 71 disrupts interferon signaling by reducing the level of interferon receptor 1. J Virol **86:**3767-3776.
211. **Hung HC, Wang HC, Shih SR, Teng IF, Tseng CP, Hsu JT.** 2011. Synergistic inhibition of enterovirus 71 replication by interferon and rupintrivir. J Infect Dis **203:**1784-1790.
212. **Mallery DL, McEwan WA, Bidgood SR, Towers GJ, Johnson CM, James LC.** 2010. Antibodies mediate intracellular immunity through tripartite motif-containing 21 (TRIM21). Proc Natl Acad Sci U S A **107:**19985-19990.
213. **McEwan WA, Hauler F, Williams CR, Bidgood SR, Mallery DL, Crowther RA, James LC.** 2012. Regulation of virus neutralization and the persistent fraction by TRIM21. J Virol **86:**8482-8491.
214. **Vaysburd M, Watkinson RE, Cooper H, Reed M, O'Connell K, Smith J, Cruickshanks J, James LC.** 2013. Intracellular antibody receptor TRIM21 prevents fatal viral infection. Proc Natl Acad Sci U S A **110:**12397-12401.
215. **Watkinson RE, Tam JC, Vaysburd MJ, James LC.** 2013. Simultaneous neutralization and innate immune detection of a replicating virus by TRIM21. J Virol **87:**7309-7313.
216. **Stoermer KA, Morrison TE.** 2011. Complement and viral pathogenesis. Virology **411:**362-373.
217. **Bonaparte RS, Hair PS, Banthia D, Marshall DM, Cunnion KM, Krishna NK.** 2008. Human astrovirus coat protein inhibits serum complement activation via C1, the first component of the classical pathway. J Virol **82:**817-827.
218. **Xu Z, Qiu Q, Tian J, Smith JS, Conenello GM, Morita T, Byrnes AP.** 2013. Coagulation factor X shields adenovirus type 5 from attack by natural antibodies and complement. Nat Med **19:**452-457.
219. **Tam JC, Bidgood SR, McEwan WA, James LC.** 2014. Intracellular sensing of complement C3 activates cell autonomous immunity. Science **345:**1256070.
220. **Protter DS, Parker R.** 2016. Principles and Properties of Stress Granules. Trends Cell Biol **26:**668-679.

221. **Tourriere H, Chebli K, Zekri L, Courselaud B, Blanchard JM, Bertrand E, Tazi J.** 2003. The RasGAP-associated endoribonuclease G3BP assembles stress granules. J Cell Biol **160:**823-831.
222. **Kedersha N, Cho MR, Li W, Yacono PW, Chen S, Gilks N, Golan DE, Anderson P.** 2000. Dynamic shuttling of TIA-1 accompanies the recruitment of mRNA to mammalian stress granules. J Cell Biol **151:**1257-1268.
223. **Tian Q, Streuli M, Saito H, Schlossman SF, Anderson P.** 1991. A polyadenylate binding protein localized to the granules of cytolytic lymphocytes induces DNA fragmentation in target cells. Cell **67:**629-639.
224. **Borghese F, Michiels T.** 2011. The leader protein of cardioviruses inhibits stress granule assembly. J Virol **85:**9614-9622.
225. **Fung G, Ng CS, Zhang J, Shi J, Wong J, Piesik P, Han L, Chu F, Jagdeo J, Jan E, Fujita T, Luo H.** 2013. Production of a dominant-negative fragment due to G3BP1 cleavage contributes to the disruption of mitochondria-associated protective stress granules during CVB3 infection. PLoS One **8:**e79546.
226. **White JP, Cardenas AM, Marissen WE, Lloyd RE.** 2007. Inhibition of cytoplasmic mRNA stress granule formation by a viral proteinase. Cell Host Microbe **2:**295-305.
227. **Ng CS, Jogi M, Yoo JS, Onomoto K, Koike S, Iwasaki T, Yoneyama M, Kato H, Fujita T.** 2013. Encephalomyocarditis virus disrupts stress granules, the critical platform for triggering antiviral innate immune responses. J Virol **87:**9511-9522.
228. **Langereis MA, Feng Q, van Kuppeveld FJ.** 2013. MDA5 localizes to stress granules, but this localization is not required for the induction of type I interferon. J Virol **87:**6314-6325.
229. **Reineke LC, Lloyd RE.** 2015. The stress granule protein G3BP1 recruits protein kinase R to promote multiple innate immune antiviral responses. J Virol **89:**2575-2589.
230. **Reineke LC, Kedersha N, Langereis MA, van Kuppeveld FJ, Lloyd RE.** 2015. Stress granules regulate double-stranded RNA-dependent protein kinase activation through a complex containing G3BP1 and Caprin1. MBio **6:**e02486.
231. **Kleifeld O, Doucet A, auf dem Keller U, Prudova A, Schilling O, Kainthan RK, Starr AE, Foster LJ, Kizhakkedathu JN, Overall CM.** 2010. Isotopic labeling of terminal amines in complex samples identifies protein N-termini and protease cleavage products. Nat Biotechnol **28:**281-288.
232. **Huesgen PF, Overall CM.** 2012. N- and C-terminal degradomics: new approaches to reveal biological roles for plant proteases from substrate identification. Physiol Plant **145:**5-17.
233. **Mahrus S, Trinidad JC, Barkan DT, Sali A, Burlingame AL, Wells JA.** 2008. Global sequencing of proteolytic cleavage sites in apoptosis by specific labeling of protein N termini. Cell **134:**866-876.
234. **Kleifeld O, Doucet A, Prudova A, auf dem Keller U, Gioia M, Kizhakkedathu JN, Overall CM.** 2011. Identifying and quantifying proteolytic events and the natural N terminome by terminal amine isotopic labeling of substrates. Nat Protoc **6:**1578-1611.
235. **Staes A, Impens F, Van Damme P, Ruttens B, Goethals M, Demol H, Timmerman E, Vandekerckhove J, Gevaert K.** 2011. Selecting protein N-terminal peptides by combined fractional diagonal chromatography. Nat Protoc **6:**1130-1141.

236. **Van Damme P, Impens F, Vandekerckhove J, Gevaert K.** 2008. Protein processing characterized by a gel-free proteomics approach. Methods Mol Biol **484:**245-262.
237. **Staes A, Van Damme P, Helsens K, Demol H, Vandekerckhove J, Gevaert K.** 2008. Improved recovery of proteome-informative, protein N-terminal peptides by combined fractional diagonal chromatography (COFRADIC). Proteomics **8:**1362-1370.
238. **Impens F, Timmerman E, Staes A, Moens K, Arien KK, Verhasselt B, Vandekerckhove J, Gevaert K.** 2012. A catalogue of putative HIV-1 protease host cell substrates. Biol Chem **393:**915-931.
239. **Jefferson T, Auf dem Keller U, Bellac C, Metz VV, Broder C, Hedrich J, Ohler A, Maier W, Magdolen V, Sterchi E, Bond JS, Jayakumar A, Traupe H, Chalaris A, Rose-John S, Pietrzik CU, Postina R, Overall CM, Becker-Pauly C.** 2013. The substrate degradome of meprin metalloproteases reveals an unexpected proteolytic link between meprin beta and ADAM10. Cell Mol Life Sci **70:**309-333.
240. **Schilling O, Barre O, Huesgen PF, Overall CM.** 2010. Proteome-wide analysis of protein carboxy termini: C terminomics. Nat Methods **7:**508-511.
241. **Van Damme P, Staes A, Bronsoms S, Helsens K, Colaert N, Timmerman E, Aviles FX, Vandekerckhove J, Gevaert K.** 2010. Complementary positional proteomics for screening substrates of endo- and exoproteases. Nat Methods **7:**512-515.
242. **Mohagheghi F, Prudencio M, Stuani C, Cook C, Jansen-West K, Dickson DW, Petrucelli L, Buratti E.** 2015. TDP-43 functions within a network of hnRNP proteins to inhibit the production of a truncated human SORT1 receptor. Hum Mol Genet doi:10.1093/hmg/ddv491.
243. **Chen S, Zhang J, Duan L, Zhang Y, Li C, Liu D, Ouyang C, Lu F, Liu X.** 2014. Identification of HnRNP M as a novel biomarker for colorectal carcinoma by quantitative proteomics. Am J Physiol Gastrointest Liver Physiol **306:**G394-403.
244. **Cui Y, Koirala D, Kang H, Dhakal S, Yangyuoru P, Hurley LH, Mao H.** 2014. Molecular population dynamics of DNA structures in a bcl-2 promoter sequence is regulated by small molecules and the transcription factor hnRNP LL. Nucleic Acids Res **42:**5755-5764.
245. **Colaert N, Helsens K, Martens L, Vandekerckhove J, Gevaert K.** 2009. Improved visualization of protein consensus sequences by iceLogo. Nat Methods **6:**786-787.
246. **Lin JY, Chen TC, Weng KF, Chang SC, Chen LL, Shih SR.** 2009. Viral and host proteins involved in picornavirus life cycle. J Biomed Sci **16:**103.
247. **Weng KF, Li ML, Hung CT, Shih SR.** 2009. Enterovirus 71 3C protease cleaves a novel target CstF-64 and inhibits cellular polyadenylation. PLoS Pathog **5:**e1000593.
248. **Fung G, Shi J, Deng H, Hou J, Wang C, Hong A, Zhang J, Jia W, Luo H.** 2015. Cytoplasmic translocation, aggregation, and cleavage of TDP-43 by enteroviral proteases modulate viral pathogenesis. Cell Death Differ **22:**2087-2097.
249. **Garmaroudi FS, Marchant D, Hendry R, Luo H, Yang D, Ye X, Shi J, McManus BM.** 2015. Coxsackievirus B3 replication and pathogenesis. Future Microbiol **10:**629-653.
250. **Marchant D, Si X, Luo H, McManus B, Yang D.** 2008. The impact of CVB3 infection on host cell biology. Curr Top Microbiol Immunol **323:**177-198.

251. **Jagdeo JM, Dufour A, Fung G, Luo H, Kleifeld O, Overall CM, Jan E.** 2015. Heterogeneous Nuclear Ribonucleoprotein M Facilitates Enterovirus Infection. J Virol **89:**7064-7078.
252. **Chase AJ, Semler BL.** 2012. Viral subversion of host functions for picornavirus translation and RNA replication. Future Virol **7:**179-191.
253. **Lloyd RE.** 2006. Translational control by viral proteinases. Virus Res **119:**76-88.
254. **Rebsamen M, Meylan E, Curran J, Tschopp J.** 2008. The antiviral adaptor proteins Cardif and Trif are processed and inactivated by caspases. Cell Death Differ **15:**1804-1811.
255. **Lenarcic EM, Landry DM, Greco TM, Cristea IM, Thompson SR.** 2013. Thiouracil cross-linking mass spectrometry: a cell-based method to identify host factors involved in viral amplification. J Virol **87:**8697-8712.
256. **Kim S, Hill A, Warman ML, Smits P.** 2012. Golgi disruption and early embryonic lethality in mice lacking USO1. PLoS One **7:**e50530.
257. **Puthenveedu MA, Linstedt AD.** 2004. Gene replacement reveals that p115/SNARE interactions are essential for Golgi biogenesis. Proc Natl Acad Sci U S A **101:**1253-1256.
258. **Griffith KJ, Chan EK, Lung CC, Hamel JC, Guo X, Miyachi K, Fritzler MJ.** 1997. Molecular cloning of a novel 97-kd Golgi complex autoantigen associated with Sjogren's syndrome. Arthritis Rheum **40:**1693-1702.
259. **Nakamura N, Rabouille C, Watson R, Nilsson T, Hui N, Slusarewicz P, Kreis TE, Warren G.** 1995. Characterization of a cis-Golgi matrix protein, GM130. J Cell Biol **131:**1715-1726.
260. **Dales S, Eggers HJ, Tamm I, Palade GE.** 1965. Electron Microscopic Study of the Formation of Poliovirus. Virology **26:**379-389.
261. **Yamaoka T, Kondo M, Honda S, Iwahana H, Moritani M, Ii S, Yoshimoto K, Itakura M.** 1997. Amidophosphoribosyltransferase limits the rate of cell growth-linked de novo purine biosynthesis in the presence of constant capacity of salvage purine biosynthesis. J Biol Chem **272:**17719-17725.
262. **Sweeney TR, Abaeva IS, Pestova TV, Hellen CU.** 2014. The mechanism of translation initiation on Type 1 picornavirus IRESs. EMBO J **33:**76-92.
263. **Cordes S, Kusov Y, Heise T, Gauss-Muller V.** 2008. La autoantigen suppresses IRES-dependent translation of the hepatitis A virus. Biochem Biophys Res Commun **368:**1014-1019.
264. **Jiang X, Kanda T, Wu S, Nakamoto S, Saito K, Shirasawa H, Kiyohara T, Ishii K, Wakita T, Okamoto H, Yokosuka O.** 2014. Suppression of La antigen exerts potential antiviral effects against hepatitis A virus. PLoS One **9:**e101993.
265. **Mukhopadhyay NK, Kim J, Cinar B, Ramachandran A, Hager MH, Di Vizio D, Adam RM, Rubin MA, Raychaudhuri P, De Benedetti A, Freeman MR.** 2009. Heterogeneous nuclear ribonucleoprotein K is a novel regulator of androgen receptor translation. Cancer Res **69:**2210-2218.
266. **Ostareck DH, Ostareck-Lederer A, Shatsky IN, Hentze MW.** 2001. Lipoxygenase mRNA silencing in erythroid differentiation: The 3'UTR regulatory complex controls 60S ribosomal subunit joining. Cell **104:**281-290.

267. **Ostareck DH, Ostareck-Lederer A, Wilm M, Thiele BJ, Mann M, Hentze MW.** 1997. mRNA silencing in erythroid differentiation: hnRNP K and hnRNP E1 regulate 15-lipoxygenase translation from the 3' end. Cell **89:**597-606.
268. **Ostareck-Lederer A, Ostareck DH, Cans C, Neubauer G, Bomsztyk K, Superti-Furga G, Hentze MW.** 2002. c-Src-mediated phosphorylation of hnRNP K drives translational activation of specifically silenced mRNAs. Mol Cell Biol **22:**4535-4543.
269. **Takimoto M, Tomonaga T, Matunis M, Avigan M, Krutzsch H, Dreyfuss G, Levens D.** 1993. Specific binding of heterogeneous ribonucleoprotein particle protein K to the human c-myc promoter, in vitro. J Biol Chem **268:**18249-18258.
270. **Ostrowski J, Kawata Y, Schullery DS, Denisenko ON, Bomsztyk K.** 2003. Transient recruitment of the hnRNP K protein to inducibly transcribed gene loci. Nucleic Acids Res **31:**3954-3962.
271. **Michelotti EF, Michelotti GA, Aronsohn AI, Levens D.** 1996. Heterogeneous nuclear ribonucleoprotein K is a transcription factor. Mol Cell Biol **16:**2350-2360.
272. **Lee SW, Lee MH, Park JH, Kang SH, Yoo HM, Ka SH, Oh YM, Jeon YJ, Chung CH.** 2012. SUMOylation of hnRNP-K is required for p53-mediated cell-cycle arrest in response to DNA damage. EMBO J **31:**4441-4452.
273. **Kaminski A, Jackson RJ.** 1998. The polypyrimidine tract binding protein (PTB) requirement for internal initiation of translation of cardiovirus RNAs is conditional rather than absolute. RNA **4:**626-638.
274. **Belov GA, Nair V, Hansen BT, Hoyt FH, Fischer ER, Ehrenfeld E.** 2012. Complex dynamic development of poliovirus membranous replication complexes. J Virol **86:**302-312.
275. **van der Schaar HM, Leyssen P, Thibaut HJ, de Palma A, van der Linden L, Lanke KH, Lacroix C, Verbeken E, Conrath K, Macleod AM, Mitchell DR, Palmer NJ, van de Poel H, Andrews M, Neyts J, van Kuppeveld FJ.** 2013. A novel, broad-spectrum inhibitor of enterovirus replication that targets host cell factor phosphatidylinositol 4-kinase IIIbeta. Antimicrob Agents Chemother **57:**4971-4981.
276. **Lin R, Tao R, Gao X, Li T, Zhou X, Guan KL, Xiong Y, Lei QY.** 2013. Acetylation stabilizes ATP-citrate lyase to promote lipid biosynthesis and tumor growth. Mol Cell **51:**506-518.
277. **Beske O, Reichelt M, Taylor MP, Kirkegaard K, Andino R.** 2007. Poliovirus infection blocks ERGIC-to-Golgi trafficking and induces microtubule-dependent disruption of the Golgi complex. J Cell Sci **120:**3207-3218.
278. **Trahey M, Oh HS, Cameron CE, Hay JC.** 2012. Poliovirus infection transiently increases COPII vesicle budding. J Virol **86:**9675-9682.
279. **Suhy DA, Giddings TH, Jr., Kirkegaard K.** 2000. Remodeling the endoplasmic reticulum by poliovirus infection and by individual viral proteins: an autophagy-like origin for virus-induced vesicles. J Virol **74:**8953-8965.
280. **Aldabe R, Carrasco L.** 1995. Induction of membrane proliferation by poliovirus proteins 2C and 2BC. Biochem Biophys Res Commun **206:**64-76.
281. **Guo Y, Punj V, Sengupta D, Linstedt AD.** 2008. Coat-tether interaction in Golgi organization. Mol Biol Cell **19:**2830-2843.
282. **Richards AL, Soares-Martins JA, Riddell GT, Jackson WT.** 2014. Generation of unique poliovirus RNA replication organelles. MBio **5:**e00833-00813.

283. **Bissig C, Gruenberg J.** 2014. ALIX and the multivesicular endosome: ALIX in Wonderland. Trends Cell Biol **24:**19-25.
284. **Murrow L, Debnath J.** 2015. ATG12-ATG3 connects basal autophagy and late endosome function. Autophagy **11:**961-962.
285. **Fisher RD, Chung HY, Zhai Q, Robinson H, Sundquist WI, Hill CP.** 2007. Structural and biochemical studies of ALIX/AIP1 and its role in retrovirus budding. Cell **128:**841-852.
286. **Zhai Q, Fisher RD, Chung HY, Myszka DG, Sundquist WI, Hill CP.** 2008. Structural and functional studies of ALIX interactions with YPX(n)L late domains of HIV-1 and EIAV. Nat Struct Mol Biol **15:**43-49.
287. **Bird SW, Maynard ND, Covert MW, Kirkegaard K.** 2014. Nonlytic viral spread enhanced by autophagy components. Proc Natl Acad Sci U S A **111:**13081-13086.
288. **Chen X, Liao J, Chen L, Qiu S, Mo C, Mao X, Yang Y, Zhou S, Chen J.** 2015. En bloc transurethral resection with 2-micron continuous-wave laser for primary non-muscle-invasive bladder cancer: a randomized controlled trial. World J Urol **33:**989-995.
289. **Robinson SM, Tsueng G, Sin J, Mangale V, Rahawi S, McIntyre LL, Williams W, Kha N, Cruz C, Hancock BM, Nguyen DP, Sayen MR, Hilton BJ, Doran KS, Segall AM, Wolkowicz R, Cornell CT, Whitton JL, Gottlieb RA, Feuer R.** 2014. Coxsackievirus B exits the host cell in shed microvesicles displaying autophagosomal markers. PLoS Pathog **10:**e1004045.
290. **Richards AL, Jackson WT.** 2012. Intracellular vesicle acidification promotes maturation of infectious poliovirus particles. PLoS Pathog **8:**e1003046.
291. **Taylor MP, Kirkegaard K.** 2007. Modification of cellular autophagy protein LC3 by poliovirus. J Virol **81:**12543-12553.
292. **Wang X, Jiang W, Yan Y, Gong T, Han J, Tian Z, Zhou R.** 2014. RNA viruses promote activation of the NLRP3 inflammasome through a RIP1-RIP3-DRP1 signaling pathway. Nat Immunol **15:**1126-1133.
293. **Jiang S, Cheng LY, Bai AM, Zhou S, Hu YJ.** 2015. Novel rare earth tungstoarsenate heteropolyoxometalates K11[Ln(AsW 11O 39) 2].xH 2O (Ln = La, Nd, Sm) binding to bovine serum albumin: spectroscopic approach. Biol Trace Elem Res **163:**275-282.
294. **Martinez-Contreras R, Cloutier P, Shkreta L, Fisette JF, Revil T, Chabot B.** 2007. hnRNP proteins and splicing control. Adv Exp Med Biol **623:**123-147.
295. **Han SP, Tang YH, Smith R.** 2010. Functional diversity of the hnRNPs: past, present and perspectives. Biochem J **430:**379-392.
296. **Lin JY, Shih SR, Pan M, Li C, Lue CF, Stollar V, Li ML.** 2009. hnRNP A1 interacts with the 5' untranslated regions of enterovirus 71 and Sindbis virus RNA and is required for viral replication. J Virol **83:**6106-6114.
297. **Chase AJ, Daijogo S, Semler BL.** 2014. Inhibition of poliovirus-induced cleavage of cellular protein PCBP2 reduces the levels of viral RNA replication. J Virol **88:**3192-3201.
298. **Dery KJ, Gaur S, Gencheva M, Yen Y, Shively JE, Gaur RK.** 2011. Mechanistic control of carcinoembryonic antigen-related cell adhesion molecule-1 (CEACAM1) splice isoforms by the heterogeneous nuclear ribonuclear proteins hnRNP L, hnRNP A1, and hnRNP M. J Biol Chem **286:**16039-16051.

299. **Hovhannisyan RH, Carstens RP.** 2007. Heterogeneous ribonucleoprotein m is a splicing regulatory protein that can enhance or silence splicing of alternatively spliced exons. J Biol Chem **282:**36265-36274.
300. **Kafasla P, Patrinou-Georgoula M, Guialis A.** 2000. The 72/74-kDa polypeptides of the 70-110 S large heterogeneous nuclear ribonucleoprotein complex (LH-nRNP) represent a discrete subset of the hnRNP M protein family. Biochem J **350 Pt 2:**495-503.
301. **Kafasla P, Patrinou-Georgoula M, Lewis JD, Guialis A.** 2002. Association of the 72/74-kDa proteins, members of the heterogeneous nuclear ribonucleoprotein M group, with the pre-mRNA at early stages of spliceosome assembly. Biochem J **363:**793-799.
302. **Lleres D, Denegri M, Biggiogera M, Ajuh P, Lamond AI.** 2010. Direct interaction between hnRNP-M and CDC5L/PLRG1 proteins affects alternative splice site choice. EMBO Rep **11:**445-451.
303. **Park E, Iaccarino C, Lee J, Kwon I, Baik SM, Kim M, Seong JY, Son GH, Borrelli E, Kim K.** 2011. Regulatory roles of heterogeneous nuclear ribonucleoprotein M and Nova-1 protein in alternative splicing of dopamine D2 receptor pre-mRNA. J Biol Chem **286:**25301-25308.
304. **Datar KV, Dreyfuss G, Swanson MS.** 1993. The human hnRNP M proteins: identification of a methionine/arginine-rich repeat motif in ribonucleoproteins. Nucleic Acids Res **21:**439-446.
305. **Tolskaya EA, Romanova LI, Kolesnikova MS, Ivannikova TA, Smirnova EA, Raikhlin NT, Agol VI.** 1995. Apoptosis-inducing and apoptosis-preventing functions of poliovirus. J Virol **69:**1181-1189.
306. **Blondel B, Autret A, Brisac C, Martin-Latil S, Mousson L, Pelletier I, Estaquier J, Colbere-Garapin F.** 2009. Apoptotic signaling cascades operating in poliovirus-infected cells. Front Biosci (Landmark Ed) **14:**2181-2192.
307. **Aidinis V, Sekeris CE, Guialis A.** 1995. Two immunologically related polypeptides of 72/74 kDa specify a novel 70-100S heterogeneous nuclear RNP. Nucleic Acids Res **23:**2742-2753.
308. **Simoes EA, Sarnow P.** 1991. An RNA hairpin at the extreme 5' end of the poliovirus RNA genome modulates viral translation in human cells. J Virol **65:**913-921.
309. **Kiesler E, Hase ME, Brodin D, Visa N.** 2005. Hrp59, an hnRNP M protein in Chironomus and Drosophila, binds to exonic splicing enhancers and is required for expression of a subset of mRNAs. J Cell Biol **168:**1013-1025.
310. **Cho S, Moon H, Loh TJ, Oh HK, Choy HE, Song WK, Chun JS, Zheng X, Shen H.** 2014. hnRNP M facilitates exon 7 inclusion of SMN2 pre-mRNA in spinal muscular atrophy by targeting an enhancer on exon 7. Biochim Biophys Acta **1839:**306-315.
311. **Marko M, Leichter M, Patrinou-Georgoula M, Guialis A.** 2014. Selective interactions of hnRNP M isoforms with the TET proteins TAF15 and TLS/FUS. Mol Biol Rep **41:**2687-2695.
312. **Bajenova OV, Zimmer R, Stolper E, Salisbury-Rowswell J, Nanji A, Thomas P.** 2001. Heterogeneous RNA-binding protein M4 is a receptor for carcinoembryonic antigen in Kupffer cells. J Biol Chem **276:**31067-31073.
313. **Gattoni R, Mahe D, Mahl P, Fischer N, Mattei MG, Stevenin J, Fuchs JP.** 1996. The human hnRNP-M proteins: structure and relation with early heat shock-induced splicing arrest and chromosome mapping. Nucleic Acids Res **24:**2535-2542.

314. **Liu YC, Kuo RL, Lin JY, Huang PN, Huang Y, Liu H, Arnold JJ, Chen SJ, Wang RY, Cameron CE, Shih SR.** 2014. Cytoplasmic viral RNA-dependent RNA polymerase disrupts the intracellular splicing machinery by entering the nucleus and interfering with Prp8. PLoS Pathog **10:**e1004199.
315. **Jorba N, Juarez S, Torreira E, Gastaminza P, Zamarreno N, Albar JP, Ortin J.** 2008. Analysis of the interaction of influenza virus polymerase complex with human cell factors. Proteomics **8:**2077-2088.
316. **Varjak M, Saul S, Arike L, Lulla A, Peil L, Merits A.** 2013. Magnetic fractionation and proteomic dissection of cellular organelles occupied by the late replication complexes of Semliki Forest virus. J Virol **87:**10295-10312.
317. **Dougherty JD, White JP, Lloyd RE.** 2011. Poliovirus-mediated disruption of cytoplasmic processing bodies. J Virol **85:**64-75.
318. **Feng Q, Langereis MA, Lork M, Nguyen M, Hato SV, Lanke K, Emdad L, Bhoopathi P, Fisher PB, Lloyd RE, van Kuppeveld FJ.** 2014. Enterovirus 2Apro targets MDA5 and MAVS in infected cells. J Virol **88:**3369-3378.
319. **Zoll J, Galama JM, van Kuppeveld FJ, Melchers WJ.** 1996. Mengovirus leader is involved in the inhibition of host cell protein synthesis. J Virol **70:**4948-4952.
320. **van Pesch V, van Eyll O, Michiels T.** 2001. The leader protein of Theiler's virus inhibits immediate-early alpha/beta interferon production. J Virol **75:**7811-7817.
321. **Nakashima N, Nakamura Y.** 2008. Cleavage sites of the "P3 region" in the nonstructural polyprotein precursor of a dicistrovirus. Arch Virol **153:**1955-1960.
322. **Nakashima N, Ishibashi J.** 2010. Identification of the 3C-protease-mediated 2A/2B and 2B/2C cleavage sites in the nonstructural polyprotein precursor of a Dicistrovirus lacking the NPGP motif. Arch Virol **155:**1477-1482.
323. **Tacon CE, Wiehler S, Holden NS, Newton R, Proud D, Leigh R.** 2010. Human rhinovirus infection up-regulates MMP-9 production in airway epithelial cells via NF-{kappa}B. Am J Respir Cell Mol Biol **43:**201-209.
324. **Tacon CE, Newton R, Proud D, Leigh R.** 2012. Rhinovirus-induced MMP-9 expression is dependent on Fra-1, which is modulated by formoterol and dexamethasone. J Immunol **188:**4621-4630.
325. **Marchant DJ, Bellac CL, Moraes TJ, Wadsworth SJ, Dufour A, Butler GS, Bilawchuk LM, Hendry RG, Robertson AG, Cheung CT, Ng J, Ang L, Luo Z, Heilbron K, Norris MJ, Duan W, Bucyk T, Karpov A, Devel L, Georgiadis D, Hegele RG, Luo H, Granville DJ, Dive V, McManus BM, Overall CM.** 2014. A new transcriptional role for matrix metalloproteinase-12 in antiviral immunity. Nat Med **20:**493-502.
326. **Malz R, Weithauser A, Tschope C, Schultheiss HP, Rauch U.** 2014. Inhibition of coagulation factor Xa improves myocardial function during CVB3-induced myocarditis. Cardiovasc Ther **32:**113-119.
327. **Ran FA, Hsu PD, Wright J, Agarwala V, Scott DA, Zhang F.** 2013. Genome engineering using the CRISPR-Cas9 system. Nat Protoc **8:**2281-2308.
328. **Smits AH, Vermeulen M.** 2016. Characterizing Protein-Protein Interactions Using Mass Spectrometry: Challenges and Opportunities. Trends Biotechnol **34:**825-834.

329. **He S, Zhao J, Song S, He X, Minassian A, Zhou Y, Zhang J, Brulois K, Wang Y, Cabo J, Zandi E, Liang C, Jung JU, Zhang X, Feng P.** 2015. Viral pseudo-enzymes activate RIG-I via deamidation to evade cytokine production. Mol Cell **58:**134-146.
330. **Kotla S, Gustin KE.** 2015. Proteolysis of MDA5 and IPS-1 is not required for inhibition of the type I IFN response by poliovirus. Virol J **12:**158.
331. **Hayden FG, Turner RB, Gwaltney JM, Chi-Burris K, Gersten M, Hsyu P, Patick AK, Smith GJ, 3rd, Zalman LS.** 2003. Phase II, randomized, double-blind, placebo-controlled studies of ruprintrivir nasal spray 2-percent suspension for prevention and treatment of experimentally induced rhinovirus colds in healthy volunteers. Antimicrob Agents Chemother **47:**3907-3916.
332. **Patick AK.** 2006. Rhinovirus chemotherapy. Antiviral Res **71:**391-396.
333. **Dragovich PS, Zhou R, Webber SE, Prins TJ, Kwok AK, Okano K, Fuhrman SA, Zalman LS, Maldonado FC, Brown EL, Meador JW, 3rd, Patick AK, Ford CE, Brothers MA, Binford SL, Matthews DA, Ferre RA, Worland ST.** 2000. Structure-based design of ketone-containing, tripeptidyl human rhinovirus 3C protease inhibitors. Bioorg Med Chem Lett **10:**45-48.
334. **Kong JS, Venkatraman S, Furness K, Nimkar S, Shepherd TA, Wang QM, Aube J, Hanzlik RP.** 1998. Synthesis and evaluation of peptidyl Michael acceptors that inactivate human rhinovirus 3C protease and inhibit virus replication. J Med Chem **41:**2579-2587.
335. **Tan J, George S, Kusov Y, Perbandt M, Anemuller S, Mesters JR, Norder H, Coutard B, Lacroix C, Leyssen P, Neyts J, Hilgenfeld R.** 2013. 3C protease of enterovirus 68: structure-based design of Michael acceptor inhibitors and their broad-spectrum antiviral effects against picornaviruses. J Virol **87:**4339-4351.
336. **Wang Y, Yang B, Zhai Y, Yin Z, Sun Y, Rao Z.** 2015. Peptidyl aldehyde NK-1.8k suppresses enterovirus 71 and enterovirus 68 infection by targeting protease 3C. Antimicrob Agents Chemother **59:**2636-2646.
337. **Nicholson DW, Thornberry NA.** 1997. Caspases: killer proteases. Trends Biochem Sci **22:**299-306.
338. **Cohen MS, Chen YQ, McCauley M, Gamble T, Hosseinipour MC, Kumarasamy N, Hakim JG, Kumwenda J, Grinsztejn B, Pilotto JH, Godbole SV, Mehendale S, Chariyalertsak S, Santos BR, Mayer KH, Hoffman IF, Eshleman SH, Piwowar-Manning E, Wang L, Makhema J, Mills LA, de Bruyn G, Sanne I, Eron J, Gallant J, Havlir D, Swindells S, Ribaudo H, Elharrar V, Burns D, Taha TE, Nielsen-Saines K, Celentano D, Essex M, Fleming TR, Team HS.** 2011. Prevention of HIV-1 infection with early antiretroviral therapy. N Engl J Med **365:**493-505.
339. **Shafer RW, Schapiro JM.** 2008. HIV-1 drug resistance mutations: an updated framework for the second decade of HAART. AIDS Rev **10:**67-84.
340. **Andreone P, Colombo MG, Enejosa JV, Koksal I, Ferenci P, Maieron A, Mullhaupt B, Horsmans Y, Weiland O, Reesink HW, Rodrigues L, Jr., Hu YB, Podsadecki T, Bernstein B.** 2014. ABT-450, ritonavir, ombitasvir, and dasabuvir achieves 97% and 100% sustained virologic response with or without ribavirin in treatment-experienced patients with HCV genotype 1b infection. Gastroenterology **147:**359-365 e351.
341. **Kwong AD, Kauffman RS, Hurter P, Mueller P.** 2011. Discovery and development of telaprevir: an NS3-4A protease inhibitor for treating genotype 1 chronic hepatitis C virus. Nat Biotechnol **29:**993-1003.

342. **Malcolm BA, Liu R, Lahser F, Agrawal S, Belanger B, Butkiewicz N, Chase R, Gheyas F, Hart A, Hesk D, Ingravallo P, Jiang C, Kong R, Lu J, Pichardo J, Prongay A, Skelton A, Tong X, Venkatraman S, Xia E, Girijavallabhan V, Njoroge FG.** 2006. SCH 503034, a mechanism-based inhibitor of hepatitis C virus NS3 protease, suppresses polyprotein maturation and enhances the antiviral activity of alpha interferon in replicon cells. Antimicrob Agents Chemother **50:**1013-1020.
343. **Perni RB, Almquist SJ, Byrn RA, Chandorkar G, Chaturvedi PR, Courtney LF, Decker CJ, Dinehart K, Gates CA, Harbeson SL, Heiser A, Kalkeri G, Kolaczkowski E, Lin K, Luong YP, Rao BG, Taylor WP, Thomson JA, Tung RD, Wei Y, Kwong AD, Lin C.** 2006. Preclinical profile of VX-950, a potent, selective, and orally bioavailable inhibitor of hepatitis C virus NS3-4A serine protease. Antimicrob Agents Chemother **50:**899-909.
344. **Pan D, Xue W, Zhang W, Liu H, Yao X.** 2012. Understanding the drug resistance mechanism of hepatitis C virus NS3/4A to ITMN-191 due to R155K, A156V, D168A/E mutations: a computational study. Biochim Biophys Acta **1820:**1526-1534.
345. **Romano KP, Ali A, Aydin C, Soumana D, Ozen A, Deveau LM, Silver C, Cao H, Newton A, Petropoulos CJ, Huang W, Schiffer CA.** 2012. The molecular basis of drug resistance against hepatitis C virus NS3/4A protease inhibitors. PLoS Pathog **8:**e1002832.
346. **Halfon P, Locarnini S.** 2011. Hepatitis C virus resistance to protease inhibitors. J Hepatol **55:**192-206.
347. **Li XD, Sun L, Seth RB, Pineda G, Chen ZJ.** 2005. Hepatitis C virus protease NS3/4A cleaves mitochondrial antiviral signaling protein off the mitochondria to evade innate immunity. Proc Natl Acad Sci U S A **102:**17717-17722.
348. **Li K, Foy E, Ferreon JC, Nakamura M, Ferreon AC, Ikeda M, Ray SC, Gale M, Jr., Lemon SM.** 2005. Immune evasion by hepatitis C virus NS3/4A protease-mediated cleavage of the Toll-like receptor 3 adaptor protein TRIF. Proc Natl Acad Sci U S A **102:**2992-2997.